2012

Assessing the capabilities of Landsat imagery for measuring fuel properties in Sydney Coastal Dry Sclerophyll Forest

Angela Cash
University of Wollongong

Assessing the capabilities of Landsat imagery for measuring fuel properties in Sydney Coastal Dry Sclerophyll Forest

Abstract

Australia is one of the most fire-prone continents in the world (King et al, 2011). Fire can be a great threat to human safety and property (Bradstock & Gill, 2001) and so it is important that effective techniques are developed to be able to predict future fire events. The amount of fuel available to burn strongly determines the likelihood of a fire occurring and the nature of the fire (e.g. severity, intensity) (Bradstock, 2010). Traditionally researchers have attempted to predict future fire events by manually measuring fuel in the field. However such methods at large spatial scales are time-consuming, costly, require man-power and are limited for regions inaccessible to humans. For these reasons remote sensing methods are becoming increasingly popular to measure fuel (Frokling et al, 2009). However, only a few studies have been conducted in Australia to investigate the potential of remote sensing for measuring fuel. Australian studies have only tested a small number of spectral indices, have not tested the effects of the understorey layers on the spectral signal over long time-periods of fuel accumulation and have not taken into consideration dead fuel components in the forest layers. This research project attempted to fill these gaps in the research by assessing the ability of Landsat 5 TM in measuring fuel loads. Seven different indices were compared in their ability to measure fuel in Sydney Coastal Dry Sclerophyll Forest, a forest characterised by a prominent understorey and the presence of both live and dead fuel. Ground truth data extracted from a fuel database for 31 sites was regressed against spectral indice values calculated from the Landsat images. Two approaches were used: Approach 1 did not account for phenological variation; Approach 2 did account for phenological variation. Results found that overall moisture indices (NDIIb5 and NDIIb7) performed the best at measuring fuel cover, as they were not greatly affected by phenological variation or hindered by the presence of dead fuel. Greenness indices (SR, NDVI, GNDVI and SAVI) performed well at measuring fuel but only when phenological effects were accounted for and dead fuel was eliminated from the GT data. When indices performed well they all improved with the addition of the elevated fuel cover layer, suggesting that in this forest type, the understorey significantly contributes to the spectral signal. SATVI was affected by phenological variations, but when this was accounted for it was not as affected by the presence of dead vegetation. The main implication from this study was that, in multiple layered forests that contain dead fuel in the layers, indices that incorporate SWIR wavelengths may prove to be more accurate and successful to use for measuring fuel than the traditional greenness indices.

Degree Type

Thesis

Degree Name

Bachelor of Science (Honours)

Department

School of Earth & Environmental Science

Advisor(s)

Laurie Chisholm

Keywords

Bushfires, fuel load, passive remote sensing, spectral indices

Assessing the capabilities of Landsat imagery for measuring fuel properties in Sydney Coastal Dry Sclerophyll Forest

Angela Cash

"This thesis is presented as part of the requirements for the award of the Degree of Bachelor of Science (Honours) University of Wollongong

October 2012

Certification

The information in this thesis is entirely the result of investigations conducted by the author, unless otherwise acknowledged, and has not been submitted in part, or otherwise, for any other degree or qualification.

Angela Cash

10 October 2012

ABSTRACT

Australia is one of the most fire-prone continents in the world (King et al, 2011). Fire can be a great threat to human safety and property (Bradstock & Gill, 2001) and so it is important that effective techniques are developed to be able to predict future fire events. The amount of fuel available to burn strongly determines the likelihood of a fire occurring and the nature of the fire (e.g. severity, intensity) (Bradstock, 2010). Traditionally researchers have attempted to predict future fire events by manually measuring fuel in the field. However such methods at large spatial scales are time-consuming, costly, require man-power and are limited for regions inaccessible to humans. For these reasons remote sensing methods are becoming increasingly popular to measure fuel (Frokling et al, 2009). However, only a few studies have been conducted in Australia to investigate the potential of remote sensing for measuring fuel. Australian studies have only tested a small number of spectral indices, have not tested the effects of the understorey layers on the spectral signal over long time-periods of fuel accumulation and have not taken into consideration dead fuel components in the forest layers. This research project attempted to fill these gaps in the research by assessing the ability of Landsat 5 TM in measuring fuel loads. Seven different indices were compared in their ability to measure fuel in Sydney Coastal Dry Sclerophyll Forest, a forest characterised by a prominent understorey and the presence of both live and dead fuel. Ground truth data extracted from a fuel database for 31 sites was regressed against spectral indice values calculated from the Landsat images. Two approaches were used: Approach 1 did not account for phenological variation; Approach 2 did account for phenological variation. Results found that overall moisture indices (NDIIb5 and NDIIb7) performed the best at measuring fuel cover, as they were not greatly affected by phenological variation or hindered by the presence of dead fuel. Greenness indices (SR, NDVI, GNDVI and SAVI) performed well at measuring fuel but only when phenological effects were accounted for and dead fuel was eliminated from the GT data. When indices performed well they all improved with the addition of the elevated fuel cover layer, suggesting that in this forest type, the understorey significantly contributes to the spectral signal. SATVI was affected by phenological variations, but when this was accounted for it was not as affected by the presence of dead vegetation. The main implication from this study was that, in multiple layered forests that contain dead fuel in the layers, indices that incorporate SWIR wavelengths may prove to be more accurate and successful to use for measuring fuel than the traditional greenness indices.

ACKNOWLEDGEMENTS

I was lucky enough to receive help and support from a number of people throughout the year. Firstly I would like to thank my three supervisors Laurie Chisholm, Ross Bradstock and Gabriele Caccamo for taking me on as an honours student. Thank you for sharing your ranges of knowledge, always giving valuable advice and continuing to encourage me throughout the year. I would like to thank Penny Watson, Bronwyn Horsey and Sandra Penman for allowing me the use of their database and giving me advice when needed. Thank you Michael Stevens and Heidi Brown for helping me overcome GIS related issues and also a big thank you to Rittick Borah for his assistance with image processing. Finally I would like to thank my fiancé Matthew Whittaker for keeping me sane throughout the year and always knowing how to cheer me up.

Table of Contents

LIST OF FIGURES

LIST OF TABLES

Chapter 1: Introduction

1.1 The problem of fire in Australia

Australia is one of the most fire-prone continents in the world (King et al, 2011). In south-eastern Australia periodic episodes of extreme fire weather (e.g. 1939, 1983, 2003 and 2009) have resulted in large, high intensity fires that have negatively affected people and property (Bradstock & Gill, 2001; King et al, 2011). In the Sydney Basin over 580,000 and 425,000 hectares of bushland were affected by fire in 2001/02 and 2002/03 fire seasons respectively (Caccamo et al, 2012). In order to reduce the impacts of extreme fire weather on communities and ecosystems, research has focused on the key factors that influence the nature of fire regimes, in terms of their severity, intensity, frequency and spatial distribution. Fuel load is considered a major factor affecting fire (Bradstock, 2010). Fuel is defined as "all material that is available to be burnt in a fire" (Brandis & Jacobson, 2003). The more fuel that is available for a fire to consume, the more severe or intense a fire can be. The availability of burnable fuel, or litter, is determined by local climatic conditions, such as weather and moisture levels (Brown & Johnstone, 2012). For example, drought will cause vegetation to dry out and senesce, creating an increase in litterfall from trees and shrubs. This dry fuel is easier to ignite and consume, so will lead to more intense and severe fires (Bradstock et al, 2010). Fire managers have implemented prescribed burnings which are designed to minimize fuel loads to reduce the intensity and severity of fires and maximise fire controllability (Gill & McCarthy, 1998; Ryan & Williams, 2011; Wittkuhn et al, 2011).

Current climate change conditions are predicted to change the accumulation rate of fuel in Australia (Bradstock, 2010), which in turn will affect the nature of fire regimes, as has already been observed in other parts of the world (e.g. Brown & Johnstone, 2012). Increases in atmospheric carbon dioxide (CO_2) have been found to favour and assist the recovery of woody vegetation (e.g. trees) after disturbance events such as fire (Lamont et al, 2011; Bond & Midgely, 2012). It is predicted that if growth of woody vegetation cover (i.e. fuel) in Australia increases, coupled with anticipated drier climatic conditions, there is a strong likelihood that future fires will be more severe (Williams et al, 2009). It is therefore crucial that suitable methods be found to predict future fuel loads.

In the past, measuring fuel loads has been done manually in the field, but fieldwork at large spatial scales is time-consuming and costly. A great number of studies have focused research on the ability of remote sensing to accurately measure fuel properties. Remote sensing instruments possess the ability to obtain information about an object without being in direct physical contact with the object (Jensen, 2007). Remote sensing methods have a number of advantages over field measurement techniques. They can obtain data over a greater spatial extent in a shorter time-frame, are cost-effective and can collect fuel data from forest regions inaccessible to humans (Frokling et al, 2009). There have been a number of previous attempts around the world to measure vegetation properties and fuel using remote sensing methods (e.g. Foody et al, 2003; Rollins et al, 2004; Krasnow et al, 2009; Reeves et al, 2009; Fatoyinbo & Armstrong, 2010; Chen et al, 2011; le Maire et al, 2011; Avitabile et al, 2012; Forzieri, 2012). In particular canopy cover has been found to be an accurate predictor variable for fuel in fire models and can be successfully determined from satellite images and photographs (Krasnow et al, 2009). A number of studies have found that spectral indices derived from remotely sensed images are strongly related to canopy cover (e.g. Franklin et al, 1991; Carreiras et al, 2006; Smith et al, 2009; Sprintsin et al, 2009; Boggs, 2010; Yang et al, 2012).

One major limitation of remote sensing methods however, is that they are site-specific and normally cannot be used across different vegetation types, so field data needs to be collected at each separate site and tested against remotely sensed data to provide the most accurate results (Bi et al, 2010; Feldpausch et al, 2011). In Australia, studies on remote sensing methods for measuring fuel are limited. Some studies have been conducted (e.g. Brandis & Jacobson, 2003; Chafer et al, 2004; Jacobson, 2010; Caccamo et al, 2012) to test the ability of remote sensing to measure fuel load or properties, but further work needs to be conducted.

Firstly, only a small range of spectral indices have been used to measure fuel properties in Australia. Most studies have relied on the commonly used Normalized Difference Vegetation Index (NDVI) (Rouse et al, 1974) and moisture-sensitive indices, such as the Normalized Difference Moisture Index (NDMI) (Gao, 1996). Caccamo et al (2011) measured fuel moisture properties using a range of MODIS-derived indices, but more research needs to be conducted to test their ability to measure fuel load using sensors with higher spatial resolutions. Secondly, Australian forests are characterised as having multiple layers of fuel (Gould et al, 2011). Jacobson (2010) conducted studies on the ability of remote sensing to measure multiple layers of fuel (i.e. canopy, shrub and surface layers) but only

conducted this study on vegetation in its first year of recovery after a fire. More research needs to be conducted to determine if remote sensing can measure fuel loads in multiple layers after fuel has had a longer time-span to recover and accumulate.

Thirdly, no studies in Australia have investigated the contribution of dead fuel to the spectral signal. Spectral indices are designed to be sensitive to live fuel properties, but Australian forests contain components of dead fuel in its multiple layers. The current study will be conducting preliminary analyses to compare the performances of a range of spectral indices, determine if understorey vegetation contributes to the spectral signal and if the presence of dead fuel affects the spectral signal.

1.2 Project Aims

Based upon the gaps in research stated above, the aims of the current project were to:

1. assess the ability of Landsat-derived spectral information for measuring fuel properties in Australian Sydney Coastal Dry Sclerophyll forest;
2. analyse the capability of Landsat-derived spectral indices to retrieve information about fuel properties of multiple forest layers; and
3. explore the influence of live and dead fuel components on vegetation spectral response.

Chapter 2: Literature Review

2.1 Introduction

Fire poses as a major hazard to the environment and humans when it is not controlled (Gill & McCarthy, 1998; Bradstock & Gill, 2001; King et al, 2011; Ryan & Williams, 2011; Wittkuhn et al, 2011). Consequently it is important to be able to understand the nature of and measure fuels that contribute to fire and be able to predict future fire events. The aim of the following chapter is to review previous research conducted on the measurement of fuel and vegetative properties in forests. Originally fuel properties in Australia have been measured manually in the field, but due to the limitations of fieldwork, research investigating the potential of remote sensing to measure fuel load is increasingly becoming popular. When refined and tested for accuracy, remote sensing methods can prove to be more advantageous over fuel measurements because they are cost and time-effective and have the ability to cover greater spatial and temporal scales (Frokling et al, 2009). The main methods for measuring fuel have been based upon determining relationships between spectral indices and vegetation properties, such as biomass or canopy cover. The current study focused upon canopy cover because in Australian dry sclerophyll forests most fuel litter originates from the canopy (Brandis & Jacobson, 2003; Gould et al, 2011). Canopy cover is also an easier variable to measure than biomass (less time-consuming and less field resources required), so it would be advantageous to find it to be an accurate variable for measuring fuel. As can be found in the literature however, the effectiveness of indices varies between locations and vegetation types. The accuracy of indices can also be affected by the presence of understorey vegetation and dead fuel, two factors that Australian research is limited in.

2.2 Australian Fuel Characteristics

The ability to accurately measure fuel loads in Australian forests is critical for fire management practices. Fine fuel (litter, bark and understorey vegetation) is the greatest contributor the fuel loads (Brandis & Jacobson, 2003). This fuel can consist of both live and dead biomass (Rollins et al, 2004) and is the greatest contributor of energy to fires (McCaw et al, 2012). In Australia, eucalypt litter fuels are not homogeneous, but can be stratified into a relatively compacted horizontal surface fuel layer with an aerated, less compacted upper

layer (Gould et al, 2011). Studies conducted on fuel structure in Australia (e.g. Gould et al, 2011) have described that forest fuel layers can be broken down into five distinct layers (Figure 1).

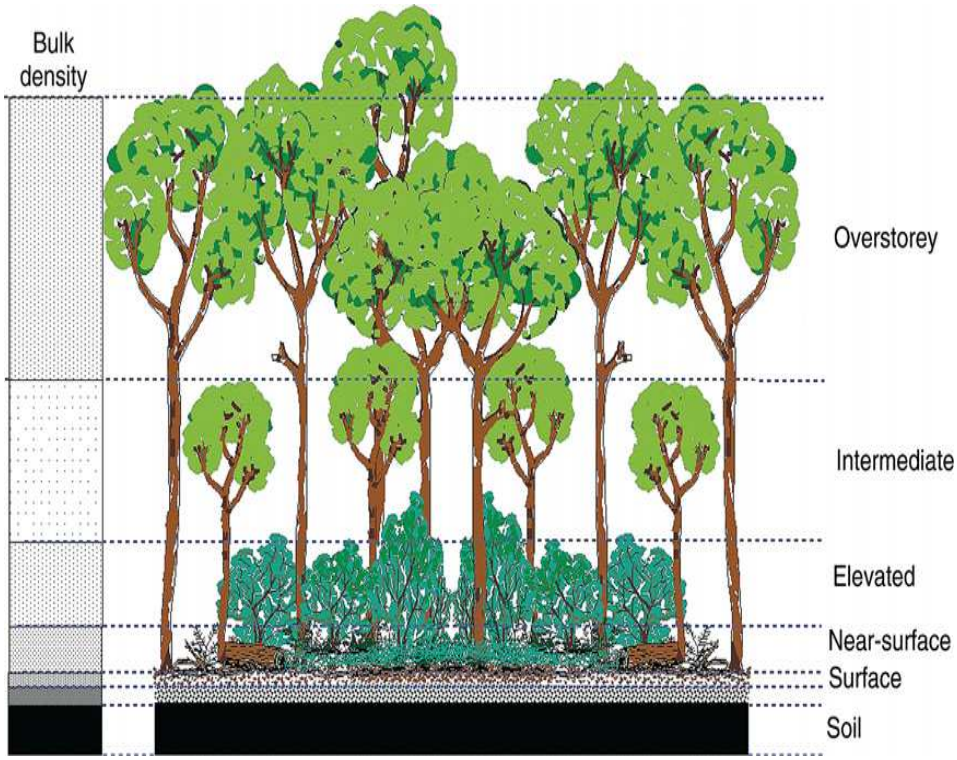

Figure 1: The visual identification of fuel layers in a typical Australian Eucalypt Forest. Source: Gould et al (2007)

The *Overstorey* layer contains the uppermost canopy layer of the forest formed by dominant and co-dominant trees. The *Intermediate* layer is a distinct under-layer consisting of shorter trees (immature overstorey species or species with intermediate stature) with crowns either below or extending into the lower part of the forest canopy. The *Elevated* layer consists of tall shrubs and other understorey plants without significant suspended material, including regeneration of overstorey species mixed with shrubs and can include both live and dead fuel material. The *Near-surface* fuel layer contains a mixture of live and dead material, consisting of grasses, low shrubs, creepers and collapsed understorey that contains suspended leaf, twig and bark material from the overstorey vegetation. Finally, the *Surface* fuel layer consists of predominantly dead material such as leaves, twigs, and bark from the higher vegetation levels. This layer provides the bulk of fuel consumed in a fire (Gould et al, 2007; Gould et al, 2011).

Olson (1963) was the first to quantify fuel in the natural environment, realising that the accumulation of litter acts as a function of continuous litter-fall and could be described using the following relationship:

$$X = L/k.(1-e^{-kt})$$

Where *X* is the litter remaining after *t*, *L* is the rate of litter fall, *k* is the loss or decomposition rate, and *t* is the period of litter fall (years). In fire-prone landscapes, the period of litter fall begins from the Time Since Fire (TSF) (Olson, 1963). Fuel load changes as a function of TSF (Figure 2).

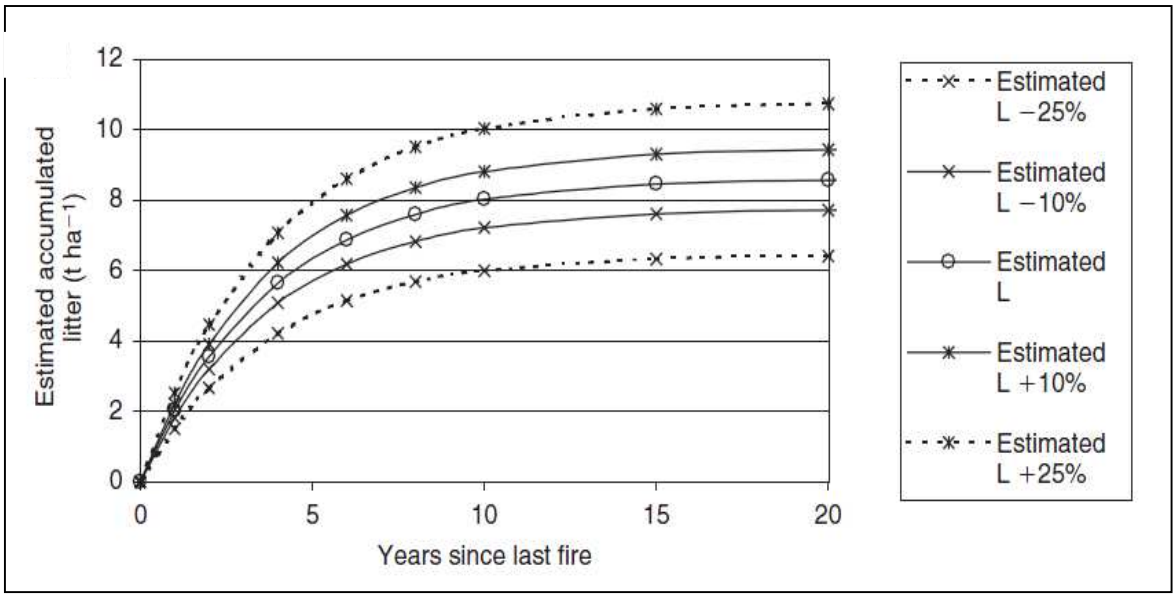

Figure 2: Pattern of litter accumulation as a function of TSF in a Eucalypt Forest. Source: Brandis & Jacobson (2003).

In the first few years after fire, the rate of fuel accumulation is greater, as vegetation growth is more productive. As the forest starts to reach a full recovery, production slows and the rate of fuel accumulation is equivalent to the rate of decomposition (Figure 2).

Based on this understanding of how fuel loads accumulate, Conroy (1998, cited in Brandis & Jacobson, 2003) adapted Olson's (1963) work to predict fuel loads in Sydney vegetation types using the following model:

$$F = a - c * (e^{-bt})$$

Where *F* is the estimated total fuel load, *a*, *b* and *c* are constants and *t* is the TSF.

Brandis and Jacobson (2003) further conducted studies on fuel accumulation in Popran National Park (NSW) using Conroy's equation and found that it was accurate in predicting fuel loads for this particular vegetation type.

A number of studies have used visual assessment techniques to measure fuel in the field and these have also been found to be useful in creating fuel models. Visual assessment techniques are important because they are non-destructive, easy to learn and allow for a number of sites to be sampled in a shorter amount of time (Brandis & Jacobson, 2003). For example, Brandis and Jacobson (2003) also tested the following model developed by Morris (1997, cited in Brandis & Jacobson, 2003) to estimate fuel loads from the visual assessment of litter cover:

$$F = (\%C_l \times D_l) + (\%V_{0\text{-}50} + \%V_{50\text{-}100} + \%V_{100\text{-}150}) / 20$$

Where *C* is percentage litter cover, *D* is litter depth and *V* is percentage volume of vegetation at heights 0-50, 50-100 and 100-150cm. Gould et al (2011) developed a visual assessment hazard score method for measuring fuel load, which was found to also be related to TSF. Gould et al (2011) formulated the following non-linear relationships to describe fuel characteristic change since last fire (adapted from Olson, 1963):

$$fp = ss(1\text{-}e^{-k \times age})$$

and

$$fp = (a \times age)/(b + age)$$

Where *fp* is the fuel parameter value (e.g. cover, depth, height, hazard rating) at a given fuel age (months) and *ss*, *k*, *a* and *b* are regression constants. More recently, Watson et al (2012) conducted studies on fuel accumulation since TSF in the Sydney Basin bioregion. Models were not developed from this study but the results did show a trend of supporting Gould et al (2011), where fuel loads (measured with visual hazard scores) showed a similar pattern of accumulation in relation to TSF (Watson et al, 2012).

Another common visually assessed fuel variable is "canopy cover", which refers to the percentage cover of the vertical projection of tree crowns within a radius of view (McElhinny et al, 2005). As most fuel originates from the canopy layer, and canopy cover has been found to be related to biomass (Suganuma et al, 2006) (and in turn biomass is an indicator of fuel load) measuring canopy cover can provide an indication of future fuel loads (Brandis &

Jacobson, 2003; McCaw et al, 2012). Canopy cover has already been found to be a useful predictor variable when predicting fire models (Krasnow et al, 2009).

Field measurement techniques have proven to be accurate at measuring fuel loads, but they are limited by a number of factors. Firstly, fuel load models are site-specific and normally cannot be used across different vegetation types, so field data needs to be collected at each separate site (Bi et al, 2010; Feldpausch et al, 2011) which is costly and time-consuming (Brandis & Jacobson, 2003). Measuring variables such as biomass can require excessive use of man-power and equipment and are difficult to employ in less accessible locations (Good et al, 2001). As a result, research is being conducted to investigate the potential of remote sensing for measuring fuel properties.

2.3 The use of Remote Sensing

Remote sensing describes the science of obtaining information about an object without being in direct physical contact with the object (Jensen, 2007). Remote sensing holds a number of advantages over field measurement techniques. Much of the time it is cost-effective, less time-consuming and can cover greater temporal and spatial scales. Because forests are widespread, vast and can be inaccessible, spaceborne remote sensing has played a huge role in overcoming these problems by providing large-scale coverage and repeated viewing with the same instrument (Frokling et al, 2009). Studies conducted have found that remote sensing has the ability to indirectly measure fundamental forest properties such as biomass, stand age, canopy height, leaf area and productivity (Frokling et al, 2009). In particular, canopy cover (which stated earlier is a successful predictor variable for future fuel loads) is a common variable that can be measured by remote sensing. Remote sensing has been found in a number of studies to accurately measure canopy cover, which can be successfully determined from satellite images and photographs (Krasnow et al, 2009).

Passive remote sensors (e.g. Landsat, MODIS, AVHRR) define objects by the measurement of reference incoming solar radiation most commonly from visible (0.4-0.7µm), Near Infrared (NIR) (0.7-1.2µm) and Short-Wave Infrared (SWIR) (1.2-2µm) wavelengths (Frokling et al, 2009). While a number of studies have used active remote sensing techniques (e.g. Lucas et al, 2006, conducted studies on measuring Australian forest structure using Lidar) the focus of this study will be on passive remote-sensing.

Healthy vegetation creates a distinct spectral signal from passive sensors (Figure 3).

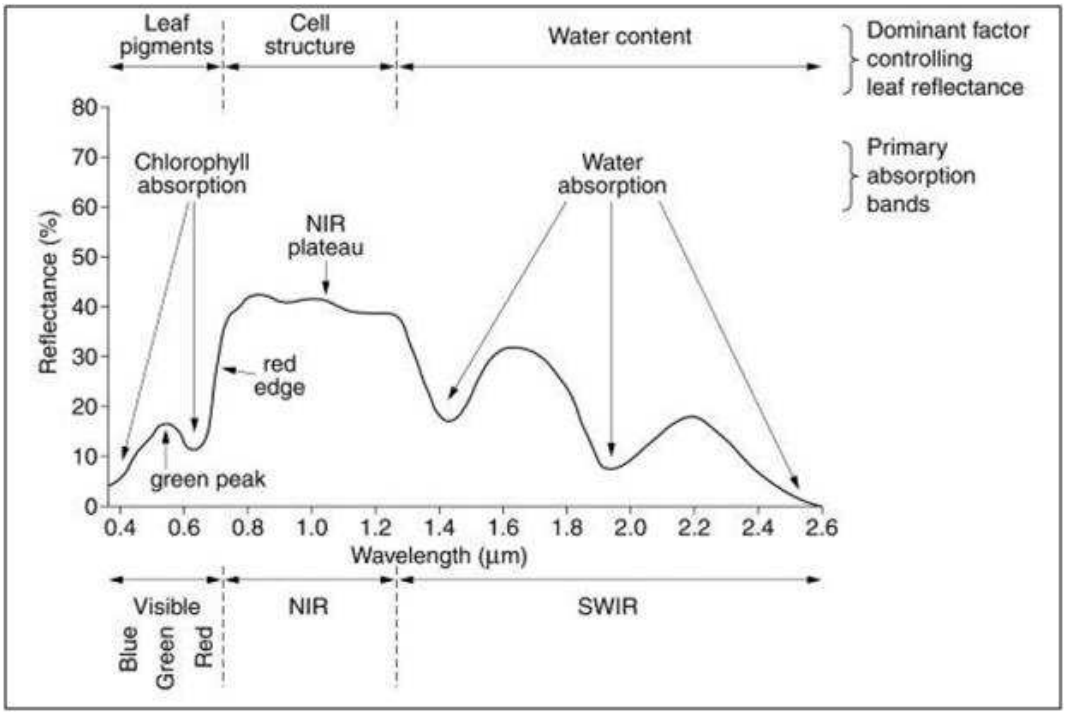

Figure 3: Spectral reflectance signal across wavelengths for healthy vegetation. Source: The Scottish Government (2009)

Landsat TM and ETM+ images in particular have been found to be useful because they are relatively inexpensive (archives are freely available online), are widely available and date back to 1984 (Resasco et al, 2007). Landsat also has an advantage over MODIS in measuring certain vegetation properties because it has a moderate spatial resolution of 30m, in comparison to MODIS which has a coarse spatial resolution of 250-1000m (Hansen et al, 2008). Landsat 5 TM measures a variety of physical properties from seven wavelength bands (Table 1).

In order to distinguish vegetation features from images a number of techniques have been employed, such as Spectral Mixture Analysis (SMA) (e.g. Somers et al, 2010; Yang et al, 2012) and geometric-optical model techniques (e.g. Scarth & Phinn, 2000; Chopping et al, 2011), but the most common methods involve using spectral indices, which the following section of this literature review will focus on.

Table 1: the Landsat 5 TM sensors comprise seven bands: bands 1-3 represent visible wavelengths (blue, green and red); band 4 represents NIR wavelengths; bands 5 and 7 represent SWIR wavelengths; band 6 represents thermal infrared wavelengths.

Landsat 5 TM Band	Wavelength (μm)	Spatial Resolution (m)
1	0.45 - 0.52	30
2	0.52 - 0.60	30
3	0.63 - 0.69	30
4	0.76 - 0.90	30
5	1.55 - 1.75	30
6	10.40 - 12.50	120
7	2.08 - 2.35	30

2.4 Spectral Indices

Spectral indices are combinations of bands that reflect different aspects of plant growth and distribution (Li et al, 2012). With the understanding of how vegetation interacts with oncoming radiation, a wide variety of spectral indices have now been developed that can indirectly measure vegetation physical properties. The most common indices have been developed to measure the "greenness" (i.e. how much visible radiation is being absorbed or reflected) or the "moisture content" of the plant. Greenness indices are based upon the principle that healthy vegetation reflects NIR due to intra- and inter- leaf scattering and absorbs most red and blue wavelengths by photosynthetic pigments (Law & Waring, 1994; Carreiras et al, 2006). As such they provide contrast between the reflectance of vegetation (which reflects NIR wavelengths) and the surrounding soils (which reflect Red wavelengths) (Tucker, 1979; Law & Waring, 1994). The most widely used greenness indices are the Simple Ratio (SR) (Birth & McVey, 1968) and the Normalized Difference Vegetation Index (NDVI) (Rouse et al, 1974). SR is calculated as:

$$\mathbf{SR = \rho_{NIR}/\rho_{red}}$$

More commonly used is NDVI, which is calculated as:

$$\mathbf{NDVI = (\rho_{NIR}-\rho_{Red})/(\rho_{NIR}+\rho_{Red})}$$

Functionally NDVI works the same as SR, but as a ratio it reduces many forms of multiplicative noise (sun illumination differences, cloud shadows, some atmospheric attenuation and some topographic variations) present in multiple bands of multiple date imagery (Jensen, 2007). NDVI has been found to be closely related to biomass, vegetation type, Leaf Area Index (LAI) and primary productivity, so represents and indirect method for measuring fuel load (Chen et al, 2011). Results for the effectiveness of greenness indices however vary across study sites. Coops et al (1997) found that a strong correlation existed between LAI and NDVI, with weaker relationships observed between LAI and SR, as NDVI is more sensitive to areas with lower LAI values. Staben and Evans (2008) found that SR was a highly effective index for discriminating between canopy covers of different vegetation communities in northern Australia. In contrast to Staben and Evans (2008), Li et al (2012) found that NDVI was the most useful for discriminating between different vegetation class types in a river forest in China. NDVI has also been used for mapping disturbance events. For example, Diaz-Delgado et al (2003) found NDVI values declined after fire events, and that these values were positively correlated with severity classes. Studies in Australia have also found that $NDVI_{diff}$ (i.e. the difference between NDVI values before and after the fire) is very effective at mapping changes in vegetation cover after disturbance from fire (e.g. Chafer et al, 2004; Lentile et al, 2006; Jacobson, 2010; Chen et al, 2011).

As common as NDVI is however, it has its limitations. For example, in highly dense vegetated regions NDVI performance can be hindered by saturation effects (Gitelson et al, 1996). To overcome this issue, a modified version of NDVI was the Green Normalized Difference Vegetation Index (GNDVI) (Gitelson et al, 1996), which is calculated as:

$$\mathbf{GNDVI = (\rho_{NIR}-\rho_{Green})/(\rho_{NIR}+\rho_{Green})}$$

GNDVI is similar to NDVI, but uses green wavelengths instead of red wavelengths to increase sensitivity to the presence of chlorophyll (Gitelson et al, 1996). It was found to be highly accurate in measuring photosynthetic rate and stress in vegetation (Gitelson et al, 1996). GNDVI has been found to perform well in studies located in highly vegetated regions (Carrieras et al, 2006). In sparsely vegetated regions however, GNDVI has been found to not have a strong relationship with canopy cover (Barati et al, 2011).

The ability of greenness indices for measuring vegetation is limited in regions with sparse vegetation, due to any surrounding soils and sand that may have a greater reflectance than the vegetation (Barati et al, 2011). Surrounding soils reflect visible wavelengths and, until soils

are fully covered by vegetation they will continue to influence traditional vegetation indices which commonly utilize the red wavelengths (Jackson & Huete, 1991). To minimize the confounding effects of soils in the background, soil adjusted vegetation indices have been developed (Carreiras et al, 2006). The first of these indices to be developed was the Soil Adjusted Vegetation Index (SAVI) (Huete, 1988). SAVI is calculated as:

$$\mathbf{SAVI = [(\rho_{NIR}-\rho_{Red})/(\rho_{NIR}+\rho_{Red}+L)]*(1+L)}$$

where *L* is a factor (ranging from 0 to 1) incorporated to minimize soil influence (Huete 1988; Kasawani et al, 2010). SAVI has been found to work much more effectively in sparsely vegetated regions, such as Mangrove swamps (Kasawani et al, 2010) and deserts (Barati et al, 2011) than NDVI. As Australian vegetation can be characterised by fairly open canopies, the current study tested soil adjusted indices in case any visible soil could influence the signal.

Another index taking the effects of soil into consideration is the Soil Adjusted Total Vegetation Index (SATVI) (Marsett et al, 2006). SATVI is calculated as:

$$\mathbf{SATVI = [(\rho_{SWIR(1.55\mu m)}-\rho_{Red})/(\rho_{SWIR(1.55\mu m)}+\rho_{Red}+L)]*(1+L) - (\rho_{SWIR(2.08\mu m}/2).}$$

SATVI works in a similar fashion to SAVI, but by incorporating short-wave infrared (SWIR) wavelengths instead of the NIR wavelengths in the ratio, the index was found to be sensitive to both green and senescent vegetation (Marsett et al, 2006). What Marsett et al (2006) found was that, when the spectral signal of healthy vegetation was compared to that of senescent vegetation, NIR wavelengths showed the greatest difference in reflectance, but SWIR wavelengths showed the least change in reflectance (slightly higher reflectance for senescent vegetation). Therefore SWIR wavelengths could potentially be used for measuring both live and dead fuel. This index has yet to be tested however in regions other than rangelands. As Australian Eucalypt forests do contain a certain amount of dead or senescent understorey vegetation, it was tested in the current study to determine if it could be effective for measuring both live and dead fuel.

Indices have also been created to measure moisture levels in vegetation. It has been found that NIR wavelengths (Gao, 1996) and SWIR wavelengths (Datt, 1999) are sensitive to water content in stacked leaves. These indices incorporate NIR (0.950-970µm) and SWIR (1.150-1.260µm and 1.520 – 1.540µm) wavelengths. SWIR wavelengths are weakly absorbed and thus penetrate more deeply into canopies which, in theory, suggests these wavelengths should

be able to measure a larger proportion of the total water in canopies (Sims & Gamon, 2003). Moisture-sensitive indices can therefore have an advantage over greenness indices, in that they can penetrate down to 8 leaf layers, whereas NDVI signals become saturated for regions with 3 or more leaf layers, due to the visible bands becoming absorbed (Gao, 1996). Carreiras et al (2006) also found that the indices incorporating SWIR bands were less affected by atmospheric effects, in comparison to other indices that use visible wavelengths. Moisture-sensitive indices have also shown to be less affected by seasonal variation. For example, De Beurs and Townsend (2008) found that defoliation in deciduous hardwood forests was more readily detected by MODIS NDII than the traditional vegetation indices Enhanced Vegetation Index (EVI), and NDVI. NDII was found to show more consistent results and consequently be better for mapping forest changes, whereas NDVI varied based upon the timing and season of the image (De Beurs & Townsend, 2008).

One main type of moisture-sensitive index is the Normalized Difference Infrared Index (NDII) (Hunt & Rock, 1989). NDII is calculated as:

$$\mathbf{NDII} = (\rho_{NIR} - \rho_{SWIR(1.55\mu m \text{ or } 2.08\mu m)}) / (\rho_{NIR} + \rho_{SWIR(1.55\mu m \text{ or } 2.08\mu m)})$$

This index provides an alternative to the Normalized Difference Water Index (NDWI) (Gao, 1996) which was developed for MODIS and hyperspectral sensors that have two or more NIR bands. Because NDII makes use of both NIR and SWIR it has the flexibility of being able to be used by a greater range of sensors. As Landsat 5 TM has two bands in the SWIR region, NDII can be calculated using TM band 5 or 7. NDII calculated with TM band 5 has also been referred to as the Normalized Difference Moisture Index (NDMI) in previous studies (e.g. Wilson & Sader, 2002; Noone et al, 2012) and also as VI5 in Carreiras et al (2006). NDII calculated with TM band 7 uses the same Landsat TM bands as the Normalized Burn Ratio (NBR) Index for Landsat TM (Miller & Yool, 2002; Lentile et al, 2006; Escuin et al, 2008) where it was found to be more sensitive for mapping burn scars. Carreiras et al (2006) referred to NDII with TM band 7 as VI7.

Previous research has found that the effectiveness of spectral indices can vary between different locations, levels of vegetation cover and the types of sensors used. Even within similar environmental regions, researchers have obtained different results using the same indices due to other local factors. A few studies around the world have run studies to compare the effectiveness of a range of indices in their ability to measure fuel properties, most commonly canopy cover. For example, Carreiras et al (2006) found that when testing

the ability of a range of indices and band combinations to measure canopy cover in evergreen oak woodlands, a multiple regression of TM bands 3, 4, 5 and 7 and NDVI out-performed other indices (SAVI, MSAVI, GNDVI, VI5 and VI7). Barati et al (2011) tested 20 spectral indices in sparsely vegetated regions and found that SAVI performed slightly better than NDVI, but none of the indices tested alone performed better in comparison to the other. Better predictions were provided when a multiple of indices were combined together (Barati et al, 2011). Kasawani et al (2010) tested a range of soil adjusted indices and found them to consistently provide accurate results when testing them across a range of mangrove landscapes, where the vegetation was sparse and soils are highly prominent. In contrast however, Yang et al (2012) tested indices in sparsely vegetated regions and found that NDVI still out-performed SAVI, even though the theory suggests that SAVI should perform well in these regions. As results have varied between sites, it is important to test a range of spectral indices potential in measuring fuel in Australian forests.

In Australian forests the range of indices that have been tested in their ability to measure vegetation properties and fuel is limited. Most studies have relied upon the use of NDVI. For example, Chafer et al (2004) used NDVI to predict fuel loads. Most studies measuring changes in vegetation have also relied mainly on moisture-sensitive indices, such as NDMI or NBR. Boer et al (2008) conducted a study to measure stands in the northern Jarrah forest in Western Australia and found that NBR was the most effective at mapping vegetation change, whereas SR and NDVI were more likely to suffer from saturation and seasonal effects. Jacobson (2010) used NDVI and NDMI to map changes in plant regrowth during the first year after a fire and found that, overall, they both performed similarly across seasons. NDMI was found to perform better after a fire, but the greatest variation between the two indices depended upon the combination of forest layers used, with NDMI showing greater potential to measure live fuel than NDVI, when under-storey layers were incorporated into the models (Jacobson, 2010). Though commonly used, the use of NDVI for measuring vegetation in Australia can be problematic, as the country often experiences fires and NDVI has been found to be less effective in detecting post-fire recovery vegetation, as seasonal variation affects the values (Buma, 2011). One study conducted by Caccamo et al (2011) tested a range of MODIS indices (4 greenness; 4 moisture) in their ability to measure moisture in vegetation, finding that indices that incorporated the SWIR bands performed the best. More research however needs to be conducted to test the effectiveness of a greater range of indices in their ability to specifically predict fuel loads in Australian forests.

2.5 Underlying effects on the remotely sensed signal

Previous research has found that the understorey vegetation can contribute to the spectral signal. Spectral indices a limited in that they do not show any indication of forest 3 dimensional structure. When radiation reflects off the earth's surface, passive remote sensors interpret it as a 2 dimensional image. As a result, Pisek et al (2010) highlights the importance of adding the understorey and canopy layers together when explaining what is contributing to the reflectance signal.

Interference from the understorey can be problematic if researchers are aiming to only measure the canopy layer. Many studies conducted in forests with sparse woody vegetation and little upper canopy cover have found an over-estimation of canopy cover, where the understorey is visible and measured by the sensor (Franklin et al, 1991; Law & Waring, 1994; Staben & Evans, 2008; Smith et al, 2009; Boggs, 2010). Smith et al (2009) suggested that NIR wavelengths should be avoided in open canopy forests if the aim is to only measure the upper canopy layer, as these wavelengths are sensitive to any vegetation visible to the sensor. The influence of the understorey has found to be a particular problem in deciduous forests, where spring greenness begins in the understorey before canopy layers have begun to grow (Resasco et al, 2007; Doktor et al, 2009). Some researchers (e.g. Franklin et al, 1991; Lu et al, 2003) were able to overcome this issue by finding that NDVI and all TM bands corresponded strongly with canopy cover during seasons where there was the greatest contrast between canopy and the understorey (i.e. understorey layer had senesced) and is therefore important to measure canopy cover in seasons appropriate to the study site (Carreiras et al, 2006; Lu et al, 2003). In Australian forests however, contribution of the understorey to the spectral signal is likely to occur all-year round, as dry sclerophyll forests are evergreen (Coops et al, 1997).

Knowing that the understorey cover layers can influence the spectral signal to a point, some studies have focused their research on investigating to what depths of forested regions passive remote sensors can actually measure. Indices are dependent on the visibility of leaves in image pixels (Somers et al, 2010), and a lot of the time, a proportion of the understorey layer is covered out of the sensor's reach by the canopy layer. The ability of passive remotes sensors to be able to measure past the canopy layer is important for studies aiming to measure multiple layers. Surface fuels are often obscured from the sensor by the canopy layer (Riano et al, 2003; Rollins et al, 2004; Krasnow et al, 2009). Studies have

found that understorey cover can be best measured by NIR wavelengths in regions where stands have the smallest canopy cover (Rautiainen et al, 2007). In past research, studies have overcome the problem of canopy saturation by incorporating multiple sensors. For example, Law and Waring (1994) used on-ground sensors such as spectrometers. Kuusk et al (2004) developed a 2-layer model for understorey (ground) vegetation using on-ground remote sensing techniques. These methods however are more time-consuming and less practical, than if one satellite sensor could be used to measure multiple layers.

As Australian forests contain multiple layers of fuel, this study was interested in testing how many forest layers could influence the spectral signal of Landsat 5 TM data. Previous studies conducted by Viedma et al (1997) found that when comparing the recovery of different forest types, the tree+shrub regions showed greater NDVI values than regions with just shrubs, suggesting the contribution to the spectral signal is a cumulative factor. A more recent study conducted by Jacobson (2010) considered multi-layer effects on spectral signal and found that the relationship between NDVI or NDMI and vegetation cover increased when the under-storey layers were added to the canopy layer. Jacobson's (2010) study however, like Viedma et al (1997) was conducted soon after a fire event (within the first year of recovery). More research needs to be conducted to assess the ability of sensors to measure multiple layers of fuel in Australian forests after longer time periods of recovery and fuel accumulation in the layers.

Another underlying factor that needs to be considered is the contribution of dead fuel to the spectral signal. Spectral indices make use of wavelengths which primarily reflect characteristics of live vegetation, whereas the aim of this study is to measure fuel, which is composed of both live (e.g. canopy foliage) and dead (e.g. litter) material. Studies have found that relationships between spectral indices and vegetation cover weakened when dead vegetation was considered (Tucker, 1979). This is because as leaves die off their cell structure changes and the reflection patterns of NIR wavelengths off leaves are modified (Doktor et al, 2009). While Marsett et al (2006) has tried to account for senescent vegetation by incorporating SWIR bands into indices, this method has not undergone enough studies outside of rangelands to prove to be robust. As Australian forests contain a significant amount of dead fuel in the layers, a spectral index that can measure both live and dead vegetation would be highly beneficial. Research needs to be conducted to determine to what extent dead fuel contributes to the vegetation signal, to see if remote sensing can accurately measure fuel cover in Australian forests that contain dead fuel.

Another limitation to using passive remote sensing for measuring understorey layers is that greenness indices can be highly affected by seasonal variation (Smith et al, 2009). As was mentioned earlier, in many forests the understorey can be deciduous with an evergreen over-storey, or both can be deciduous with different growth rates, which would cause an issue with wanting to study the cumulative effects of forest layers on spectral signal (Ahl et al, 2006; Doktor et al, 2009). Australian forests are evergreen so have the advantage of being live all year round. However, the greenness still displays phenological variation in the canopy based upon the season, and the understorey grass growth can be highly variable, with most perennials growing in relation to rainfall, regardless of season (Williams, 1970).

When testing the ability of passive remote sensing for measuring live and dead fuel properties in Australian forests, it is therefore important to take into consideration the effects of the understorey, understand the limitations of indices when measuring mixes of live and dead fuel and the effects of seasonal variation.

Chapter 3: Site Description

3.1 Introduction

The current study was set in the Sydney Basin Bioregion. The following chapter provides a brief description of landscapes observed in the region, local climatic conditions, and how the interaction of these two factors have lead to the growth of the diversely vegetated forests. The current study focused upon vegetation data collected in Sydney Coastal Dry Sclerophyll (SCDS) Forest, so a description of this forest type will be given, as well as an explanation for how it has evolved to survive and depend upon fire.

3.2 Site Description

The study region was located on the central East coast of Australia in the Sydney Basin Bioregion, New South Wales. The bioregion extends from just north of Batemans Bay to Nelson Bay on the Central Coast and almost as far west as Mudgee. It covers an area of 3,624,008 hectares and occupies about 4.53 percent of New South Wales. It encompasses the city of Sydney and the towns of Wollongong, Nowra, Newcastle, Cessnock, Muswellbrook and the Blue Mountains towns such as Katoomba and Mt Victoria (Figure 4).

Geologically the Sydney Basin consists of a basin filled with near horizontal sandstones and shales of Permian to Triassic age that overlie older basement rocks of the Lachlan Fold Belt. The sedimentary rocks have been subject to uplift with gentle folding and minor faulting during the formation of the Great Dividing Range (NSW Government Environment and Heritage, 2011).

These past geological processes have all lead to creating the vast variety of landscapes observed in this region. Much of the Basin landscape is elevated sandstone plateau, with the exceptions being the Hunter Valley and the low-lying Cumberland Plain The coast is characterised by an escarpment that has formed on the eastern side of the inland plateaux

(Taylor, 1970). Along the coast there can be observed cliffs, beaches and estuaries, confined barrier systems, dunes and coastal lakes (NSW Government Environment & Heritage, 2011).

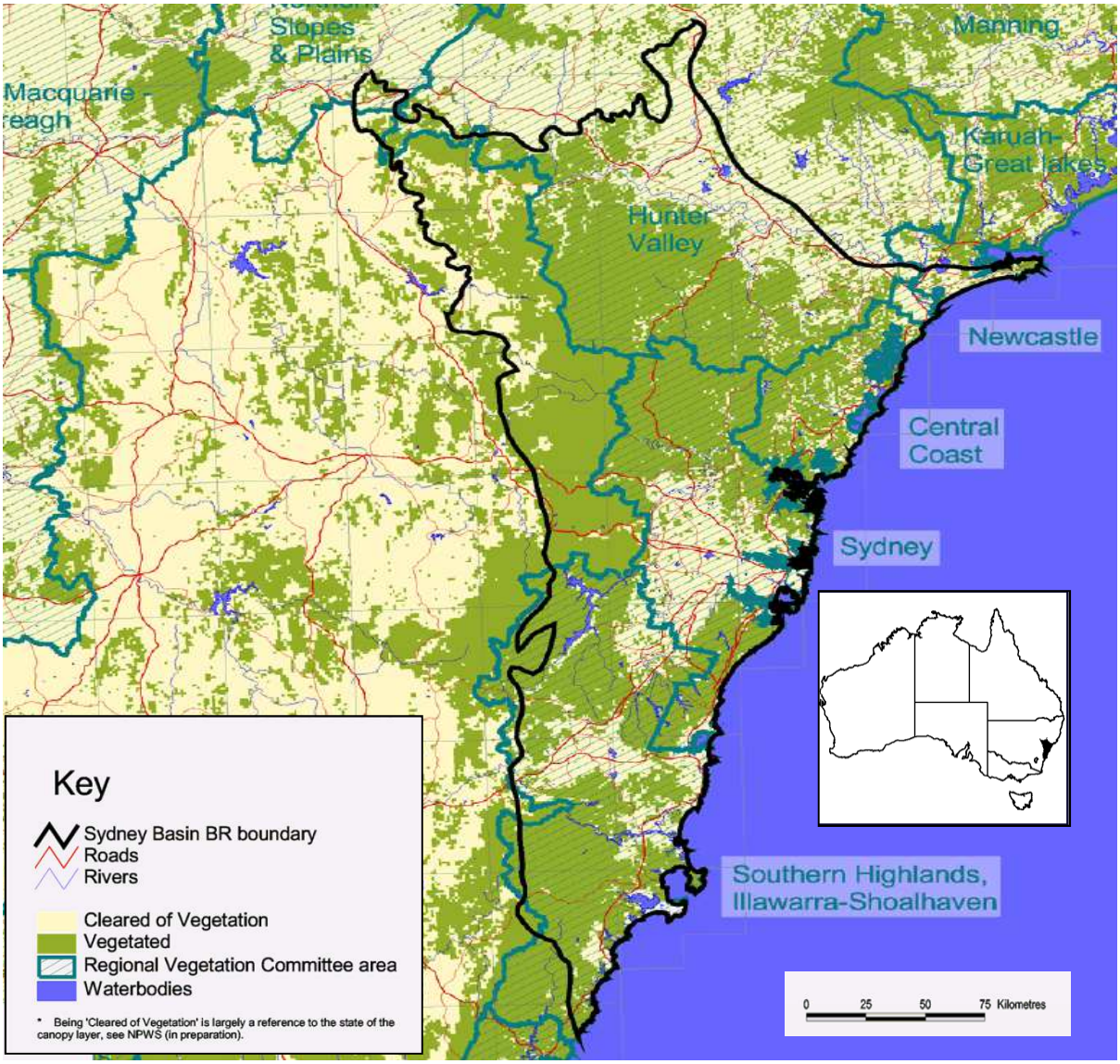

Figure 4: Sydney Basin Bioregion, New South Wales. Source: NSW Government Environment and Heritage (2011).

The Sydney Basin covers a large part of the catchments of the Hawkesbury-Nepean, Hunter and Shoalhaven river systems. West of the escarpment, rivers have eroded the inland plateau blocks to form deep sandstone gorges (NSW Government Environment & Heritage, 2011).

The Sydney Basin Bioregion predominantly experiences temperate climate characterized by warm summers with no dry season. A sub-humid climate occurs across significant areas in the northeast of the bioregion. A small area in the west of the bioregion around the Blue Mountains falls in a montane climate zone, where snow occasionally falls (NSW Government Environment & Heritage, 2011). Rain can occur throughout the year, but varies across the bioregion in relation to altitude and distance from the coast, with wetter regions being close

to the coast or in higher altitudes. An east-west rainfall gradient is evident across the remnant plateaus and follows down the cliffs of the inland gorges. Higher temperatures are experienced along the coast and in the Hunter valley and areas of lower temperature are experienced in the higher plateaux and western edge (NSW Government Environment & Heritage, 2011).

As a result of the variable topography interacting with current climatic conditions, the bioregion is characterised by highly diverse forests. The most common forest types in this region are the dry sclerophyll forests.

3.3 Dry Sclerophyll Vegetation

Dry Sclerophyll (DS) forests are characterised by an incredibly diverse range of vegetation (Keith, 2004). The upper canopies of most DS forests are dominated by eucalypts (Keith, 2004). DS forests are often characterised by a prominent under-storey structure of shrubs (characterised by many quintessential Australian wildflowers, such as waratahs, banksias and wattles) or grasses. The sparse ground covers of these forests are comprised mainly of sclerophyllous sedges (Keith, 2004).

Since the start of the Australian continent drying 15-20 million years ago, Sclerophyllous species have evolved to overcome a number of harsh factors in their environment, such as dryness, infertile soil and fire events (Keith, 2004).

Australia is a landscape that experiences regular fire events and the native vegetation have evolved a range of strategies, or recovery mechanisms, for surviving and reproducing after fire (Keith, 2004). Many species are able to resprout after a fire from protected living tissues that are either contained in organs beneath the soil (e.g. lignotubers) or within the trunk and branches under thick insulating barks (e.g. epicormic strands) (Keith, 2004; Keith et al, 2007; Vivian et al, 2008; Lamont, 2011). Other species have adopted an obligate seeder mechanism, where the original tree is often burnt but seeds are stored or protected in such a way that they are not destroyed by the fire (Keith et al, 2007; Vivian et al, 2008).

Just as fire plays a role in the biodiversity structure of native forests, the forest properties in turn have an influence on the nature of fires. Due to recovery mechanisms a number of

native species rely upon fire events to promote seed germination, production and sprouting (Lentile, 2006; Vivian et al, 2008). Some species store seeds in protective woody fruits that are stimulated to open from the heat of fire (serotiny), while other plants when scorched are stimulated to grow rapidly and flower profusely (Keith, 2004). Because of this dependence upon fire, the vegetation has evolved to be flammable. Eucalypt litter is coarse and decays slowly so it builds up for a fire event. Many species have flammable and loosely attached bark and the green leaves contain highly flammable oils and resins that act as a catalyst to promote combustion before the leaves are fully dry (CSIRO, 2011). As such, the local vegetation plays a role in the spread of bushfires.

Fire severity and intensity also varies based upon the diversity of the vegetation, depending upon the vegetation's topographic location and its access to water (Hammill & Bradstock, 2006). Trees need enough access to moisture to produce burnable vegetation, but not so much that it cannot dry out enough to fully burn (Bradstock, 2010). Less severe fires will remain confined to the understorey vegetation, which contains dead fuel, but conditions where fires can become more severe, such as if the vegetation located on a high ridge and exposed to wind, the fire can reach the canopy layer (Bradstock, 2010).

3.3.1 Sydney Coastal Dry Sclerophyll Forest

The current study focused upon Sydney Coastal Dry Sclerophyll (SCDS) forests, which are unique to the Sydney Basin region. This type of forest is the most diverse and extensive of the DS forests in Australia, containing over 100 different kinds of native species, covering 1.4 million (Keith, 2004). It can be found in the coastal reserves between Port Stephens and Sussex Inlet, including Brisbane Water, Ku-ring-gai Chase and Royal national parks, and also in the lower Blue Mountains and eastern parts of Morton Plateau. SC DS Forests grow below 700 metres elevation and have an average rainfall of 1000 to 1300+ millimetres. Like other DS forests, its species composition varies with topography and moisture (Keith, 2004). Many species have developed specialized characteristics to suit their habitat, such as rock overhangs, seepage zones and 'ironstone' soils have very distinct and endemic plant communities. Eucalypt growth is highly driven by access to moisture, with canopies of 10 metres or less observed on exposed ridges or plateaus where drainage is poor, but may exceed 25 metres in sheltered gullies with moist but freely draining soils (Keith, 2004).

Chapter 4: Methods

4.1 Introduction

The purpose of the current study was to assess the capability of Landsat images for measuring canopy cover. Relationships between Ground Truth (GT) Data and spectral indices derived from the Landsat images were explored. The GT Data was obtained from a fuel database collected and comprised together in a prior study by Watson et al (2012). Spectral data was obtained using a range of Landsat 5 TM images. Data was analysed based upon the following steps:

1. Images underwent pre-processing to correct for atmospheric and topographic effects;
2. Seven spectral indices were calculated for each image and values were then extracted from these in locations that corresponded to the locations of the GT data.
3. The relationships between spectral data and the GT data were then analysed using standard least squares regressions and tested for significance using one-way ANOVA tests to obtain an F value.

4.2 Ground Truth Data

Ground-truth data was selected from a Fuel Hazard database complied from data collected in a previous study by Watson et al (2012). The purpose of the study by Watson et al (2012) was to measure the accumulation of fuel loads across a variety of Australian forests in relation to TSF. A large number of vegetation variables and fuel measurements were collected for the database from the canopy, elevated, near-surface and surface forest layers (e.g. percentage cover, fuel hazard scores, fuel height). Based upon previous research that has found that most fuel originates from the canopy (Brandis & Jacobson, 2003) the current study conducted tests on the variable “canopy cover”. As was noted in Chapter 2, canopy cover has been found in a number of studies to be strongly related to the spectral signal of passive remote sensors (e.g. Franklin et al, 2001; Carreiras et al, 2006; Staben & Evans, 2008; Smith et al, 2009). “Elevated cover” and “near-surface cover” were also incorporated into the analysis, as those layers also contribute to fuel load and contain fuel which has fallen from the canopy (Gould et al, 2011). To account for differences between vegetation types, all points studied were chosen from the SCDS Forest, as different vegetation types can have

different effects on the spectral signal (Hammill & Bradstock, 2006). This left a data set of 31 points collected between 20 July 2009 and 9 April 2010 (see Appendix A for site information and raw data values). Data points were located on the NSW south-eastern coastal region between 33°18'29" (encompassing the region from Popran National Park to Northern Sydney) and 34°13'24" (Royal National Park region) (Figure 5).

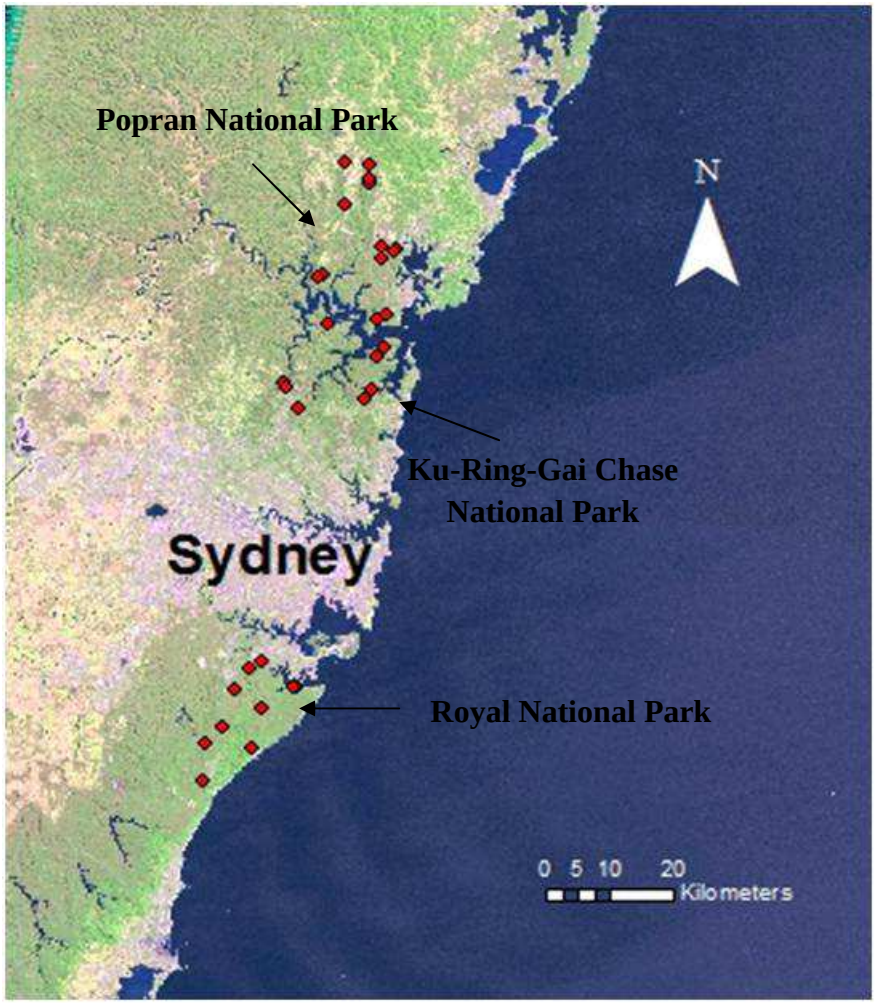

Figure 5: Field collection sites for GT data points (red dots) surrounding the Sydney region. Major national parks are labelled.

4.3 Remote sensing data

Landsat 5 TM images were downloaded from the *USGS Earth Explorer* (USGS, 2012) website free of charge. All images were delivered as Level 1T products (already geo-registered and had some terrain correction) (Table 2).

Table 2: List of Landsat 5 TM images used in the current study

Date	Path	Row
5 Jul 2009	89	84
21 Jul 2009	89	83
28 Jul 2009	90	84
22 Aug 2009	89	83
23 Sep 2009	89	83
23 Sep 2009	89	84
10 Nov 2009	89	83
10 Nov 2009	89	84
12 Dec 2009	89	83
12 Dec 2009	89	84
18 Mar 2010	89	83
18 Mar 2010	89	84
10 Sep 2010	89	83
10 Sep 2010	89	84

4.3.1 Pre-processing

All of the Landsat 5 TM images were atmospherically corrected using the FLAASH (Fast Line-of-sight Atmospheric Analysis of Spectral Hypercubes) tool in *ENVI 4.8* (Exelis Visual Information Solutions, 2010), which uses a MODTRAN-4 atmospheric correction algorithm (Guanter et al, 2009). FLAASH atmospherically corrects images by selecting dark surface pixels in the image based upon the at-sensor radiances at channels near 660nm and 2100nm. It has been found affective to use on multi-temporal data to remove non-uniform atmospheric effects (Moses et al, 2012). It was chosen to use in this study because FLAASH removes Raleigh scattering and amplifies NIR reflectance, so is suitable for measuring vegetation properties (Moses et al, 2012).

Firstly images needed to undergo a "radiance calibration" so they were in the appropriate format for FLAASH. They then had to be converted to BIL (or BIP) as FLAASH does not recognise BSQ files (Figure 6).

A number of input parameters were required to run the FLAASH correction tool (Table 3).

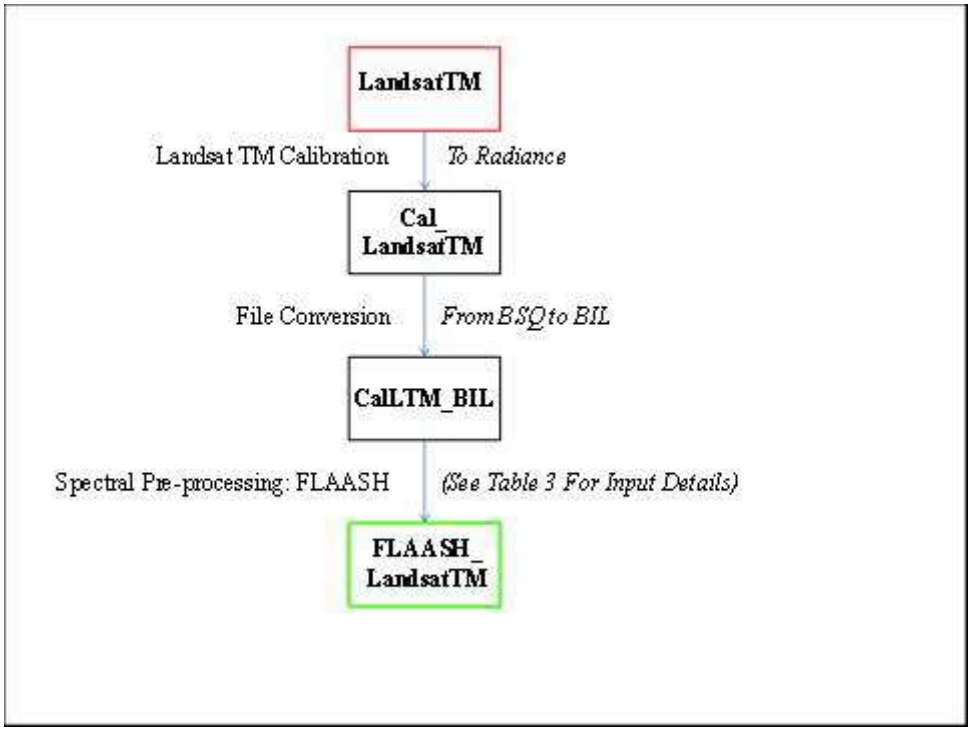

Figure 6: Schematic diagram showing steps involved in the atmospheric correction. The red box shows the original input image and the green box shows the final output image.

Table 3: Summary of input parameters for FLAASH.

Parameter	Input value
Scale Factor	10
Latitude & Longitude	Unique to each image
Flight Date & Time	Unique to each image
Altitude	705km for Landsat 5 TM
Average Ground Elevation	0.230km
Atmospheric Model	Mid-Latitude Summer
Aerosol Model	Tropospheric
Aerosol Retrieval	2 Band (K-T), limits bands 3-7
Initial Visibility	20-40km. FLAASH automatically changed this value

A scale factor of 10 was entered so that the pixels would be scaled from the unit [W/(m^2*sr*μm)] to the appropriate unit of [μW/(cm^2*sr*nm)].

The parameters Latitude & Longitude, and Flight Date & Time were stored in each image's own Metadata File. The altitude information for Landsat 5 TM was stored in FLAASH. The average ground elevation was calculated from a 30m resolution SRTM derived Digital

Elevation Model (DEM) (Geoscience Australia, 2011) covering the extent of the study site. Information for the Atmospheric Model was available from the *Atmospheric Correction Module version 4.7* (Exelis Visual Information Solutions, 2009). "Mid-Latitude Summer" was chosen based upon the latitudinal information and season that the image was taken in. "Tropospheric" was chosen, as the images were acquired over calm and clear land and points were not located in high density urban/ industrial regions. "Rural" and "urban" models were also tested but values did not significantly change between the different models. Aerosol retrieval was used to subtract any potential shadow pixels and the band limit chosen was band 3 to 7 (these covered the required wavelength range for this tool). A visibility of 40km was selected, as most images used were chosen with little cloud cover. During the process however FLAASH did sometimes automatically change this value.

All images were also topographically corrected. Preliminary analysis tested two topographic correction methods: the *Cosine Correction* (Teillet et al, 1982, cited by Riaño et al, 2003; Jensen, 2007) and the *C-Correction* (Teillet et al, 1982, cited by Riaño et al, 2003; Jensen, 2007). The *Cosine Correction* assumes the surface displays Lambertian behaviours and was tested because it is the most simple and widely used correction method (Riaño et al, 2003; Vicente-Serrano et al, 2008). For the *cosine correction*, the following equation was applied to each pixel in the image:

$$\mathbf{L_H = L_T\ (\cos \textit{z} / \cos \textit{i}\ )}$$

Where L_H is the radiance for a horizontal surface, L_T is the radiance observed over the inclined terrain, *z* is the solar zenith angle and *i* is the incidence angle with respect to the surface normal. *z* was obtained by working out the difference between 90 degrees and the angle of elevation (stored in the each image's Metadata file). For the purpose of this correction it was converted to radians. *i* was obtained by creating a shaded relief image from the DEM. This was done for each individual image. Some of the images required image-to-mage registration with the shaded relief image.

Preliminary testing found that the *Cosine Correction* "over-corrected" the images (shaded regions appeared overly illuminated and sections originally illuminated by the incoming radiation were dulled). Statistically it also did not perform well, reducing the mean and increasing the standard deviations for each band. As a result the *C Correction* was then used. The *C Correction* method assumes non-Lambertian behaviour of the radiation, has been widely used and in general has been found to be the most accurate topographic correction

method (Vicente-Serrano et al, 2008; Riaño et al, 2003). The following equation was applied to each pixel for the *C Correction* method:

$$\mathbf{L_H = L_T\,[(\cos z + c_k)/(\cos i + c_k)]}$$

Where c_k adds the c co-efficient to the equation, where: $\boldsymbol{c_k = b_k/m_k}$. The parameters $\boldsymbol{b_k}$ and $\boldsymbol{m_k}$ are obtained from the regression equation $\mathbf{L_T = b_k + m_k i}$, as it is assumed that a linear relationship exists between the observed radiance and the incidence angle for images not yet corrected. The topographic correction steps are summarised in the following schematic (Figure 7).

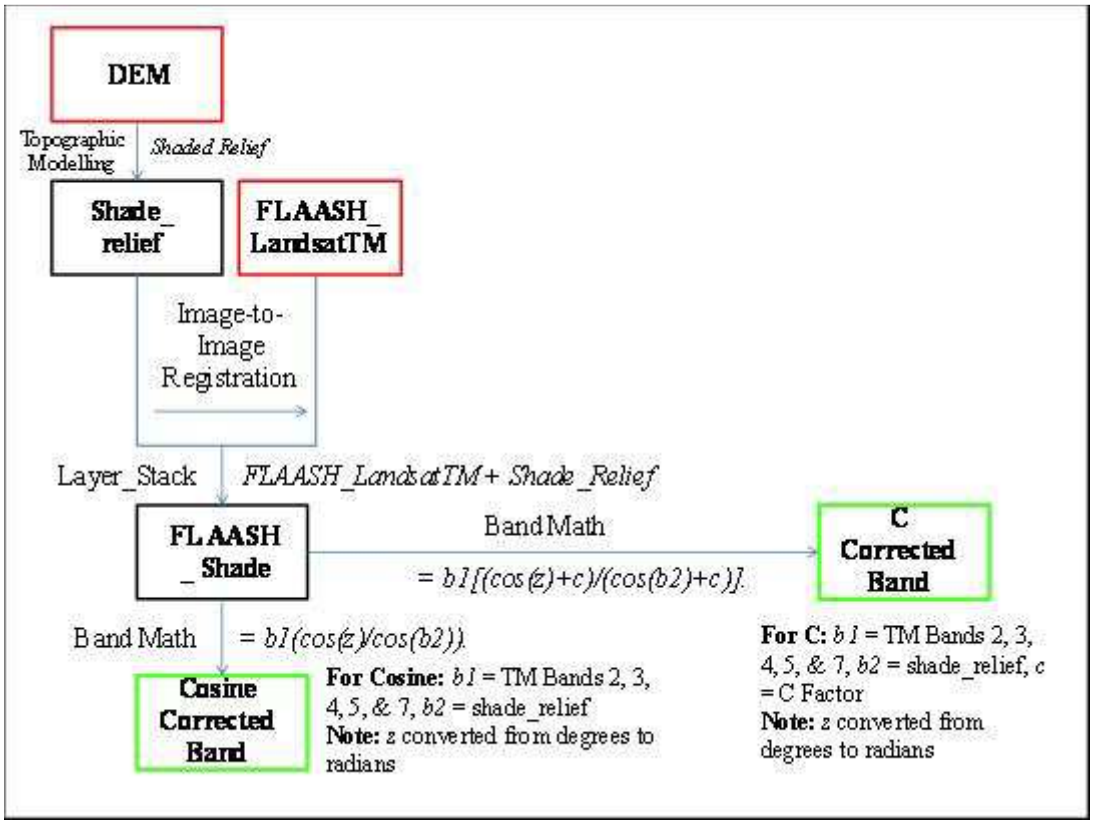

Figure 7: Schematic summarizing the processes performed for the Cosine Correction. This process was performed on each individual Landsat image. Red boxes show the original input images and green boxes show the final outputs.

In comparison to the *Cosine Correction* method, the *C Correction* method performed better statistically (showed greater mean values and lower standard deviations for bands) it was visible in the images that shaded regions had reduced. In comparison to values not topographically corrected however the *C Correction* did not make a great difference. This

could be due to the fact that points were not sampled in regions of particularly complex topography.

After applying the atmospheric and topographic corrections, each of the bands for each image were imported into *ArcGIS ArcMap* (ESRI, 2009) as separate TIFF images so that spectral indices (Table 4) could be calculated (Figure 8) (see Appendix B for example images for each of the indices).

Table 4: Formulas for spectral indices calculated, with TM2, TM3, TM4, TM5 and TM7 representing Landsat 5 TM bands 2, 3, 4, 5, and 7 respectively. The L Factor in SAVI and SATVI = 0.5 where soil conditions are unknown.

Spectral Index	Formula
Simple Ratio	TM4/TM3
NDVI	(TM4-TM3)/(TM4+TM3)
GNDVI	(TM4-TM2)/(TM4+TM2)
SAVI	[(1+L)(TM4-TM3)]/(T4+TM3+0.5)
SATVI	[(TM5-TM3)/(TM5+TM3+L)]*(1+L)-(TM7/2)
NDII(b5)	(TM4-TM5)/(TM4+TM5)
NDII(b7)	(TM4-TM7)/(TM4+TM7)

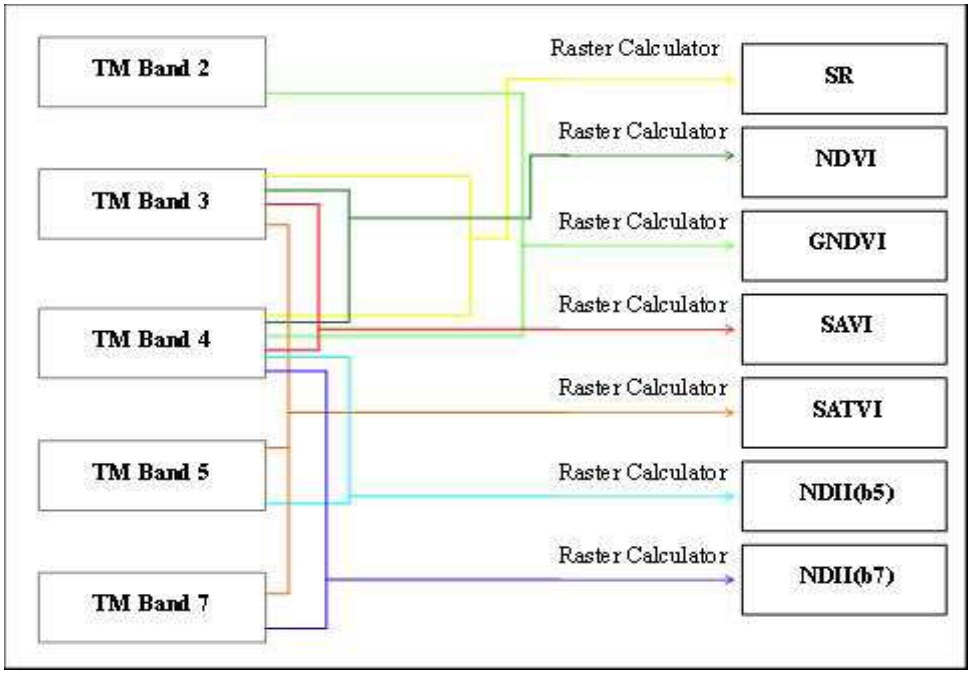

Figure 8: Schematic diagram of band data layers used to calculate indices in ArcMap. These processes were repeated for all images used. Note: Bands 1 (Blue) and 6 (Thermal IR) were not used to calculate any of the indices.

Finally spectral indices values were extracted from pixels in close spatial proximity to field plots (Figure 9).

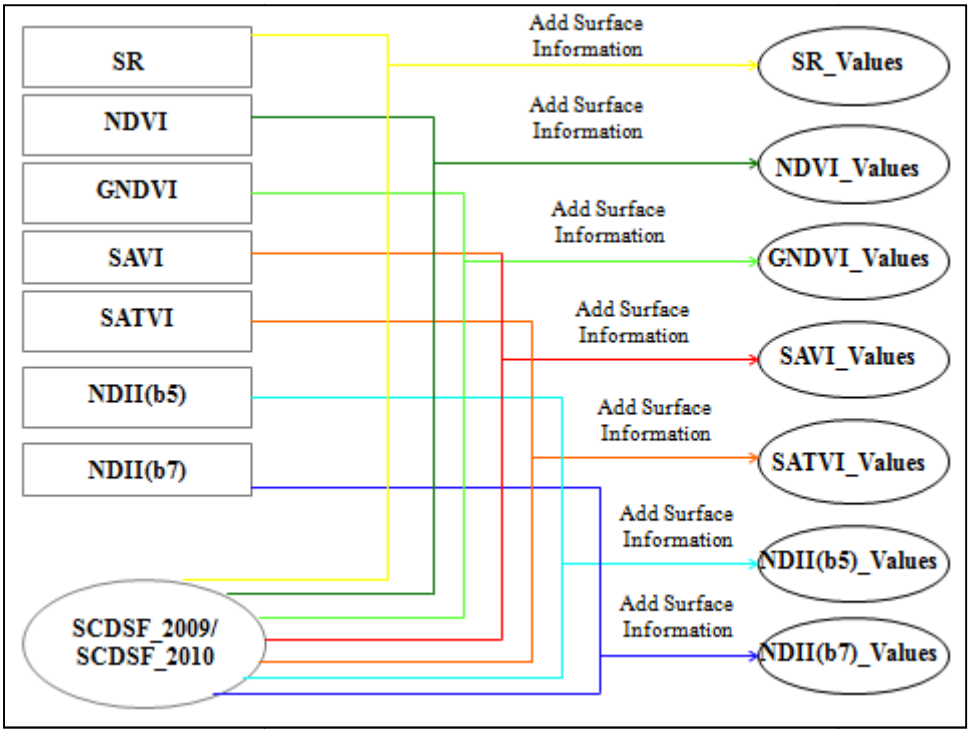

Figure 9: Schematic diagram of layers and tools used to extract pixel values from Spectral Indices. The values were extracted from the SI data sets to the attribute tables for the shapefiles. These processes were repeated for each of the Landsat images used.

4.4 Analysis approaches

The spectral indices values were regressed on fuel cover ground truth data. Two different sets of spectral indices values were prepared for the regression analysis using the following two approaches:

Approach 1:

Spectral indices values for GT data were extracted from Landsat 5 TM images acquired in close temporal proximity to field visits were used (Table 5).

Table 5: Summary showing which Landsat images the spectral indices values for GT data points were extracted from.

SiteLabel	GT Field Collection Date	Landsat Image Acquisition Date
PS005	20-Jul-09	21-Jul-09
PS009	03-Aug-09	21-Jul-09
PS010	06-Aug-09	28-Jul-09
PS015	24-Aug-09	21-Aug-09
PS019	24-Aug-09	21-Aug-09
PS020	25-Aug-09	21-Aug-09
PS021	25-Aug-09	21-Aug-09
PS023	25-Aug-09	21-Aug-09
PS024	31-Aug-09	21-Aug-09
PS025	31-Aug-09	21-Aug-09
PS026	31-Aug-09	21-Jul-09
PS028	31-Aug-09	05-Jul-09
PS029	01-Sep-09	21-Jul-09
PS031	07-Sep-09	23-Sep-09
PS033	07-Sep-09	23-Sep-09
PS037	30-Sep-09	23-Sep-09
PS038	30-Sep-09	23-Sep-09
PS045	14-Oct-09	23-Sep-09
PS046	14-Oct-09	23-Sep-09
PS050	22-Oct-09	10-Nov-09
PS051	22-Oct-09	10-Nov-09
PS056	28-Oct-09	10-Nov-09
PS057	04-Nov-09	10-Nov-09
PS078	17-Feb-10	18-Mar-10
PS079	17-Feb-10	18-Mar-10
PS080	18-Feb-10	18-Mar-10
PS081	18-Feb-10	18-Mar-10
PS082	25-Feb-10	18-Mar-10
PS083	25-Feb-10	18-Mar-10
PS099	09-Apr-10	18-Mar-10

This approach minimizes the possibility of disturbance events occurring between the GT collection date and the image collection date that may have changed the vegetation cover (Carreiras et al, 2006).

However, the disadvantage of relating variables which change at a slow rate, such as fuel cover in evergreen forests (Specht, 1972), with spectral indices acquired at different times of

the year is that the relationships are more influenced by phenology and seasonality patterns (Specht, 1972; Pook, 1984). For instance, changes in the spectral index value of a given pixel can be highly dynamic across the year due to variations in vegetation seasonal properties such as greenness (Specht, 1972; Ellis & Hatton, 2008), but its fuel cover value, in the absence of disturbance, generally remains the same (Specht, 1972; Pook, 1984; Boer et al, 2008). Preliminary tests found that spectral reflectance values for each site were either uniformly greater or lower in different seasons for greenness indices SR, NDVI, GNDVI and SAVI (see Appendix C). A second approach was used in this study to try and account for this.

Approach 2:

The second set of spectral indices was prepared trying to account for the effect of phenology and seasonality on remotely-sensed information (Specht, 1972; Ellis & Hatton, 2008; Smith et al, 2009). The normalization of the spectral indices values was achieved by using remotely sensed data acquired at the same time of the year. This approach allowed for comparison across sites at the same phenological state. Specifically, GT data collected in 2009 (ranging from July to November) were extracted from images collected on the same date (23 September 2009) and the data points collected in 2010 (ranging from February to April) were extracted from images captured on 10 September 2010.

Both sets of spectral indices were finally regressed on ground truth samples of fuel cover (canopy, elevated and near-surface cover) with the aims to:

1. Compare spectral indices performance in measuring fuel cover;
2. Analyse the effect on the relationships between spectral indices and fuel cover after adding understorey layers; and
3. Analysing the contribution of both live and dead fuel in the layers to the spectral signal.

4.5 Analysis of remotely sensed and GT fuel cover data

Relationships between spectral indices values and fuel cover were analysed by calculating R^2 values based upon linear ($y = mx + b$) or logarithmic ($y = mLn(x) + b$) relationships. The significance of each relationship was tested by calculating the F value of a one-way ANOVA.

Relationships between fuel cover layers and litter cover were tested to confirm that the upper layers were related to the litter and could therefore be used as surrogates for predicting surface fuel (Table 6).

Table 6: Summary of variables used to determine whether relationships existed between the forest layers and the surface fuel cover (percentage leaf litter). If the total for canopy + elevated + near-surface cover exceeded 100 percent, the amount was automatically rounded down to 100, as any cover amount over this was assumed to be accounted for by overlap of layers.

Fuel layer, x	y
Canopy	Litter
Elevated	Litter
Near-Surface	Litter
Elevated + Near-Surface	Litter
Canopy + Elevated	Litter
Canopy + Near-Surface	Litter
Canopy + Elevated + Near-Surface	Litter

To test the ability of spectral indices to measure fuel cover, R^2 values were calculated to show relationship strength between spectral indices values and fuel cover layers. Firstly indices were tested to see if they could measure individual layers (i.e. only canopy, only elevated or only near-surface cover). Secondly, indices were tested to determine if they measured fuel in a "cumulative" manner (i.e. canopy + elevated cover, and then canopy + elevated + near-surface cover) (Table 7), based upon the idea that the contribution of under-storey layers to the spectral signal of the upper layer is cumulative (e.g. Lu et al, 2003; Pisek et al, 2010).

The ability of spectral indices to predict fuel cover was also tested when only considering the live fuel components in the Elevated and Near-Surface layers. The canopy layer is assumed to contain predominantly all live fuel, but the elevated and near-surface layers both contain a portion of dead fuel. Knowing the percentage of dead fuel in each of the elevated and near-surface layers, this amount was subtracted from those layers so that only the amount of live fuel was taken into consideration (Table 8).

Table 7: Summary of relationships tested between spectral indices and forest layers using a standard regression method.

Spectral index, x	Fuel layer, y
SR, NDVI, GNDVI, SAVI, SATVI, NDIIb5, NDIIb7	Canopy
SR, NDVI, GNDVI, SAVI, SATVI, NDIIb5, NDIIb7	Elevated
SR, NDVI, GNDVI, SAVI, SATVI, NDIIb5, NDIIb7	Near-Surface
SR, NDVI, GNDVI, SAVI, SATVI, NDIIb5, NDIIb7	Canopy + Elevated
SR, NDVI, GNDVI, SAVI, SATVI, NDIIb5, NDIIb7	Canopy + Elevated + Near-Surface

Table 8: Summary of relationships tested between spectral indices and forest layers (live components only) using a standard regression method.

Spectral index, x	Forest layer, y
SR, NDVI, GNDVI, SAVI, SATVI, NDIIb5, NDIIb7	Elevated (Live)
SR, NDVI, GNDVI, SAVI, SATVI, NDIIb5, NDIIb7	Near-Surface (Live)
SR, NDVI, GNDVI, SAVI, SATVI, NDIIb5, NDIIb7	Canopy + Elevated (Live)
SR, NDVI, GNDVI, SAVI, SATVI, NDIIb5, NDIIb7	Canopy + Elevated (Live) + Near-Surface (Live)

Chapter 5: Results

5.1 Introduction

The following chapter summarises the results found in the current study. Firstly the results obtained for the relationships between fuel cover layers and litter cover are presented. Secondly results obtained from Approach 1 (phenological variation not accounted for) are presented. Thirdly, results obtained from Approach 2 (phenological variation accounted for) are presented. Scatter-plots for all relationships tested can be viewed in Appendix D.

5.2 Relationships between forest fuel cover layers and litter cover

The strength of relationships were tested between forest fuel cover layers (canopy, elevated and near-surface) and litter cover to confirm that upper forest layers are related to litter cover and, as a result, can be used as a surrogate to predict surface fuel. Results found that litter cover becomes more strongly related to fuel cover layers as they are progressively added (Table 9).

Table 9: The strength of relationships between forest fuel layers (canopy, elevated, near-surface, canopy + elevated, and canopy + elevated +near-surface) and litter cover.

y	Fuel cover, x	Pearson's *r* value
Litter	Canopy	0.35
Litter	Elevated	0.32
Litter	Near-Surface	0.5
Litter	Canopy + Elevated	0.66
Litter	Canopy + Elevated + Near-Surface	0.73

5.3 Results for Approach 1

The first set of spectral indices (obtained from Landsat images captured in close proximity to GT data collection dates) were tested in their ability to measure fuel layers (canopy, elevated and near-surface) taking into consideration both live and dead fuel components (Table 10 and Table 11).

Table 10: Relationships between spectral indices and separate forest fuel cover layers (canopy, elevated and near-surface). Results are based upon conducting analyses using both live and dead fuel components.

Spectral Indices	Canopy R_2	Significance (α=0.05)	Elevated R_2	Significance (α=0.05)	Near-Surface R_2	Significance (α=0.05)
SR	0	n/a	0.01	p > 0.05	0	n/a
NDVI	0	n/a	0	n/a	0	n/a
GNDVI	0	n/a	0	n/a	0	n/a
SAVI	0	n/a	0.01	p > 0.05	0	n/a
SATVI	0.02	p > 0.05	0.03	p > 0.05	0	n/a
NDIIb5	0.04	p > 0.05	0.13	p > 0.05	0	n/a
NDIIb7	0.04	p > 0.05	0.11	p > 0.05	0	n/a

Spectral indices were found to not be able to measure individual fuel cover layers, as all relationships were found to be non-significant (Table 10).

Table 11: Relationships between spectral indices and the accumulation of forest fuel cover layers (canopy + elevated, and canopy + elevated + near-surface). Results are based upon conducting analyses using both live and dead fuel components.

Spectral Indices	Canopy + Elevated R_2	Significance (α=0.05)	Canopy + Elevated + Near-Surface R_2	Significance (α=0.05)
SR	0.02	p > 0.05	0	n/a
NDVI	0.01	p > 0.05	0.01	p > 0.05
GNDVI	0	n/a	0	n/a
SAVI	0.01	p > 0.05	0.01	p > 0.05
SATVI	0	n/a	0	n/a
NDIIb5	0.32	p < 0.05	0.12	p > 0.05
NDIIb7	0.29	p < 0.05	0.11	p > 0.05

The moisture-sensitive spectral indices (NDIIb5 and NDIIb7) were found to be able to measure fuel loads after the addition of elevated cover to canopy cover. They could not however measure fuel after the addition of near-surface cover. The other five indices remained unable to measure fuel cover when understorey layers were added (Table 11).

In summary, all spectral indices showed an inability to measure canopy cover on its own (non-significant relationships). After the addition of elevated cover to canopy cover

however, indices NDIIb5 and NDIIb7 showed an ability to measure cover, while the other five indices remained ineffective. None of the indices showed an ability to measure fuel cover after the addition of near-surface cover (Figure 10).

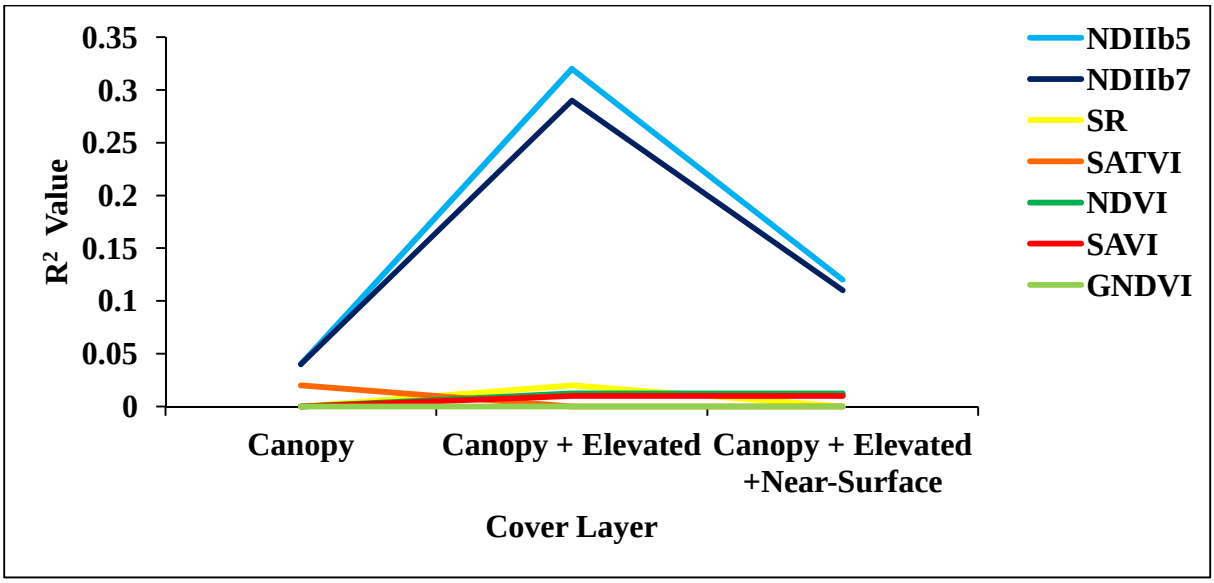

Figure 10: Change in R^2 value as forest layers are progressively added, using multiple Landsat images. The only significant R^2 values were obtained for NDIIb5 vs canopy + elevated ($p < 0.05$), and NDIIb7 vs canopy + elevated ($p < 0.05$).

The second part of Approach 1 summarises results obtained when dead fuel components were eliminated and only live fuel was considered. With the elimination of dead fuel, all spectral indices still showed an inability to predict individual fuel cover layers (Table 12).

Table 12: Relationships between spectral indices and fuel cover layers (elevated and near-surface). Results are based upon conducting analyses with the live fuel components only.

Spectral Index	Elevated R_2	Significance (α=0.05)	Near-Surface R_2	Significance (α=0.05)
SR	0.01	p > 0.05	0.03	p > 0.05
NDVI	0	n/a	0.01	p > 0.05
GNDVI	0	n/a	0	n/a
SAVI	0	n/a	0.01	p > 0.05
SATVI	0.01	p > 0.05	0	n/a
NDIIb5	0.15	p > 0.05	0.07	p > 0.05
NDIIb7	0.15	p > 0.05	0.04	p > 0.05

Spectral indices did not show a major improvement in their ability to measure the accumulation of fuel cover when dead fuel was eliminated (Table 13). Significant results

remained (p < 0.05) for moisture-sensitive indices (NDIIb5 and NDIIb7) *vs* canopy + elevated cover, but these results did not improve with the removal of dead fuel components from elevated and near-surface fuel cover layers (Table 13).

Table 13: Relationships between spectral indices and the accumulation of forest fuel cover layers (canopy + elevated, and canopy + elevated + near-surface). Results are based upon conducting analyses with live fuel components only.

Spectral Index	Canopy + Elevated R_2	Significance (α=0.05)	Canopy + Elevated + Near-SurfaceR_2	Significance (α=0.05)
SR	0.01	p > 0.05	0	n/a
NDVI	0.01	p > 0.05	0	n/a
GNDVI	0	n/a	0	n/a
SAVI	0.01	p > 0.05	0	n/a
SATVI	0	n/a	0	n/a
NDIIb5	0.3	p < 0.05	0.07	p > 0.05
NDIIb7	0.31	p < 0.05	0.08	p > 0.05

In summary, when only live fuel was considered the ability of the greenness and soil adjusted indices (SR, NDVI, GNDVI, SAVI and SATVI) to measure fuel remained low, even after the cumulative addition of elevated and near-surface layers to canopy cover (Figure 11). NDIIb5 and NDIIb7 showed a significant improvement in their ability to measure fuel after the addition of the elevated fuel cover layer, but this relationship declined after the addition of the near-surface fuel cover (Figure 11).

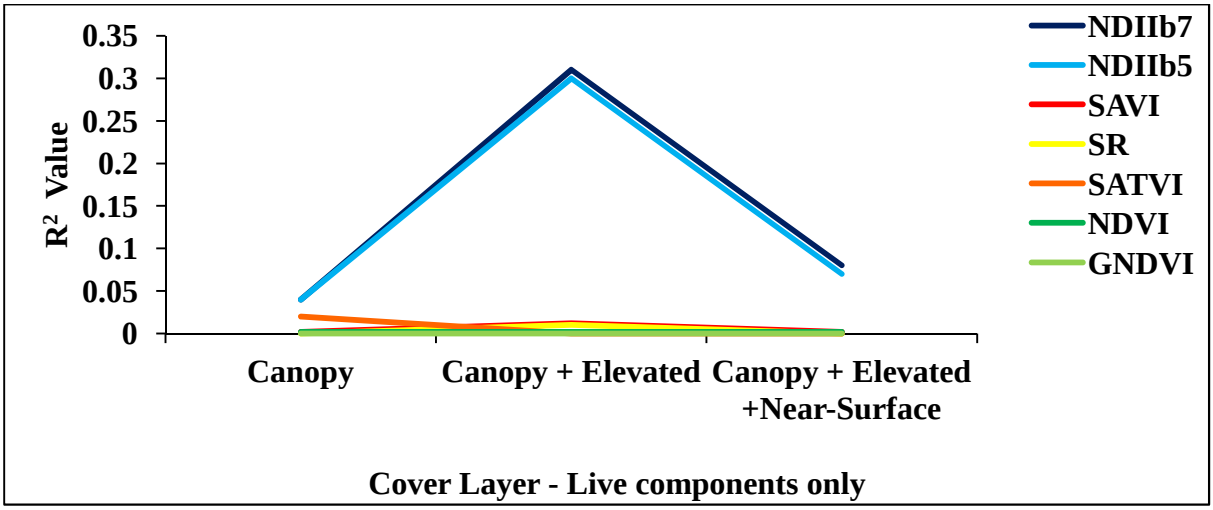

Figure 11: Change in R^2 value as forest layers are progressively added, only considering live fuel components. The only significant R^2 values were obtained for NDIIb7 vs canopy + elevated (p < 0.05) and NDIIb5 vs canopy + elevated (p < 0.05).

5.4 Results for Approach 2

When the second set of spectral indices (extracting spectral values for all GT data points from September images only i.e. all GT data points collected in 2009 were assigned spectral values from September 2009 images; all GT data points collected in 2010 were assigned spectral values from September 2010 images) were tested in their ability to measure fuel layers (canopy, elevated and near-surface) taking into consideration both live and dead fuel components. All indices showed the potential to measure canopy cover (all significant relationships, $p < 0.05$), but not for the elevated and near-surface cover layers (Table 14).

Table 14: Relationships between spectral indices and forest fuel cover layers (canopy, elevated and near-surface). Results are based upon conducting analyses using both live and dead fuel components.

Spectral Index	Canopy R_2	Significance (α=0.05)	Elevated R_2	Significance (α=0.05)	Near-Surface R_2	Significance (α=0.05)
SR	0.27	p < 0.05	0	n/a	0.01	p > 0.05
NDVI	0.22	p < 0.05	0	n/a	0.01	p > 0.05
GNDVI	0.23	p < 0.05	0	n/a	0.01	p > 0.05
SAVI	0.22	p < 0.05	0	n/a	0.01	p > 0.05
SATVI	0.18	p < 0.05	0.02	p > 0.05	0	n/a
NDIIb5	0.19	p < 0.05	0.04	p > 0.05	0	n/a
NDIIb7	0.19	p < 0.05	0.03	p > 0.05	0	n/a

All indices showed the potential to measure canopy cover with the addition of the elevated cover layer (all significant relationships, $p < 0.05$). After the addition of the near-surface cover layer however, this potential diminished (non-significant relationships, $p > 0.05$) (Table 15).

In summary, all indices showed the potential to measure canopy cover, with indices calculated from visible and NIR wavelengths (SR, NDVI, GNDVI and SAVI) showing slightly higher R^2 values than indices that incorporate SWIR wavelengths (SATVI, NDIIb5 and NDIIb7). However, after the addition of elevated cover, indices incorporating the SWIR wavelengths significantly increased in their ability to predict fuel. In contrast, the indices calculated from visible and NIR wavelengths showed a decline in potential or little change in their ability to measure fuel. The potential to measure fuel decreased for all indices after the addition of near-surface cover (Figure 12).

Table 15: Relationships between spectral indices and the accumulation of forest fuel cover layers (canopy + elevated, and canopy + elevated + near-surface). Results are based upon conducting analyses using both live and dead fuel components.

Spectral Index	Canopy + Elevated R_2	Significance (α=0.05)	Canopy + Elevated + Near-Surface R_2	Significance (α=0.05)
SR	0.16	$p < 0.05$	0.05	$p > 0.05$
NDVI	0.19	$p < 0.05$	0.05	$p > 0.05$
GNDVI	0.16	$p < 0.05$	0.04	$p > 0.05$
SAVI	0.19	$p < 0.05$	0.03	$p > 0.05$
SATVI	0.29	$p < 0.05$	0.09	$p > 0.05$
NDIIb5	0.36	$p < 0.05$	0.14	$p > 0.05$
NDIIb7	0.32	$p < 0.05$	0.12	$p > 0.05$

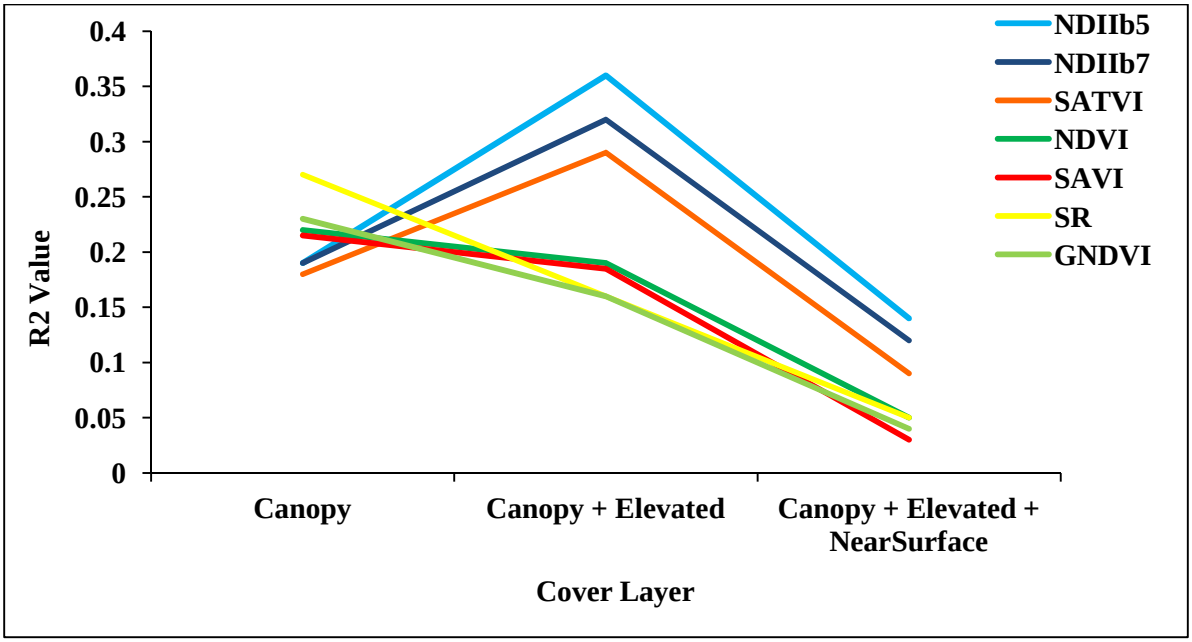

Figure 12: Change in R^2 value as fuel layers are progressively added, considering both live and dead fuel.

The second part of Approach 2 summarises results obtained when dead fuel components were eliminated and only live fuel was considered. With the elimination of dead fuel, all spectral indices still showed an inability to predict fuel cover for the elevated and near-surface cover layers when considered individually (Table 16).

Table 16: Relationships between spectral indices and fuel cover layers (elevated and near-surface). Results are based upon analyses using live fuel components only.

Spectral Indices	Elevated R_2	Significance (α=0.05)	Near-Surface R_2	Significance (α=0.05)
SR	0.01	p > 0.05	0.06	p > 0.05
NDVI	0.04	p > 0.05	0.07	p > 0.05
GNDVI	0.03	p > 0.05	0.08	p > 0.05
SAVI	0.04	p > 0.05	0.07	p > 0.05
SATVI	0.08	p > 0.05	0.05	p > 0.05
NDIIb5	0.09	p > 0.05	0.14	p > 0.05
NDIIb7	0.09	p > 0.05	0.1	p > 0.05

Spectral indices all showed a significant improvement in their potential to measure fuel after elevated cover was added to canopy cover (Table 17), in contrast to when dead fuel was incorporated and only NDIIb5, NDIIb7 and SATVI showed improvements (Table 15).

Table 17: Relationships between spectral indices and the accumulation of forest fuel cover layers (canopy + elevated, and canopy + elevated + near-surface). Results are based upon analyses using live fuel components only.

Spectral Indices	Canopy + Elevated R_2	Significance (α=0.05)	Canopy + Elevated + Near-SurfaceR_2	Significance (α=0.05)
SR	0.36	p < 0.05	0.08	p > 0.05
NDVI	0.37	p < 0.05	0.08	p > 0.05
GNDVI	0.34	p < 0.05	0.07	p > 0.05
SAVI	0.37	p < 0.05	0.08	p > 0.05
SATVI	0.44	p < 0.05	0.03	p > 0.05
NDIIb5	0.46	p < 0.05	0.08	p > 0.05
NDIIb7	0.46	p < 0.05	0.1	p > 0.05

In summary, when only considering live fuel components, all spectral indices showed a significant improvement in their ability to measure fuel cover, with NDIIb5, NDIIb7 and SWIR showing the greater improvement. All spectral indices declined in their ability to predict fuel after the addition of near-surface cover (Figure 13).

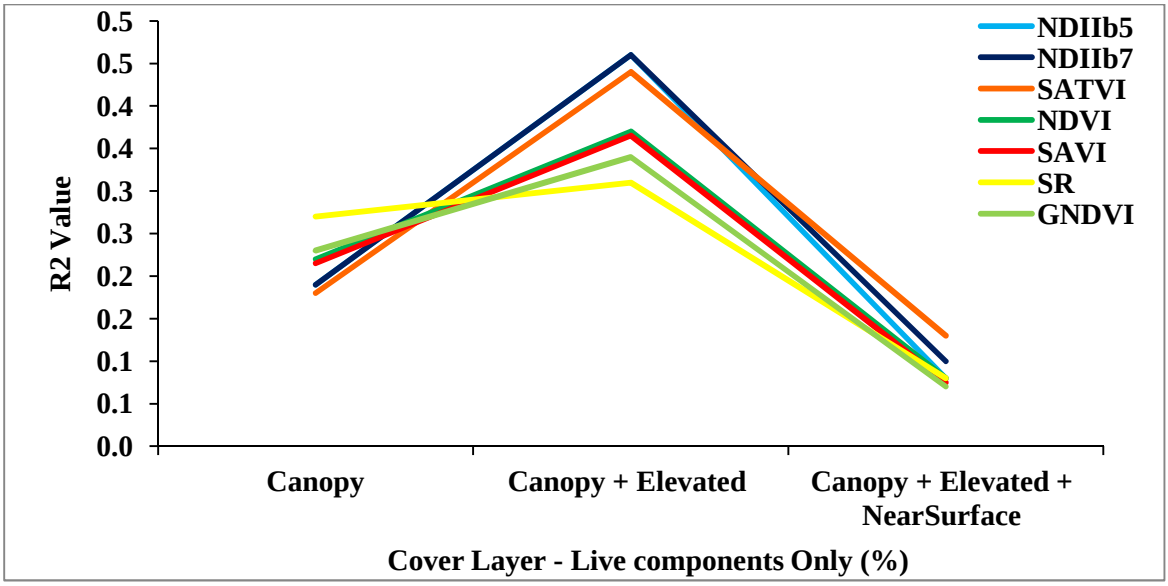

Figure 13: Change in R^2 value as forest layers are progressively added, only considering the live fuel components.

Chapter 6: Discussion

6.1 Introduction

The aims of this study were, firstly: to assess the ability of Landsat-derived spectral information for measuring fuel properties in Australian SCDS forest, secondly; to analyse the capability of Landsat-derived spectral indices to retrieve information about fuel properties of multiple forest layers, and thirdly; to explore the influence of live and dead fuel components on vegetation spectral response. For each of these aims, the effect of phenological variation on the spectral signal was also taken into consideration. The following chapter discusses the implications of the results obtained for each aim. As spectral indices behaved differently depending upon which set of spectral values was used (i.e. from Approach 1 or Approach 2), the following chapter will discuss results separately based upon the method they were obtained from. Limitations of the current study will also be discussed with recommendations for future research.

6.2 Synthesis of results: Approach 1

Approach 1 was designed so that Landsat images were accurately portraying the properties of the GT data, by extracting spectral information from images taken at the time closest to the date of collection of GT data points. Using this approach, there was a significant difference in the behaviour of spectral indices. Greenness indices (SR, NDVI, GNDVI, SAVI and SATVI) all showed no potential for measuring fuel cover, which does not support other previous research (e.g. Franklin et al, 1991; Lu et al, 2003; Carreiras et al, 2006; Staben & Evans, 2008; Smith et al, 2009; Jacobson, 2010). With the addition of the two understorey layers, elevated and near-surface cover, the relationships between greenness indices and fuel cover remained non-significant ($p < 0.05$) (Figure 10 and Figure 11). The elimination of dead fuel from the elevated and near-surface cover layers also did not change the results for greenness indices using this approach (Figure 11). In contrast however, moisture indices (NDIIb5 and NDIIb7) did show potential for measuring fuel. When only canopy cover was considered moisture indices showed non-significant relationships ($p < 0.05$). However, after the addition of elevated cover to canopy cover, their potential to measure fuel cover significantly increased (Figure 10). After the elimination of dead fuel in the elevated and

near-surface cover layers, the relationship between moisture indices and fuel cover did not improve (Figure 11). The addition of near-surface cover did not change the weak relationships between the five greenness indices and fuel cover, and caused relationships between moisture indices and fuel cover to weaken (Figure 10 and Figure 11).

The main implication found from the results of Approach 1 is that, when using data collected over multiple seasons (in this study's case, over 9 months), greenness indices will be affected by phenological effects (Chen et al, 2011). Moisture indices however, do not appear to be significantly affected by changes in phenology, supporting previous research conducted by Gond et al (1999) and De Beurs & Townsend (2008). Even though chlorophyll and moisture tend to be proportional to each other in many forests (i.e. healthy vegetation has high levels of both, unhealthy has low levels of both) chlorophyll content is not always proportional to moisture content (Ceccato et al, 2001). For example, Gond et al (1999) found that greenness in eucalypt leaves changed seasonally, whereas moisture content had less variation across seasons. These findings suggest that in forest-types with variable phenology, moisture indices could prove to be of more practical use, as they may not need to undergo normalization processes in order to accurately measure fuel cover, which could save time and reduce error. When using greenness indices in this particular forest type it is highly important to apply a phenological normalization factor to the spectral values in order to obtain accurate results.

6.3 Synthesis of results: Approach 2

Approach 2 was designed in an attempt to account for phenological variation. When spectral values for GT data points were extracted from images acquired in the same season (i.e. GT data points collected in 2009 had spectral values extracted from September 2009; GT data points collected in 2010 had spectral values extracted from September 2010), a greater number of relationships between spectral indices and cover variables began to be observed. Results found that all spectral indices showed potential for measuring canopy cover, with the indices calculated from visible and NIR wavelengths (SR, NDVI, GNDVI and SAVI) showing slightly stronger relationships with canopy cover than the other three indices that incorporated SWIR wavelengths (SATVI, NDIIb5 and NDIIb7). After the addition of elevated cover however, a clear split in strength of relationships could be seen between the

indices calculated from visible and NIR wavelengths, and indices that incorporate SWIR wavelengths (NDIIb5, NDIIb7 and SATVI) (Figure 12). In this case results appeared to imply that after the addition of elevated cover, the visible and NIR indices suffered from saturation, whereas the SWIR indices did not. These findings also support Jacobson (2010) who found that, after the addition of understorey cover layers of fuel to the canopy, NDMI (similar index to NDIIb5) performed better than NDVI at measuring the fuel cover.

The performance of indices however once again changed when dead fuel was eliminated from elevated and near-surface cover layers. When only live fuel was considered, the four visible and NIR indices also showed a strengthening in potential to measure fuel cover like the SWIR indices did, but SWIR indices still remained stronger (Figure 13). These findings show that indices calculated from visible and NIR wavelengths are highly dependent upon measuring live fuel properties and that dead fuel does not contribute to the signal for these wavelengths (Law & Waring, 1994; Li et al, 2012). These findings support previous research that has found that dead vegetation negatively affects the performance of greenness indices (Tucker, 1979; Marsett et al, 2006; Doktor et al, 2009). Results also imply that SWIR indices are better at measuring understorey layers, due to the ability of SWIR waves to penetrate further into the canopy, whereas visible wavelengths are absorbed by the top layer of the canopy (Gao, 1996; Sims & Gamon, 2003) limiting the measuring ability of indices calculated from these wavelengths in multiple-layered forests. Results also suggested that SWIR indices are less affected by the presence of dead fuel. In previous studies it has been found that the greatest change in spectral signal between live and senescent/damaged vegetation is observed in the NIR wavelengths (NIR reflectance greatly decreases for unhealthy vegetation), whereas SWIR wavelengths showed less of a change in signal (the reflectance of SWIR does increase for unhealthy vegetation, but always to a great extent) (Marsett et al, 2006) and damaged vegetation (Olsson et al, 2012). For example, the basis behind Marsett et al (2006) developing SATVI was that, in rangelands, the reflectance of SWIR wavelengths did not greatly change between healthy and dying grasses (unlike NIR reflectance), so an index could be developed using these wavelengths to measure both live and dead vegetation.

The main implication from Approach 2 is that, in SCDS Forests, when phenological effects are accounted for, all indices have the potential to be able to measure fuel cover. SWIR indices did appear to perform better in multi-layered forests and were less affected by the

presence of dead fuel. They could therefore be more useful for measuring fuel in both the canopy and understorey layers. As SWIR indices are less affected by the presence of dead fuel, they could potentially be more accurate in measuring fuel in SCDS forests where dead fuel is often present in multiple layers.

The main issue with Approach 2 however is that, while major disturbance events were unlikely to have occurred during the study period (i.e. fire events are accounted for), the GT data was not monitored to account for any unknown changes to cover. Future research should therefore monitor data collection sites if only one image is used for points collected over multiple months to provide more accuracy to the method.

For both approaches 1 and 2 the addition of the near-surface cover layer did not appear to be contributing to the spectral signal. This supports other previous studies that have found that remote sensors are limited in their ability to penetrate down to the near-surface layers (Law & Waring, 1994; Riano et al, 2003; Kuusk et al, 2004; Rollins et al, 2004; Rautianinen et al, 2007; Krasnow et al, 2009; Somers et al, 2010). This implies that Landsat cannot directly measure surface fuel, but can still measure higher levels (canopy and elevated cover) to predict future fuel loads. In SCDS forests the spectral signal is influenced by canopy trees and, to a significant level, understorey shrubs. In this particular forest type, researchers therefore have to account for the contribution of the understorey when using remote sensing to measure fuel cover.

6.4 Limitations of the current study

The current study provided an initial analysis of the potential of Landsat 5 TM to measure fuel cover in SCDS forests and in turn, how factors such as the understorey, dead fuel and phenology can affect the spectral signal. Future studies could improve on the current studies results in a few ways. Firstly, when data collected over multiple seasons is used together, phenological effects need to be normalized for greenness indices. By normalizing the data, future studies could also determine to what extent moisture indices are, or are not affected by phenological variation (i.e. if results can still be improved for these indices). If only one image is used to extract spectral values for all points then data sites need to be monitored to ensure changes in spectral value are only due to phenological variation and not any unknown disturbances. Secondly, larger data sets could be collected from all seasons to assess whether indices perform differently in their ability to measure fuel cover between different seasons.

Chapter 7: Conclusions

Based upon the findings of the current study, the following conclusions can be made:

1. Remote sensing shows the potential to measure fuel properties in Sydney Coastal Dry Sclerophyll Forests.
2. The elevated fuel cover layer does contribute to the spectral signal when the effects of phenology and the presence of dead fuel (for greenness indices) are accounted for. The near-surface fuel cover layer was not found to improve spectral indices abilities in measuring fuel cover, which suggests that the sensor cannot measure fuel down to this forest level.
3. The components of live and dead fuel do have an effect on the spectral signal, in particular for indices that are calculated from visible and NIR wavelengths. Indices that are calculated from SWIR wavelengths also showed a stronger relationship with fuel cover after the elimination of dead fuel when phenology was accounted for.
4. When comparing the seven indices, their performances varied between approaches 1 and 2:
    i. Greenness indices (SR, NDVI, GNDVI, SAVI and SATVI) were highly affected by phenological variation. When this factor was accounted for however they showed a great potential for measuring forest fuel. They performed best when only live fuel was considered.
    ii. Moisture indices (NDIIb5 and NDIIb7) appear to not be as affected by phenological or seasonal variation. They also appear to be able to penetrate further into the canopy, as relationships between the signal and cover became significantly stronger after elevated cover was added to canopy cover. They are also less affected by the presence of dead fuel, as their performance still improved with the addition of elevated cover to canopy cover, without elimination of the dead fuel component.
    iii. The performance of SATVI varied. It was highly affected by phenological effects in Approach 1 similar to the other indices greenness indices (due to its red wavelength band). However, when phenology was accounted for SATVI showed a similar pattern of performance to the moisture indices, where it was less affected by the presence of dead fuel (due to its SWIR wavelength bands).

7.1 Recommendations:

Bushfire managers that use remote sensing to predict fuel in SCDS forests need to account for the contribution of understorey and both live and dead fuel to the spectral signal. The findings of the current study imply that greater spectral index values suggest greater fuel cover, therefore Landsat images can be used to try and predict where the greatest loads of future fuel will occur. Moisture indices could prove to be more accurate at measuring fuel in this particular forest type than traditional greenness indices, because they are less affected by variations caused by phenology and disturbance events. If greenness indices are used, the data needs to be normalized, or alternatively, researchers could analyse data from different seasons separately. Using one set of spectral values from one image for all the GT data may rule out phenological variation and save time when it comes to the processing of data, but sites need to be monitored to ensure no unknown changes in vegetation cover occur between the GT collection date and the Landsat image acquisition date. Due to their SWIR wavelengths, moisture indices may be able to penetrate deeper into the forest layers, so should prove to be more effective at measuring multiple layers of fuel. With these factors considered future research could also study the effectiveness of alternative indices, such as SATVI, in their ability to measure dead fuel. When phenological variation was accounted for, SATVI showed potential for measuring fuel in a multiple-layered forest that contains dead fuel in the layers. Future research could test this index or develop one based upon similar principles that suits Australian vegetation better.

In summary, all spectral indices performed well at predicting fuel cover, but moisture indices could be more suited to SCDS forests. They are less affected by phenological variation and have a greater ability to measure fuel in the understorey, which for forests containing multiple layers of fuel would provide a more accurate estimate of future fuel loads. Moisture indices are also not as greatly hindered by the presence of dead fuel and do not suffer from saturation from measuring multiple layers to the extent that greenness indices do. Moisture indices could therefore prove to be the best measurement option at predicting future fuel loads in Australian multi-layered forests to prevent bush fire events.

References

Ahl, D. E., Gower, S. T., Burrows, S. N., Shabanov, N. V., Myneni, R. B. & Knyazikhin, Y. 2006. Monitoring spring canopy phenology of a deciduous broadleaf forest using MODIS. *Remote Sensing of Environment* **104**, 88-95.

Avitabile, V., Baccini, A., Friedl, M. A. & Schmullius, C. 2012. Capabilities and limitations of Landsat and land cover data for aboveground woody biomass estimation of Uganda. *Remote Sensing of Environment* **117**, 366-380.

Barati, S., Rayegani, B., Saati, M., Sharifi, A. & Nasri, M. 2011. Comparison the accuracies of different spectral indices for estimation of vegetation cover fraction in sparse vegetated areas. *The Egyptian Journal of Remote Sensing and Space Sciences* **14**, 49 -56.

Bi, H., Long, Y., Turner, J., Lei, Y., Snowdon, P., Li, Y., Harper, R., Zerihun, A. & Ximenes, F. 2010. Additive prediction of aboveground biomass for *Pinus radiata* (D. Don) plantations. *Forest Ecology and Management* **259**, 2301-2314.

Birth, G.S. & McVey, G.R. 1968. Measuring the colour of growing turf with a reflectance spectrophotometer. *Agronomy Journal* **60**, 640–643.

Boer, M. M., Macfarlane, C., Norris, J., Sadler, R. J., Wallace, J. & Grierson, P F. 2008. Mapping burned areas and burn severity patterns in SW Australian eucalypt forest using remotely-sensed changes in leaf area index. *Remote Sensing of Environment* **112**, 4358–4369.

Boggs, G. S. 2010. Assessment of SPOT 5 and QuickBird remotely sensed imagery for mapping tree cover in savannas. *International Journal of Applied Earth Observation and Geoinformation* **12**, 217–224.

Bureau of Meteorology 2012. 'Climate Data Online.' accessed 30/08/2012, http://www.bom.gov.au/climate/data/

Bond, W. J. & Midgley, G. F. 2012. Carbon Dioxide and the uneasy interactions of trees and savannah grasses. *Philosophical Transactions of the Royal Society* **367**, 601-612.

Bradstock, R. A., & Gill, A. M. 2001. Living with fire and biodiversity at the urban edge: in search of sustainable solution to the human protection problem in southern Australia. *Journal of Mediterranean Ecology* **2**, 179–195.

Bradstock R. A. 2010. A biogeographic model of fire regimes in Australia: current and future implications. *Global Ecology and Biogeography* **19**, 145-158.

Bradstock, R. A., Hammill, K. A., Collins, L. & Price, O. 2010. Effects of weather, fuel and terrain on fire severity in topographically diverse landscapes of south-eastern Australia. *Landscape Ecology* **25**, 607-619.

Brandis, K. & Jacobson, C. 2003. Estimation of vegetative fuel loads using Landsat TM imagery in New South Wales, Australia. *International Journal of Wildland Fire* **12**, 185-194.

Brown, C. D. & Johnstone, J. F. 2012. Once burned, twice shy: repeat fires reduce seed availability and alter substrate constraints on *Picea mariana* regeneration. *Forest Ecology and Management* **266**, 34–41.

Caccamo, G., Chisholm, L. A., Bradstock, R. A. & Puotinen, M. L. 2011. Assessing the sensitivity of MODIS to monitor drought in high biomass ecosystems. *Remote Sensing of Environment* **115**, 2626–2639.

Caccamo, G., Chisholm, L. A., Bradstock, R. A., Puotinen, M. L. & Pippen, B. G. 2012. Monitoring live fuel moisture content of heathland, shrubland and sclerophyll forest in south-eastern Australia using MODIS data. *International Journal of Wildland Fire* **21**(3), 257-269.

Carreiras, J. M. B., Pereira, J. M. C., Pereira, J. S. 2006. Estimation of tree canopy cover in evergreen oak woodlands using remote sensing. *Forest Ecology and Management* **223**, 45–53.

Ceccato, P., Flasse, S., Tarantola, S., Jacquemoud, S., & Gregoire, J. M. 2001. Detecting vegetation leaf water content using reflectance in the optical domain. *Remote Sensing of Environment* **77**, 22–33.

Chafer, C. J., Noonan, M. & Macnaught, E. 2004. The post-fire measurements of fire severity and intensity in the Christmas 2001 Sydney wildfires. *International Journal of Wildland Fire* **13**, 227-240.

Chen, F., Weber, K. T., Anderson, J. & Gokhal, B. 2011. Assessing the susceptibility of semiarid rangelands to wildfires using Terra MODIS and Landsat Thematic Mapper data. *International Journal of Wildland Fire* **20**, 690–701.

Chopping, M., Schaaf, C. B., Zhao, F., Wang, Z., Nolin, A. W., Moisen, G. G., Martonchik, J. V. & Bull, M. 2011. Forest structure and aboveground biomass in the southwestern United States from MODIS and MISR. *Remote Sensing of Environment* **115**, 2943-2953.

Conroy, R. 1998. *Fuel assessment guide for the Sydney region*. Available from the NSW National Parks and Wildlife Service, Sydney.

Coops, N., Delahaye, A. & Pook, E. 1997. Estimation of Eucalypt Forest Leaf Area Indexon the South Coast of New South Wales using Landsat MSS Data. *Australian Journal of Botany* **45**, 757-769.

CSIRO 2011. 'Bushfire in Australia.' accessed 02/10/2012, http://www.csiro.au/Organisation-Structure/Divisions/EcosystemSciences/BushfireInAustralia.aspx

Datt B. 1999. Remote sensing of water content in eucalyptus leaves. *Australian Journal of Botany* **47**, 909–923.

De Beurs, K. M. & Townsend, P. A. 2008. Estimating the effect of gypsy moth defoliation using MODIS. *Remote Sensing of Environment* **112**, 3983–3990.

Díaz-Delgado, R., Lloret, F. & Pons, X. 2003. Influence of fire severity on plant regeneration by means of remote sensing imagery. *International Journal of Remote Sensing* **24**(8), 1751-1763.

Doktor, D., Bondeau, A., Koslowski, D. & Badeck, F.-W. 2009. Influence of heterogeneous landscapes on computed green-up dates based on daily AVHRR NDVI observations. *Remote Sensing of Environment* **113**, 2618–2632.

Ellis, T. W. & Hatton, T. J. 2008. Relating leaf area index of natural eucalypt vegetation to climate variables in southern Australia. *Agricultural Water Management* **95**, 743-747.

Escuin, S., Navarro, R. & Fernández P. 2008. Fire severity assessment by using NBR (Normalized Burn Ratio) and NDVI (Normalized Difference Vegetation Index) derived from LANDSAT TM/ETM images. *International Journal of Remote Sensing* **29**(4), 1053-1073.

Exelis Visual Information Solutions 2009. *Atmospheric Correction Module: QUAC and FLAASH User's Guide.* Exelis Visual Information Solutions, Boulder, Colorado. Accessed 04/06/2012, http://www.exelisvis.com/portals/0/pdfs/envi/Flaash_Module.pdf

Fatoyinbo, T. E. & Armstrong, A. H. 2010. Remote characterization of biomass measurements: case study of Mangrove forests. Biomass. In: 'Biomass'. (Ed. M. Momba & F. Bux.). Available from *InTech*, accessed 03/04/2012, http://www.intechopen.com/books/biomass/remote-characterization-of-biomass measurements-case-study-of-mangrove-forests

Feldpausch, T.R., Banin, Phillips, O. L., Baker, T. R., Lewis, S. L., Quesada, C.A., Affum -Baffoe, K., Arets, E. J. M. M., Berry, N. J., Bird, M., Brondizio, E. S., de Camargo, P., Chave, J., Djagbletey, G., Domingues, T. F., Drescher, M., Fearnside, P. M.,

França, M B., Fyllas, N. M., Lopez-Gonzalez, G., Hladik, A., Higuchi, N., Hunter, M. O., Iida, Y., Salim, K. A., Kassim, A. R., Keller, M., Kemp, J., King, D. A., Lovett, J. C., Marimon, B. S., Marimon-Junior, B. H., Lenza, E., Marshall, A. R., Metcalfe, D. J., Mitchard, E. T. A., Moran, E. F., Nelson, B. W., Nilus, R., Nogueira, E. M., Palace, M., Patiño, S., Peh, K. S.-H., Raventos, M. T., Reitsma, J. M., Saiz, G., Schrodt, F., Sonké, B., Taedoumg, H. E., Tan, S., White, L., Wöll, H. & Lloyd, J.0 2011. Height-diameter allometry of tropical forest trees. *Biogeosciences* **8**, 1081 1106.

Foody, G. M., Boyd, D. S. & Cutler, M. E. J. 2003. Predictive relations of tropical forest biomass from Landsat TM data and their transferability between regions. *Remote Sensing of Environment* **85**, 463-474.

Forzieri, G. 2012. Satellite retrieval of woody biomass for energetic reuse of riparian vegetation. *Biomass and Bioenergy* **36**, 432-438.

Franklin, J., Davis, F. W. & Lefebre, P. 1991. Thematic Mapper analysis of tree cover in semiarid woodlands using a model of canopy shadowing. *Remote Sensing of Environment* **36**, 189-202.

Frokling, S., Palace, M. W., Clark, D. B., Chambers, J. Q., Shugart, H. H. & Hurtt, G. C. 2009. Forest disturbance and recovery: A general review in the context of spaceborne remote sensing of impacts on aboveground biomass and canopy structure. *Journal of Geophysical Research* **114**, G00E02, doi:10.1029/2008JG000911.

Gao, B. 1996. NDWI – A Normalized Difference Water Index for remote sensing of vegetation liquid water from space. *Remote Sensing of Environment* **58**(3), 257-266.

Gill, M. & McCarthy, M. A. 1998. Intervals between prescribed fires in Australia: what intrinsic variation should apply? *Biological Conservation* **85**, 161-169.

Gitelson, A. A., Kaufman, Y. J. & Merzlyak, M. N. 1996. Use of a green channel in remote sensing of global vegetation from EOS-MODIS. *Remote Sensing of Environment* **58**, 289-298.

Gond, V., De Pury, D. G. G., Veroustraete, F. & Reinhart, C. 1999. Seasonal variations inleaf area index, leaf chlorophyll, and water content; scaling-up to estimate fAPAR and carbon balance in a multilayer, multispecies temperate forest. *Tree Physiology* **19**, 673-679.

Good, N. M., Paterson, M., Brack, C. & Mengersen, K. 2001. Estimating tree component biomass using variable probability sampling methods. *Journal of Agricultural, Biological, and Environmental Statistics* **6**(2), 258-267.

Gould J. S., McCaw W. L., Cheney N. P., Ellis P. F., Knight I. K. & Sullivan A. L. 2007. *Project Vesta. Fire in Dry Eucalypt Forest: Fuel Structure, Fuel Dynamics and Fire Behaviour*. Ensis-CSIRO, Canberra, and WA Department of Environment and Conservation, Perth.

Gould, J. S., McCaw, W. L. & Cheney, N. P. 2011. Quantifying fine fuel dynamics and structure in dry eucalypt forest (*Eucalyptus marginata*) in Western Australia for fire management. *Forest Ecology and Management* **262**, 531–546.

Guanter, L., Richter, R. & Kaufmann, H. 2009. On the application of the MODTRAN4 atmospheric radiative transfer code to optical remote sensing. *International Journal of Remote Sensing* **30**(6), 1407–1424.

Hammill, K. A. & Bradstock, R. A. 2006. Remote sensing of fire severity in the Blue Mountains: influence of vegetation type and inferring fire intensity. *International Journal of Wildland Fire* **15**, 213-226.

Hansen, M. C., Stehman, S. V., Potapov, P. V., Loveland, T. R., Townshend, J. R. G., DeFries, R. S., Pittman, K. W., Arunarwati, B., Stolle, F., Steininger, M. K., Carroll, M. & DiMiceli, C. 2008. Humid tropical forest clearing from 2000 to 2005quantified by using multitemporal and multiresolution remotely sensed data. *Proceedings of the National Academy of Sciences of the United State of America* **105**(27), 9439-9444.

Huete, A. R. 1988. A soil-adjusted vegetation index (SAVI). *Remote Sensing of Environment* **25**, 295–309.

Hunt, E. R. & Rock, B. N. 1989. Detection of changes in leaf water content using near- and middle-infrared reflectances. *Remote Sensing of Environment* **30**, 43-54.

Jackson, R. D. & Huete, A. R. 1991. Interpreting vegetation indices. *Preventive Veterinary Medicine* **11**, 185-200.

Jacobson, C. R. 2010. Use of linguistic estimates and vegetation indices to assess post-fire vegetation regrowth in woodland areas. *International Journal of Wildland Fire* **19**, 94-103.

Jensen, J. R. 2007. *Remote sensing of the environment: an earth resource perspective*. (2nd edition). Pearson Prentice Hall, Upper Saddle River, NJ.

Kasawani, I., Norsaliza, U. & Mohd Hasmadi, I. 2010. Analysis of spectral vegetation indices related to soil-line for mapping mangrove forests using satellite imagery. *Applied Remote Sensing Journal* **1**(1), 25-31.

Keith, D. 2004. *Ocean shores to desert dunes: the native vegetation of New South Wales and the ACT*. The Department of Environment and Conservation, Hurstville, NSW.

Keith, D. A., Holman, L., Rodoreda, S., Lemmon, J. & Bedward, M. 2007. Plant functional types can predict decade-scale changes in fire-prone vegetation. *Journal of Ecology* **95**(6), 1324-1337.

King, K. J., de Ligt, R. M. & Cary, G. J. 2011. Fire and carbon dynamics under climate change in south-eastern Australia: insights from FullCAM and FIRESCAPE modeling. *International Journal of Wildland Fire* **20**, 563-577.

Krasnow, K., Schoennagel, T. & Veblen, T. T. 2009. Forest fuel mapping and evaluation of LANDFIRE fuel maps in Boulder County, Colorado, USA. *Forest Ecology and Management* **257**, 1603-1612.

Kuusk, A., Lang, M. & Nilson, T. 2004. Simulation of the reflectance of ground vegetation in sub-boreal forests. *Agricultural and Forest Meteorology* **126**, 33–46.

Lamont, B. B., Enright, N. J. & He, T. 2011. Fitness and evolution of resprouters in relation to fire. *Plant Ecology* 212, 1945-1957.

Law, B. E. & Waring, R. H. 1994. Remote sensing of Leaf Area Index and radiation intercepted by understory vegetation. *Ecological Applications* **4**(2), 272-279.

Le Maire, G., Marsden, C., Nouvellon, Y., Grinand, C., Hakamada, R., Stape, J. & Laclau, J. 2011. MODIS NDVI time-series allow the monitoring of *Eucalyptus* plantation biomass. *Remote Sensing of Environment* **115**, 2613-2625.

Lentile, L. B., Holden, Z. A., Smith, A. M. S., Falkowski, M. J., Hudak, A. T., Morgan, P., Lewis, S. A., Gessler, P. E. & Benson, N. C. 2006. Remote sensing techniques to assess active fire characteristics and post-fire effects. *International Journal of Wildland Fire* **15**, 319-345.

Li, X., Wang, H., Long, H., Wei, D. & Bao, Y. 2012. A model for the estimation of fractional vegetation cover based on the relationship between vegetation and soil moisture. *International Journal of Remote Sensing* **33**(11), 3580–3595.

Lu, H., Raupach, M. R., McVicar, T. R. & Barrett, D. J. 2003. Decomposition of vegetation cover into woody and herbaceous components using AVHRR NDVI time series. *Remote Sensing of Environment* **86**, 1-18.

Lucas, R. M., Cronin, N., Moghaddam, M., Lee, A., Armston, J., Bunting, P. & Witte, C. 2006. Integration of radar and Landsat-derived foliage projected cover for woody regrowth mapping, Queensland, Australia. *Remote Sensing of Environment* **100**, 388 406.

Marsett, R. C., Qi, J., Heilman, P., Biedenbender, S. H., Watson, M. C., Amer, S., Weltz, M., Goodrich, D. & Marsett, R. 2006. Remote Sensing for grassland management in the arid southwest. *Rangeland Ecology and Management* **59**(5), 530-540.

McCaw, W. L., Gould, J. S., Cheney, N. P., Ellis, P. F. M. & Anderson, W.R. 2012. Changes in behaviour of fire in dry eucalypt forest as fuel increases with age. *Forest Ecology and Management* **271**, 170–181.

McElhinny, C., Gibbons, P., Brack, C. & Bauhus, J. 2005. Forest and woodland stand structural complexity: its definition and measurement. *Forest Ecology and Management* **218**, 1-24.

Miller, J. D. & Yool, S. R. 2002. Mapping forest post-fire canopy consumption in several overstory types using multi-temporal Landsat TM and ETM data. *Remote Sensing of Environment* **82**, 481-496.

Morris, R. 2007. *Fuel sampling. Central Coast district fuel sampling manual 2/1997*. New South Wales National Parks and Wildlife Service, Sydney.

Moses, W. J., Gitelson, A. A., Perk, R. L., Gurlin, D., Rundquist, D. C., Leavitt, B. C., Barrow, T. M. & Brakhage, P. 2012. Estimation of chlorophyll-*a* concentration in turbid productive waters using airborne hyperspectral data. *Water Research* **46**, 993 1004.

New South Wales Government: Environment and Heritage 2011. *The Sydney Basin Bioregion*. accessed 14/09/2012, http://www.environment.nsw.gov.au/resources/nature/sydneyBasin.pdf

Noone, M. D., Sader, S. A. & Legaard, K. R. 2012. Are forest disturbance rates composition influenced by changing ownerships, conservation easements, and land certification? *Forest Science* **58**(2), 119-129.

Olson, J. S. 1963. Energy storage and the balance of producers and decomposers in ecological systems. *Ecology* **44**(2), 322-331.

Olsson, P., Jönsson, A. M. & Eklundh, L. 2012. A new invasive insect in Sweden - *Physokermes inopinatus*: tracing forest damage with satellite based remote sensing. *Forest Ecology and Management* **285**, 29-37.

Pisek, J., Chen, J. M., Alikas, K. & Deng., F. 2010. Impacts of including forest understory brightness and foliage clumping information from multiangular measurements on leaf area index mapping over North America. *Journal of Geophysical Research* **115**, G03023, doi:10.1029/2009JG001138.

Pook, E. W. 1984. Canopy dynamics of *Eucalyptus maculata* Hook. II. Canopy leaf area balance. *Australian Journal of Botany* **32,** 405-13.

Rautiainen, M., Suomalainen, J., Mõttus, M., Stenberg, P., Voipio, P., Peltoniemi, J. & Manninen, T. 2007. Coupling forest canopy and understory reflectance in the Arctic latitudes of Finland. *Remote Sensing of Environment* **110**, 332-343.

Reeves, M. C., Ryan, K. C., Rollins, M. G. & Thompson, T. G. 2009. Spatial fuel data products of the LANDFIRE Project. *International Journal of Wildland Fire* **18**, 250 267.

Resasco, J., Hale, A. N., Henry, M. C. & Gorchov, D. L. 2007. Detecting an invasive shrub in a deciduous forest understory using late-fall Landsat sensor imagery. *International Journal of Remote Sensing* **28**(16), 3739-3745.

Riaño, D., Chuvieco, E., Salas, J. & Aguado, I. 2003. Assessment of different topographic corrections in Landsat-TM data for mapping vegetation types. *IEEE Transactions on Geoscience and Remote Sensing* **41**(5), 1056-1061.

Rollins, M. G., Keane, R. E. & Parsons, R. A. 2004. Mapping fuels and fire regimes using remote sensing, ecosystem simulation, and gradient modeling. *Ecological Applications* **14**(1), 75-95.

Rouse, J. W., Haas, R. W., Schell, J. A., Deering, D. W. & Harlan, J.C. 1974. *Monitoring the vernal advancement and retrogradation (greenwave effect) of natural vegetation*. NASA/GSFCT Type III Final Report, Greenbelt, MD,USA.

Ryan, C. M. & Williams, M. 2011. How does fire intensity and frequency affect miombo woodland tree populations and biomass? *Ecological Applications* **21**(1), 48–60.

Scarth, P. & Phinn, S. 2000. Determining forest structural attributes using an inverted Geometric-Optical Model in mixed Eucalypt forests, Southeast Queensland, Australia. *Remote Sensing of Environment* **71**, 141-157.

Scottish Government 2009. *Assessing the Extent and Severity of Erosion on the Upland Organic Soils of Scotland using Earth Observation: A GIFTSS Implementation Test*. accessed 14/09/2012, http://www.scotland.gov.uk/Publications/2009/11/06110108/0

Sims, D. A. & Gamon, J. A. 2003. Estimation of vegetation water content and photosynthetic tissue area from spectral reflectance: a comparison of indices based on liquid water and chlorophyll absorption features. *Remote Sensing of Environment* **84**, 526-537.

Smith, A. M. S., Falkowski, M. J., Hudak, A. T., Evans, J. S., Robinson, A. P. & Steele, C. M. 2009. A cross-comparison of field, spectral, and lidar estimates of forest canopy cover. *Canadian Journal of Remote Sensing* **35**(5), 447-459.

Somers, B., Verbesselt, J., Ampe, E. M., Sims, N., Verstraeten, W. W. & Coppin, P. 2010. Spectral mixture analysis to monitor defoliation in mixed-aged *Eucalyptus globules* Labill plantations in southern Australia using Landsat 5-TM and EO-1 Hyperion data. *International Journal of Applied Earth Observation and Geoinformation* **12**, 270 277.

Specht, R. L. 1972. Water use by perennial evergreen plant communities in Australia and Papua New Guinea. *Australian Journal of Botany* **20**, 273-299.

Sprintin, M., Karnieli, A., Sprintin, S., Cohen, S. & Berliner, P. 2009. Relationships between stand density, and canopy structure in a dryland forest as estimated by ground-based measurements and multi-spectral spaceborne images. *Journal of Arid Environments* **73**, 955-962.

Staben, G. & Evans, K. 2008. Estimates of tree canopy loss as a result of Cyclone Monica, in the Magela Creek catchment northern Australia. *Austral Ecology* **33**, 562-569.

Suganuma, H., Abe, Y., Taniguchi, M., Tanouchi, H., Utsugi, H., Kojima, T. & Yamada, K. 2006. Stand biomass estimation method by canopy coverage for application to remote sensing in an arid area of Western Australia. *Forest Ecology and Management* **222**, 75-87.

Taylor, G. 1970. *Sydneyside Scenery*. Angus & Robertson, Sydney, NSW.

Teillet, P.M., Guindon, B. & Goodenough, D.G. 1982. On the slope-aspect correction of multispectral scanner data. *Canadian Journal of Remote Sensing* **8**, 84-106.

Tucker, C. J. 1979. Red and photographic infrared linear combinations for monitoring vegetation. *Remote Sensing of Environment* 8, 127-150.

United States Geological Survey: Earth Explorer (2012). accessed 04/06/2012, http://earthexplorer.usgs.gov/

Vicente-Serrano, S. M., Pérez-Cabello, F. & Lasanta, T. 2008. Assessment of radiometric correction techniques in analyzing vegetation variability and change using time series of Landsat images. *Remote Sensing of Environment* **112**, 3916–3934.

Viedma, O., Meliá, J., Segarra, D. & García-Haro, J. 1997. Modeling rates of ecosystem recovery after fires by using Landsat TM data. *Remote Sensing of Environment* **61**(3), 383-398.

Vivian, L. M., Cary, G. J., Bradstock, R. A. & Gill, A. M. 2008. Influence of fire severity on the regeneration, recruitment and distribution of eucalypts in the Cotter River Catchment, Australian Capital Territory. *Austral Ecology* **33**, 55-67.

Watson, P., Penman, S. & Horsey, B. 2012. *Data from the UoW fuel hazard study, by vegetation type and time-since-fire*. Centre for Environmental Risk Management of Bushfires, University of Wollongong (UoW).

Williams, O. B. 1970. Population dynamics of two perennial grasses in Australian semi-arid grassland. *Journal of Ecology* **58**(3), 869-875.

Williams, R. J., Bradstock, R. A., Cary, G. J., Enright, N. J., Gill, A. M., Liedloff, A. C., Lucas, C., Whelan, R. J., Anderson, A. N., Bowman, D. M. J. S., Clarke, P. J., Cook, G D., Hennessy, K. J. & York, A. 2009. *Interactions between climate change, fire regimes and biodiversity in Australia – a preliminary assessment*. Report to the Department of Climate Change and Department of the Environment, Water, Heritage and the Arts, Canberra.

Wilson, E. H. & Sader, S. A. 2002. Detection of forest harvest type using multiple dates of Landsat TM imagery. *Remote Sensing of Environment* **80**, 385-396.

Wittkuhn, R. S., McCawb, L., Wills, A. J., Robinson, R., Andersen, A. N., Van Heurcka, P., Farr, J., Liddelow, G. & Cranfield, R. 2011. Variation in fire interval sequences has minimal effects on species richness and composition in fire-prone landscapes of south-west Western Australia. *Forest Ecology and Management* **261**, 965-978.

Yang, J., Weisberg, P. J. & Bristow, N. A. 2012. Landsat remote sensing approaches for monitoring long-term tree cover dynamics in semi-arid woodlands: Comparison of vegetation indices and spectral mixture analysis. *Remote Sensing of Environment* **119**, 62-71.

Appendix A: Ground Truth Data collection location details

SiteLabel	TSF (yrs)	TSF (category)	Easting	Northing	UTM Zone	Site Location	Collection Date
PS005	2.5	1	327240	6272531	56	Ku-ring-gai Chase NP	20/07/2009
PS009	3.6	1	342633	6298266	56	Brisbane Water NP	3/08/2009
PS010	7.7	2	312922	6217983	56	Garrawarra Hospital	6/08/2009
PS015	6.6	2	340256	6298742	56	Brisbane Water NP	24/08/2009
PS019	4.1	1	342298	6298168	56	Brisbane Water NP	24/08/2009
PS020	35	3	338429	6309034	56	Brisbane Water NP	25/08/2009
PS021	35	3	338356	6309872	56	Brisbane Water NP	25/08/2009
PS023	0.5	1	338296	6312239	56	Brisbane Water NP	25/08/2009
PS024	6.6	2	340210	6296778	56	Brisbane Water NP	31/08/2009
PS025	15.6	3	331196	6294038	56	Popran NP	31/08/2009
PS026	7.8	2	330466	6293815	56	Popran NP	31/08/2009
PS028	7.8	2	341047	6287803	56	Brisbane Water NP	31/08/2009
PS029	18.8	3	339619	6286891	56	Brisbane Water NP	1/09/2009
PS031	15.7	3	334404	6305611	56	Popran	7/09/2009
PS033	7.8	2	334599	6312681	56	Popran NP	7/09/2009
PS037	0.7	1	315382	6220353	56	Royal NP	30/09/2009
PS038	0.7	1	315628	6220343	56	Royal NP	30/09/2009
PS045	15.8	3	326790	6227136	56	Royal NP	14/10/2009
PS046	15.8	3	326456	6227151	56	Royal NP	14/10/2009
PS050	5.1	1	321663	6231137	56	Royal NP	22/10/2009
PS051	7.8	2	319736	6230017	56	Royal NP	22/10/2009
PS056	7.8	2	321692	6223538	56	Royal NP	28/10/2009
PS057	15.8	3	320063	6217182	56	Royal NP	4/11/2009
PS078	2.3	1	340602	6282214	56	Ku-ring-gai Chase NP	17/02/2010
PS079	16.1	3	339533	6280816	56	Ku-ring-gai Chase NP	17/02/2010
PS080	6.1	2	337632	6273931	56	Ku-ring-gai Chase NP	18/02/2010
PS081	6.1	2	338961	6275518	56	Ku-ring-gai Chase NP	18/02/2010
PS082	16.1	3	332048	6286358	56	Muogamarra NR	25/02/2010
PS083	5	1	325107	6276747	56	Berowra Valley RP	25/02/2010
PS099	8.3	2	317461	6226543	56	Royal NP	9/04/2010

*TSF = Time Since Last Fire

SiteLabel	Canopy (%)	Elevated (%)	Elevated Live (%)	Elevated Dead (%)	Near Surface (%)	Near Surface Live (%)	Near Surface Dead (%)	Litter (%)
PS005	13.75	18.75	15.23	3.52	17.50	14.22	3.28	22.50
PS009	26.67	18.33	11.92	6.42	26.67	17.33	9.33	91.67
PS010	35.71	11.43	8.00	3.43	30.00	11.57	18.43	100.00
PS015	14.00	30.00	27.60	2.40	24.00	14.40	9.60	96.00
PS019	20.00	16.00	11.20	4.80	30.00	21.60	8.40	92.00
PS020	24.00	24.00	19.68	4.32	54.00	33.48	20.52	98.00
PS021	22.00	52.00	29.12	22.88	44.00	24.64	19.36	98.00
PS023	10.00	18.00	3.24	14.76	22.00	18.48	3.52	32.00
PS024	22.00	38.00	31.16	6.84	18.00	13.32	4.68	72.00
PS025	28.00	20.00	13.20	6.80	28.00	8.40	19.60	92.00
PS026	14.00	26.00	23.40	2.60	30.00	14.40	15.60	80.00
PS028	16.00	28.00	23.52	4.48	40.00	24.80	15.20	78.00
PS029	22.00	32.00	15.36	16.64	22.00	2.64	19.36	86.00
PS031	22.00	36.00	20.88	15.12	22.00	6.16	15.84	98.00
PS033	38.00	18.00	13.68	4.32	40.00	9.60	30.40	100.00
PS037	30.00	10.00	3.00	7.00	6.00	2.76	3.24	46.00
PS038	27.14	7.14	1.73	5.41	5.71	1.88	3.84	31.43
PS045	41.43	12.86	9.92	2.94	35.71	6.12	29.59	100.00
PS046	11.43	34.29	26.94	7.35	21.43	5.20	16.22	97.14
PS050	38.00	4.00	3.76	0.24	16.00	8.00	8.00	88.00
PS051	26.00	36.00	33.12	2.88	34.00	16.32	17.68	100.00
PS056	27.14	31.43	28.29	3.14	20.00	11.14	8.86	95.71
PS057	20.00	38.57	28.65	9.92	35.71	11.73	23.98	100.00
PS078	17.14	20.00	18.29	1.71	21.43	18.67	2.76	34.29
PS079	18.57	47.14	35.02	12.12	30.00	14.14	15.86	100.00
PS080	22.00	22.00	20.24	1.76	20.00	12.80	7.20	94.00
PS081	20.00	27.14	23.27	3.88	22.86	15.02	7.84	94.29
PS082	28.57	31.43	22.90	8.53	37.14	13.27	23.88	97.14
PS083	35.71	14.29	12.45	1.84	34.29	20.57	13.71	97.14
PS099	48.57	14.29	13.67	0.61	25.71	11.76	13.96	100.00

Appendix B: Spectral indices images

Example images for each of the spectral indices, calculated from the 23 September 2009 Landsat 5 TM images. Images labelled "A" represent the data collection regions north of Sydney, and images labelled "B" represent the data collection region south of Sydney.

Simple Ratio (SR):

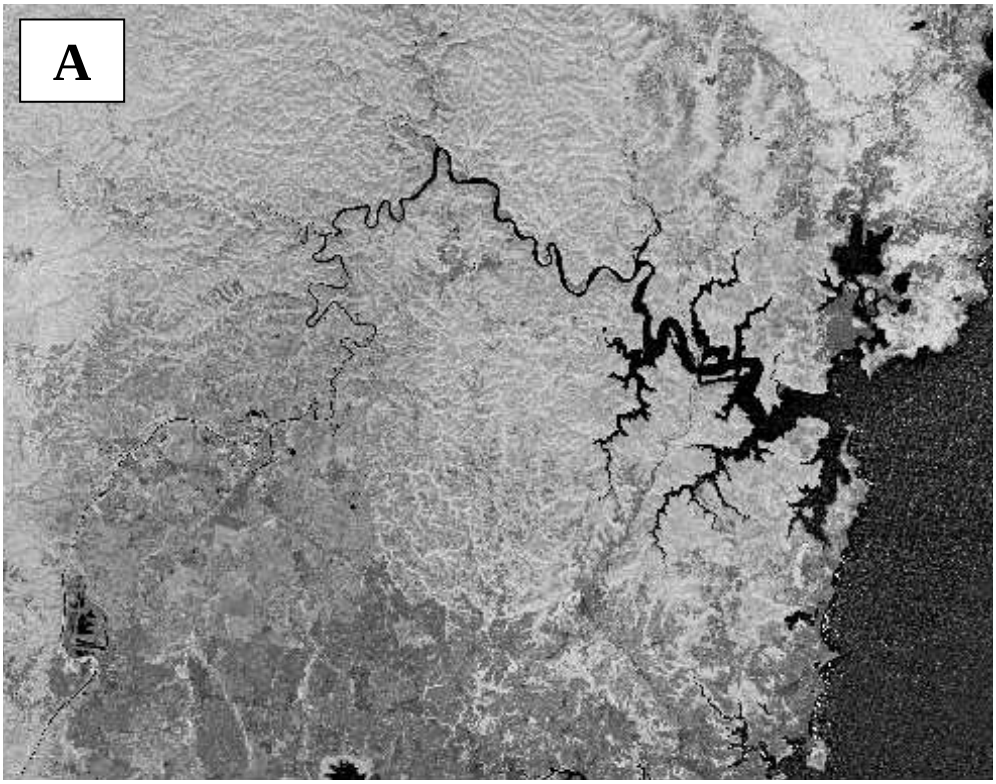

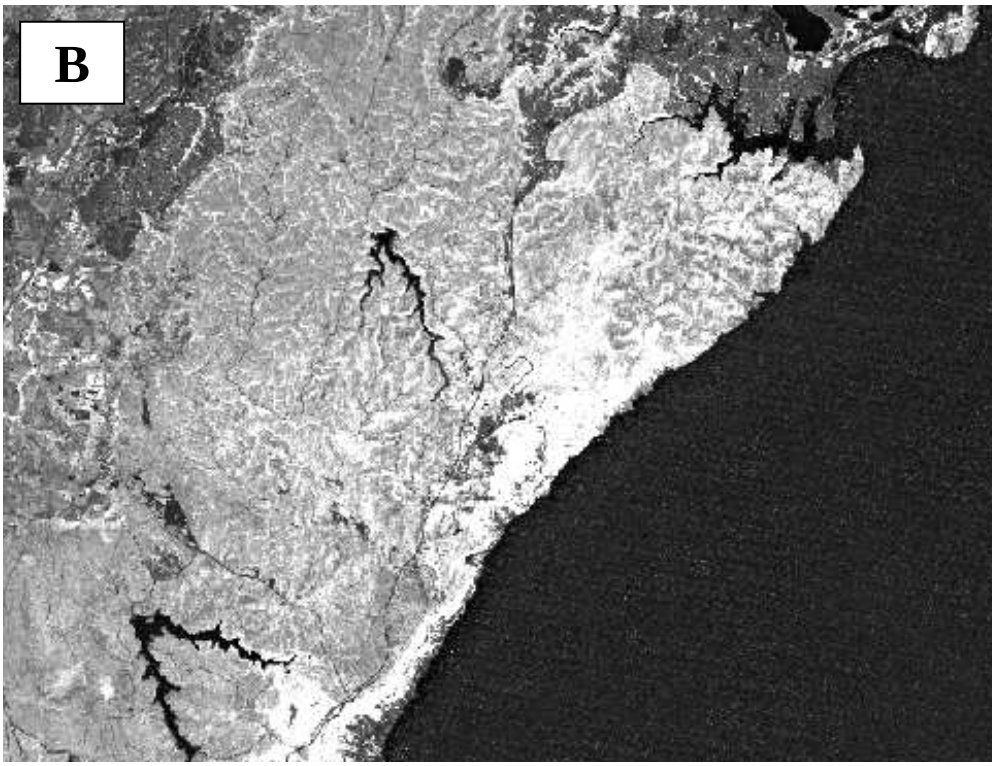

Normalized Difference Vegetation Index (NDVI):

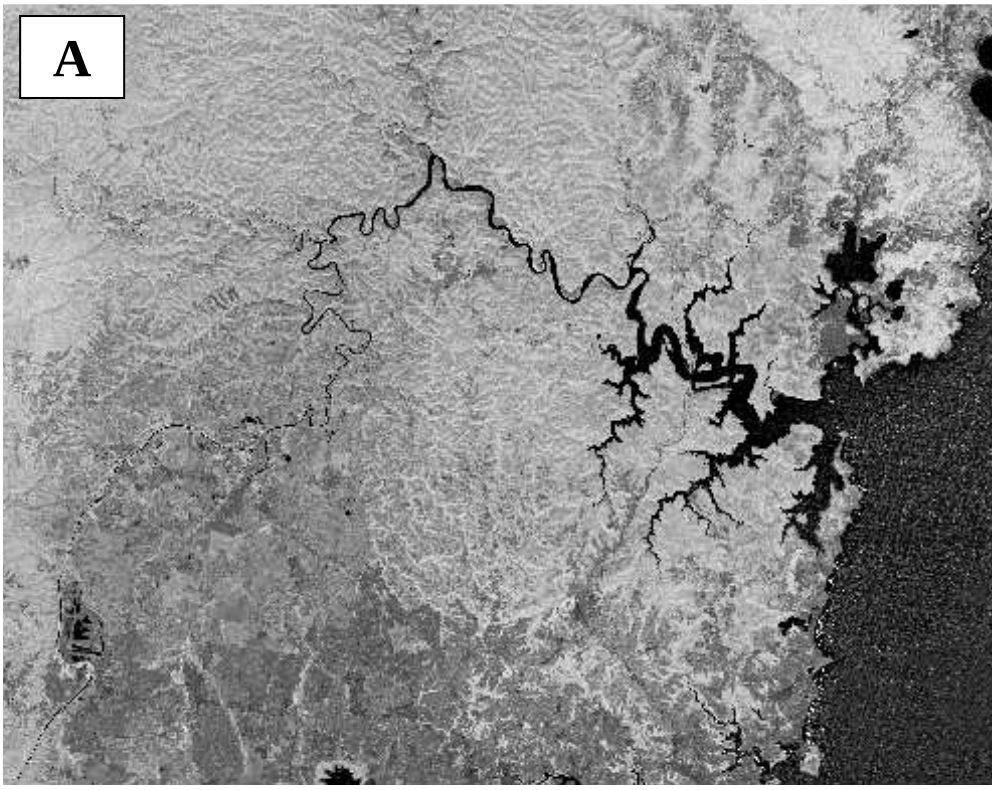

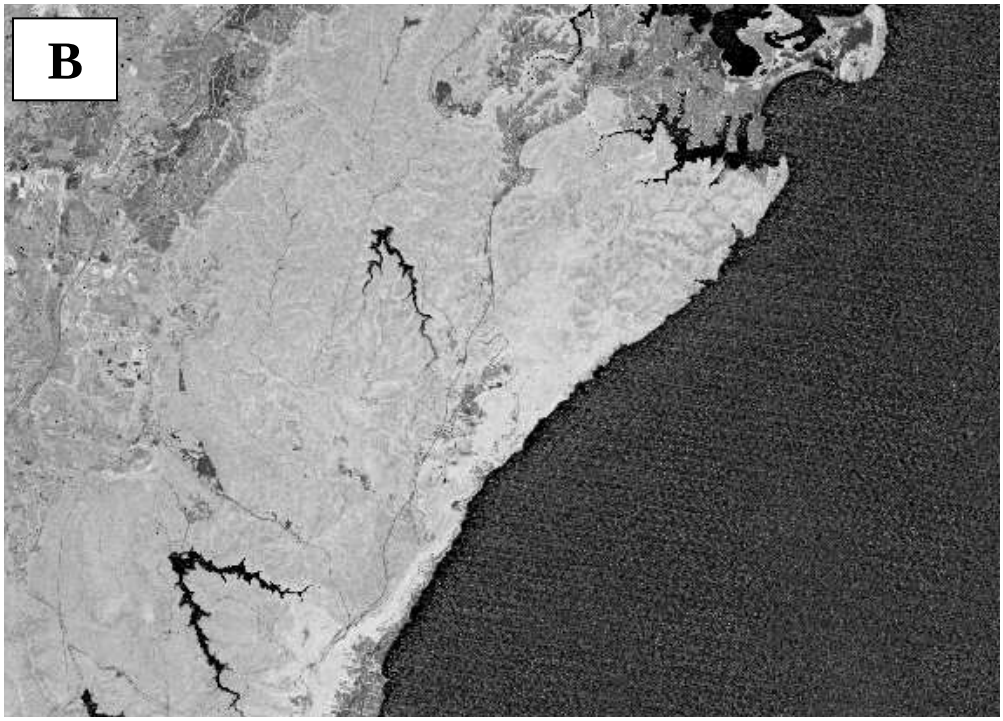

Green Normalized Difference Vegetation Index (GNDVI):

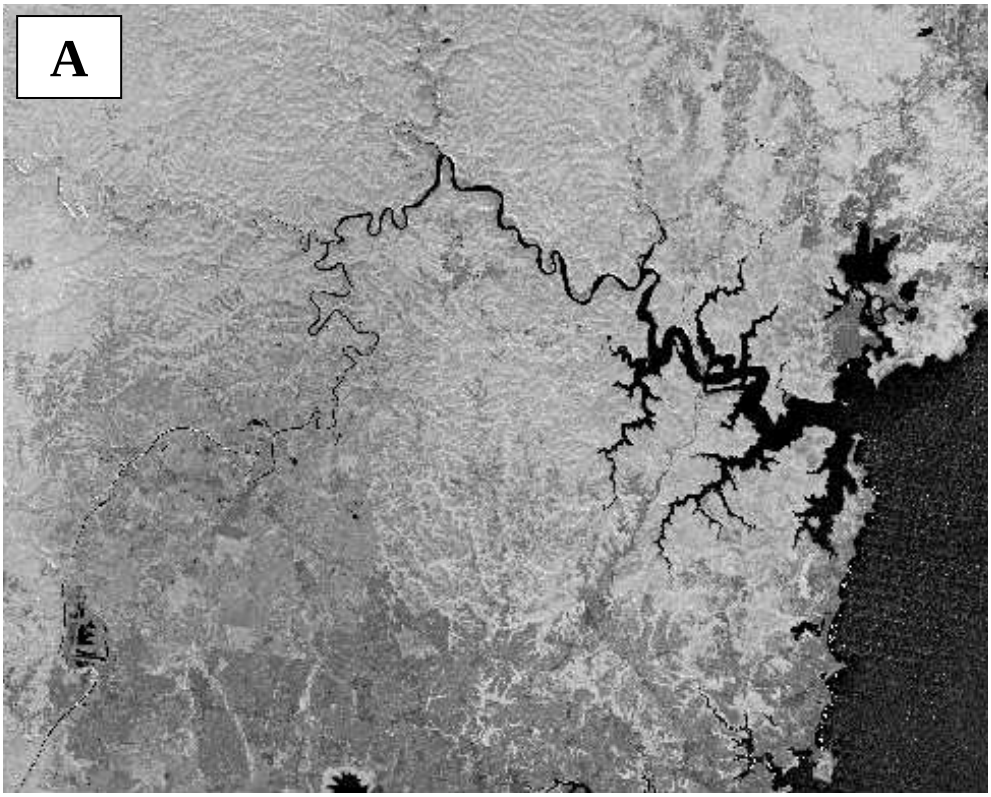

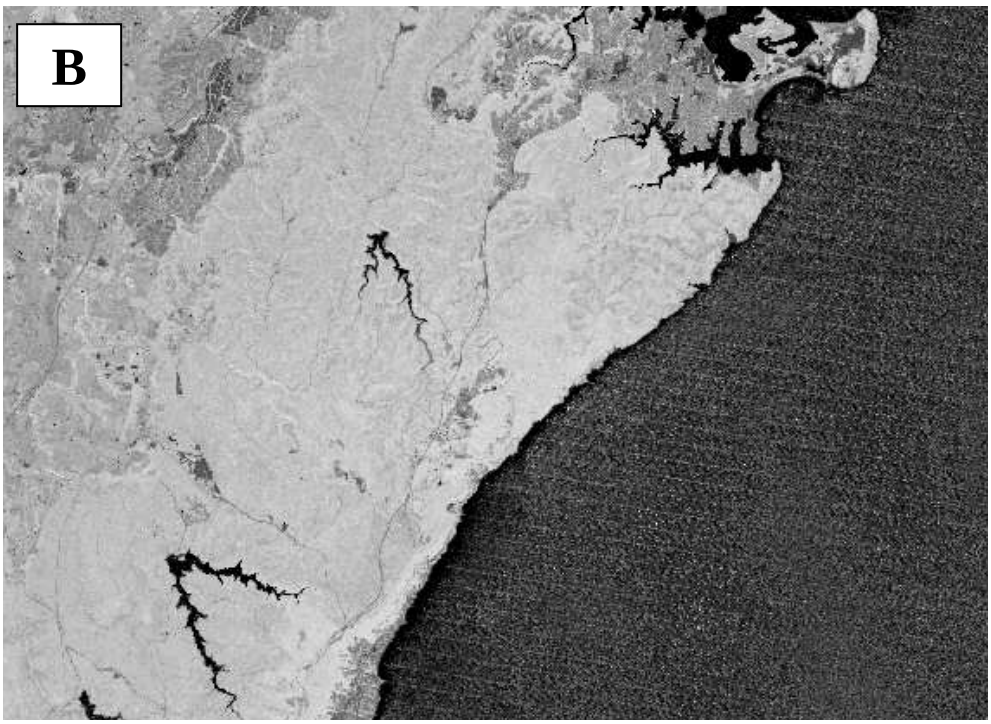

Soil-Adjusted Vegetation Index (SAVI):

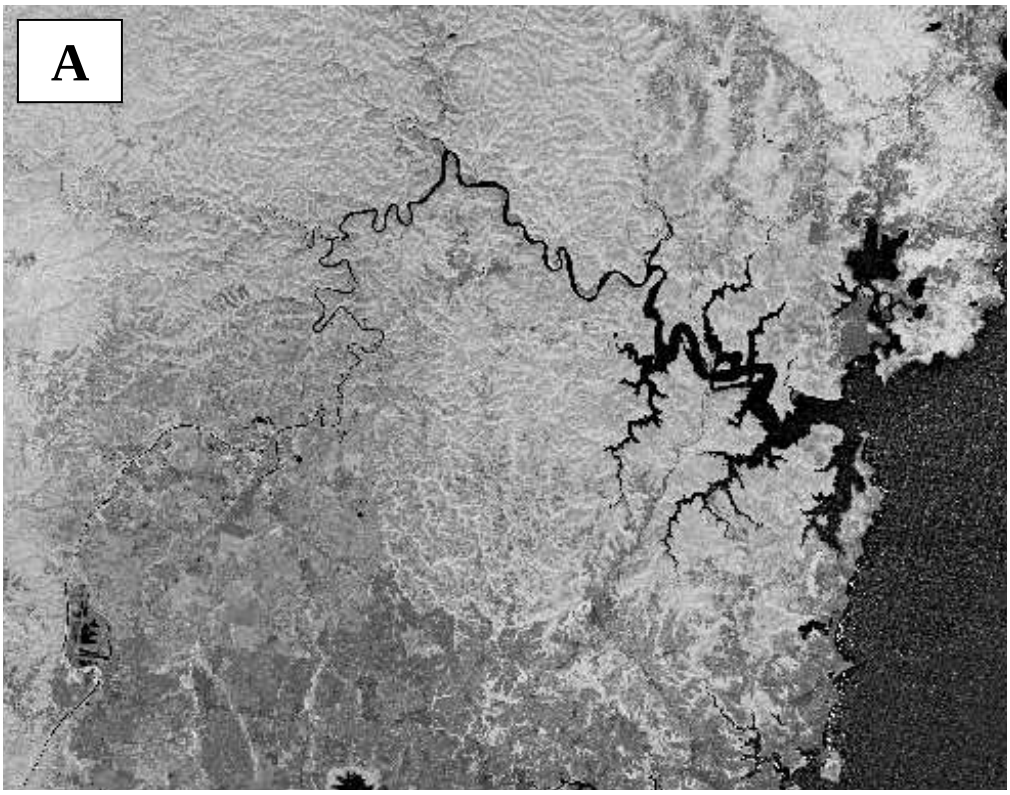

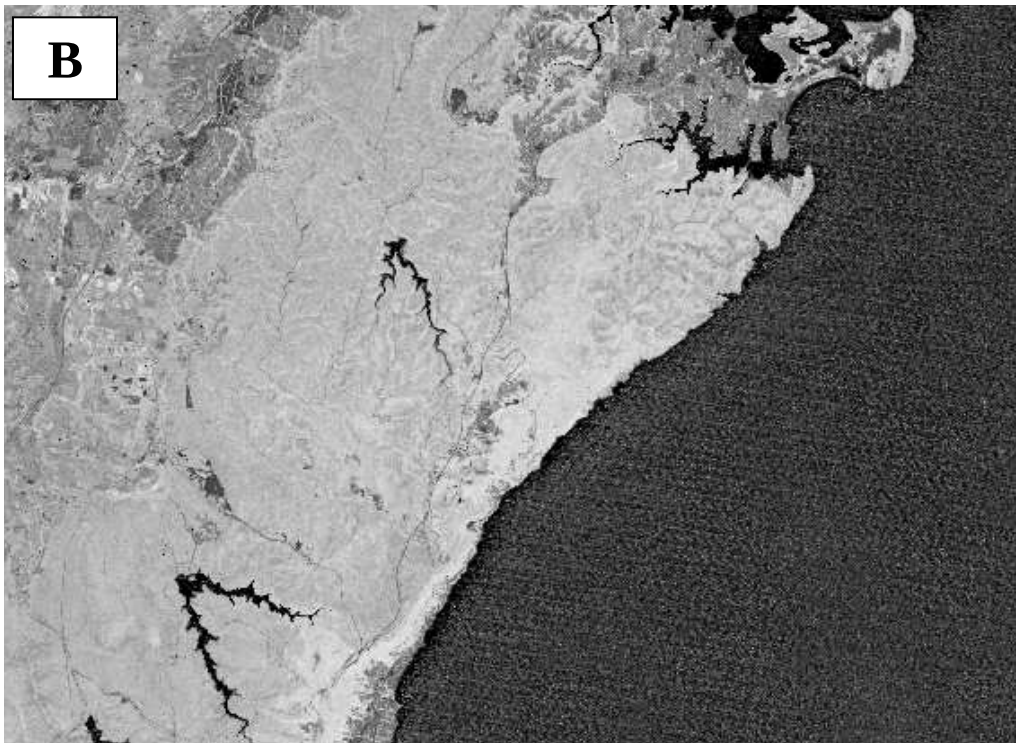

Soil Adjusted Total Vegetation Index (SATVI):

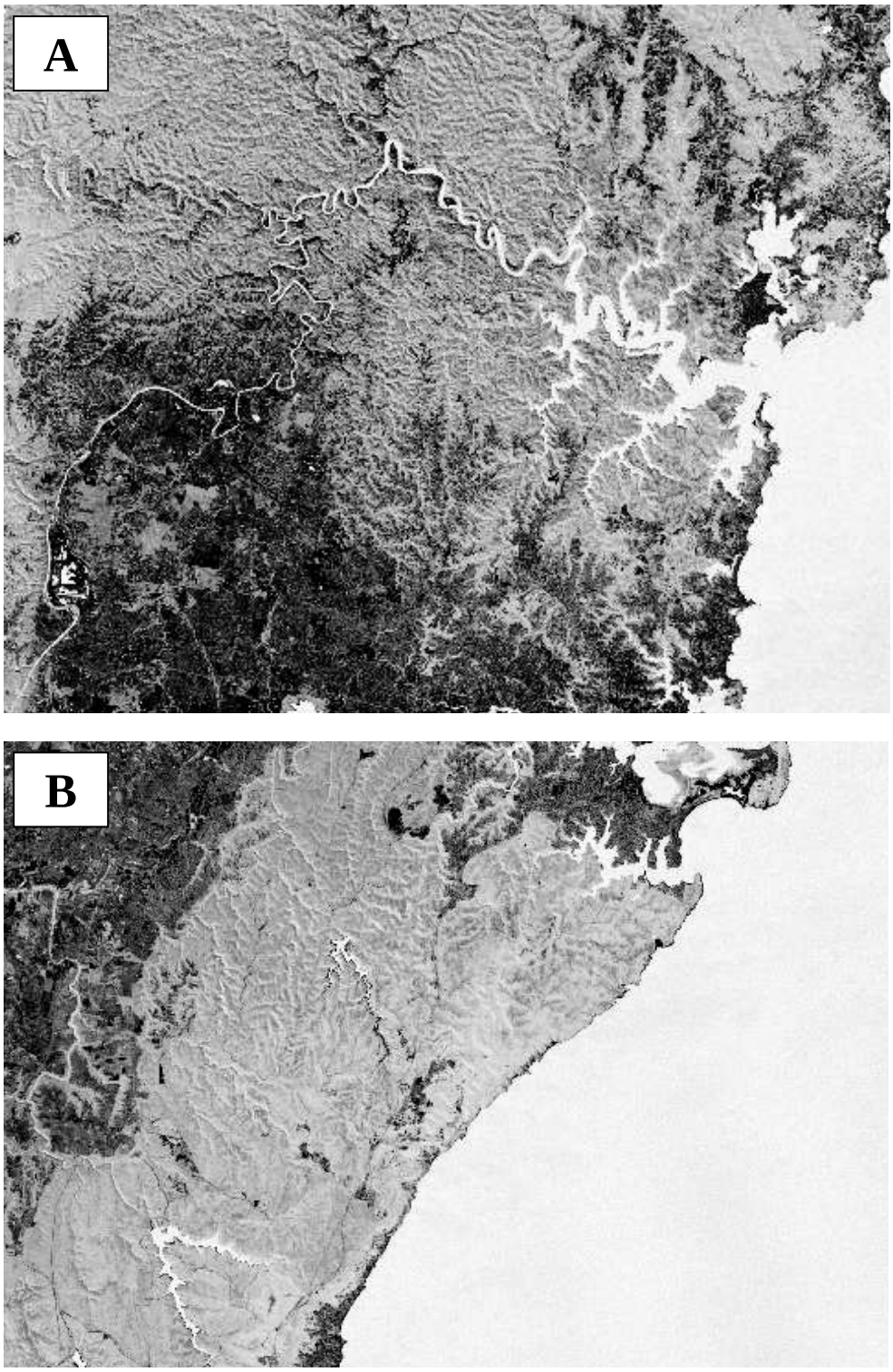

Normalized Difference Infrared Index, TM Band 5 (NDIIb5):

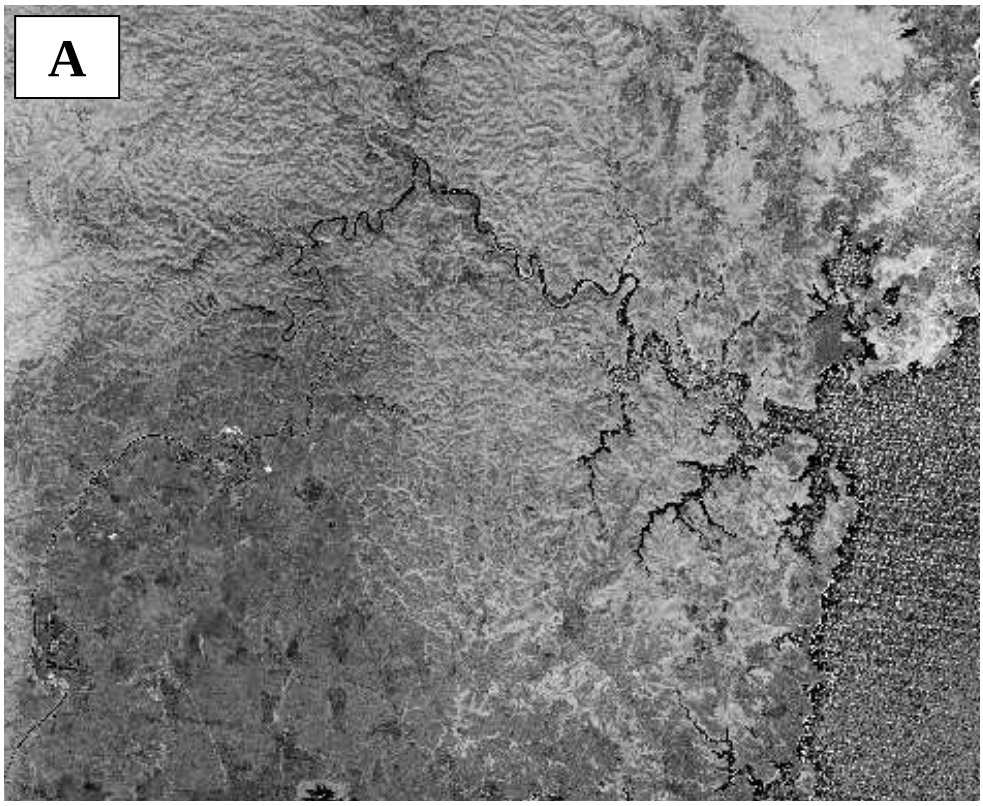

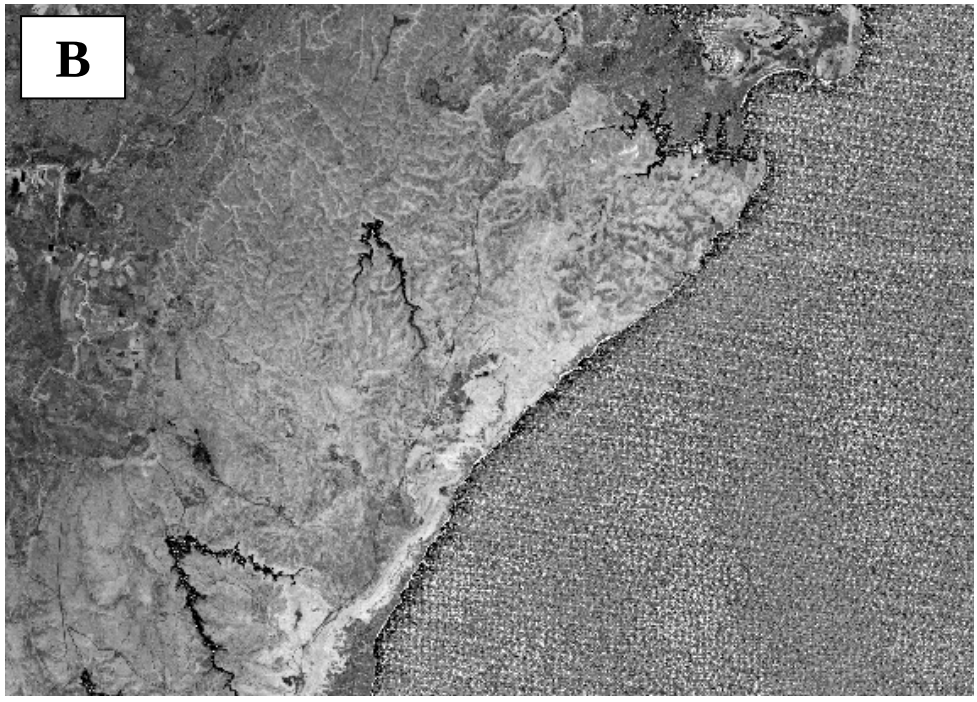

Normalized Difference Infrared Index, TM Band 7 (NDIIb7):

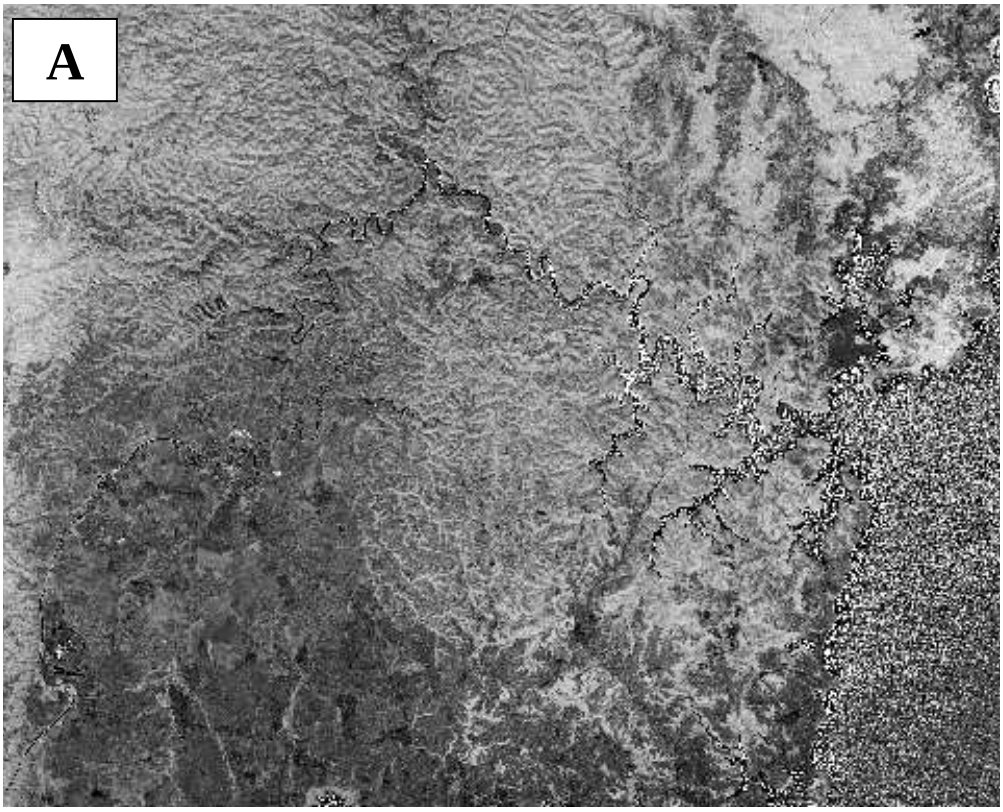

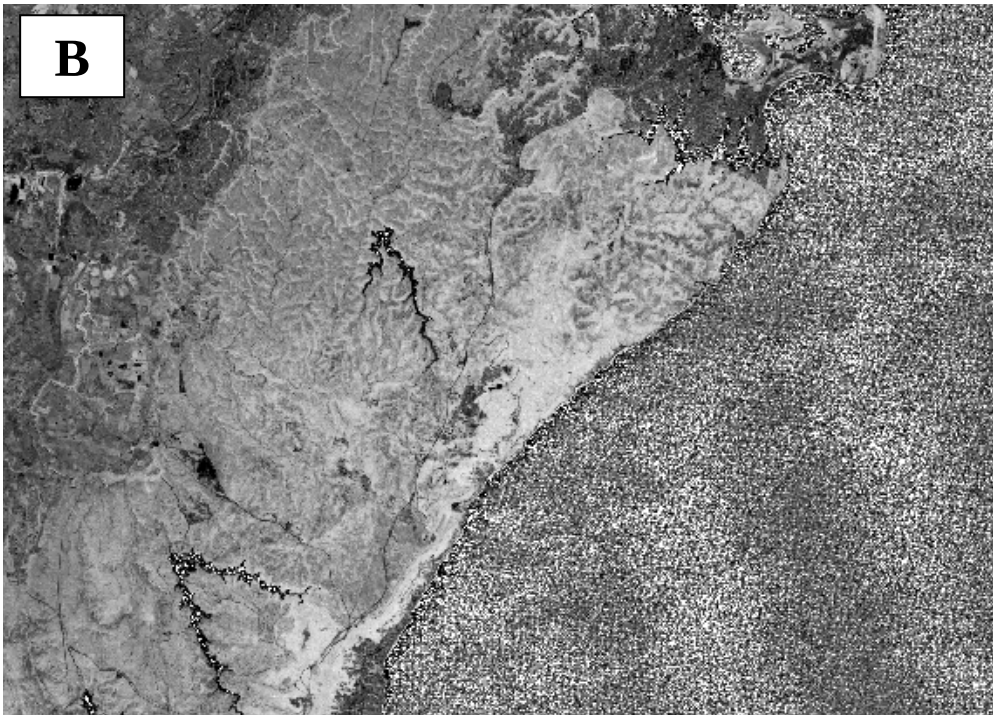

Appendix C: Spectral index values obtained for each site in different seasons

Indices calculated from visible and NIR wavelengths (SR, NDVI, GNDVI and SAVI) showed differences in spectral reflectance between seasons. Indices calculated from NIR and SWIR wavelengths (NDIIb5 and NDIIb7) showed less of a contrast in spectral reflectance between seasons. The pattern for SATVI is less uniform in difference between seasons and this variation can probably be attributed to the fact it is calculated from both visible and SWIR wavelengths.

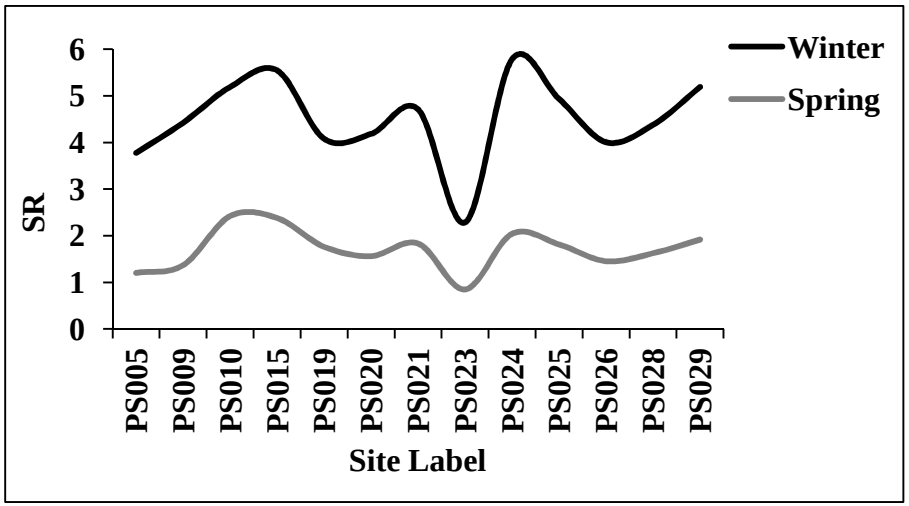

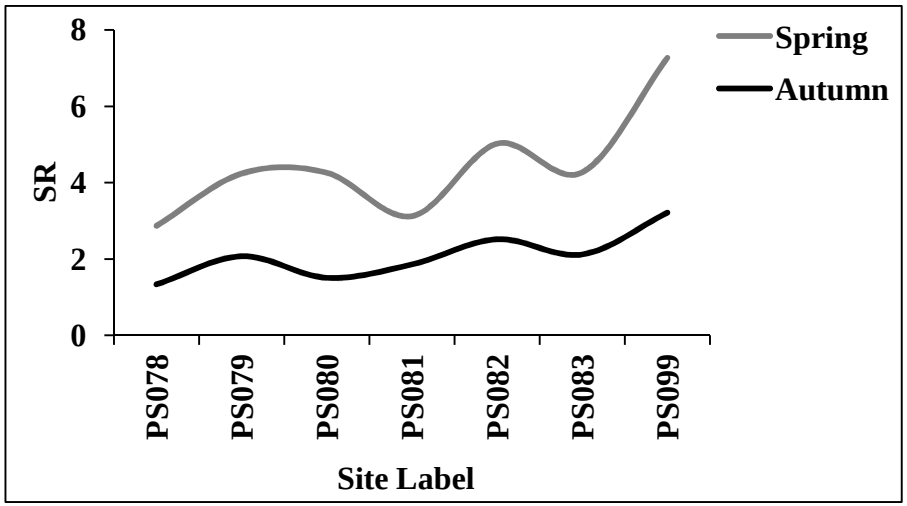

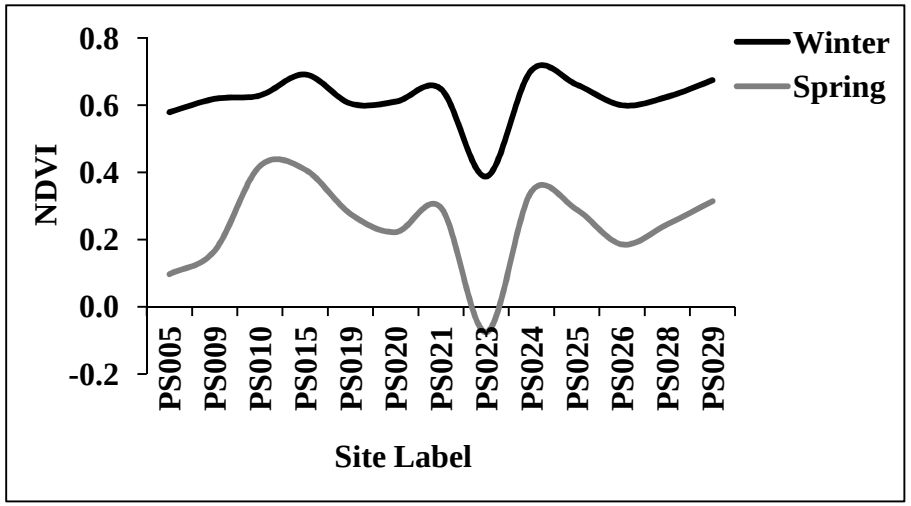
0.8
0.6
0.4
0.2
0.0
-0.2
NDVI
Winter
Spring
PS005
PS009
PS010
PS015
PS019
PS020
PS021
PS023
PS024
PS025
PS026
PS028
PS029
Site Label


0.8
0.6
0.4
0.2
0.0
NDVI
Spring
Autumn
PS078
PS079
PS080
PS081
PS082
PS083
PS099
Site Label


0.8
0.6
0.4
0.2
0.0
-0.2
GNDVI
Winter
Spring
PS005
PS009
PS010
PS015
PS019
PS020
PS021
PS023
PS024
PS025
PS026
PS028
PS029
Site Label

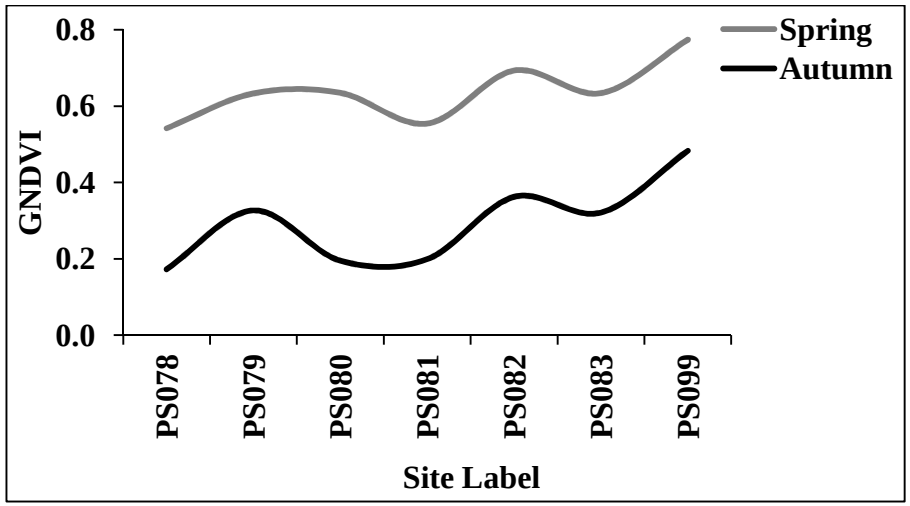
0.8
0.6
0.4
0.2
0.0
GNDVI
Spring
Autumn
PS078
PS079
PS080
PS081
PS082
PS083
PS099
Site Label

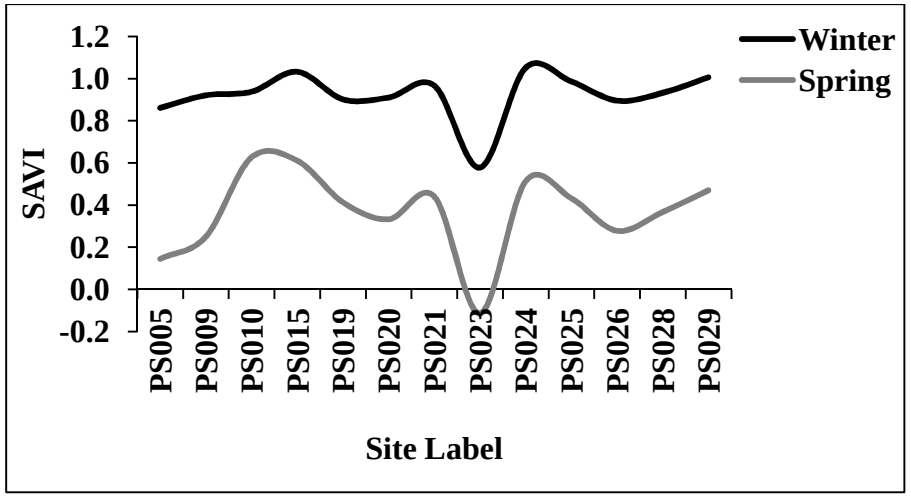
1.2
1.0
0.8
0.6
0.4
0.2
0.0
-0.2
SAVI
Winter
Spring
PS005
PS009
PS010
PS015
PS019
PS020
PS021
PS023
PS024
PS025
PS026
PS028
PS029
Site Label

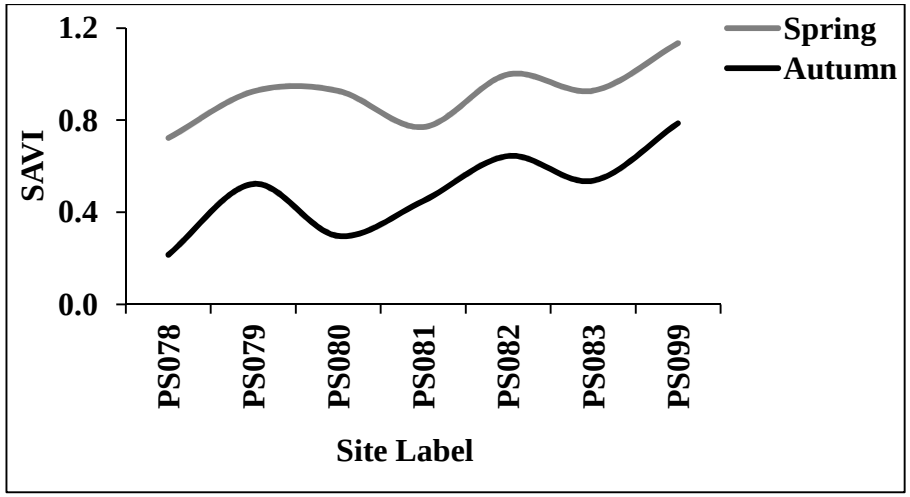
1.2
0.8
0.4
0.0
SAVI
Spring
Autumn
PS078
PS079
PS080
PS081
PS082
PS083
PS099
Site Label

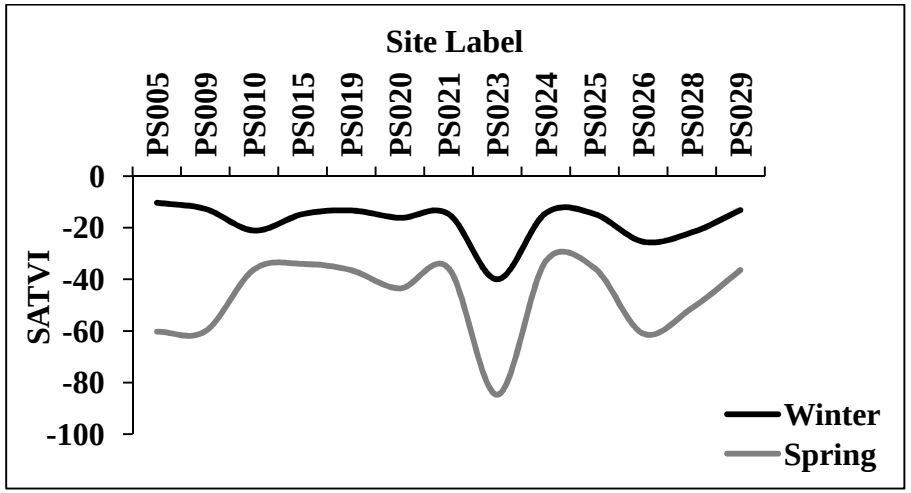
Site Label
PS005
PS009
PS010
PS015
PS019
PS020
PS021
PS023
PS024
PS025
PS026
PS028
PS029
0
-20
-40
-60
-80
-100
SATVI
Winter
Spring

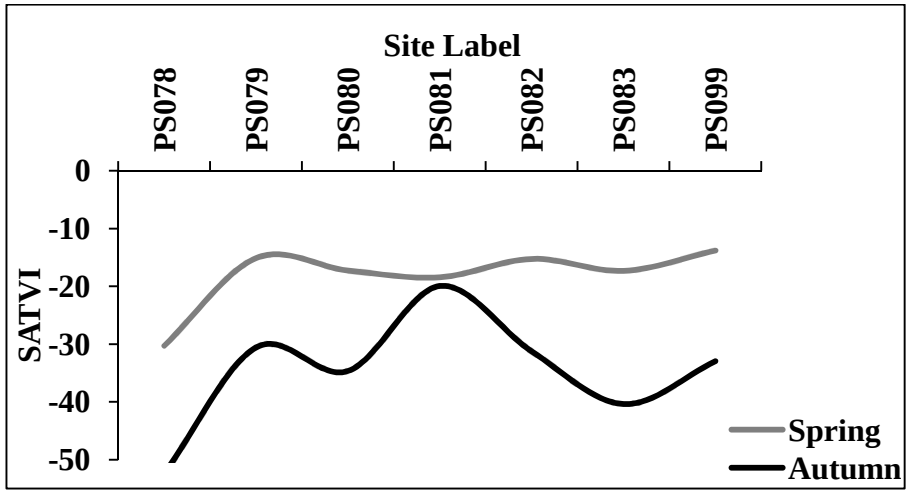
Site Label
PS078
PS079
PS080
PS081
PS082
PS083
PS099
0
-10
-20
-30
-40
-50
SATVI
Spring
Autumn

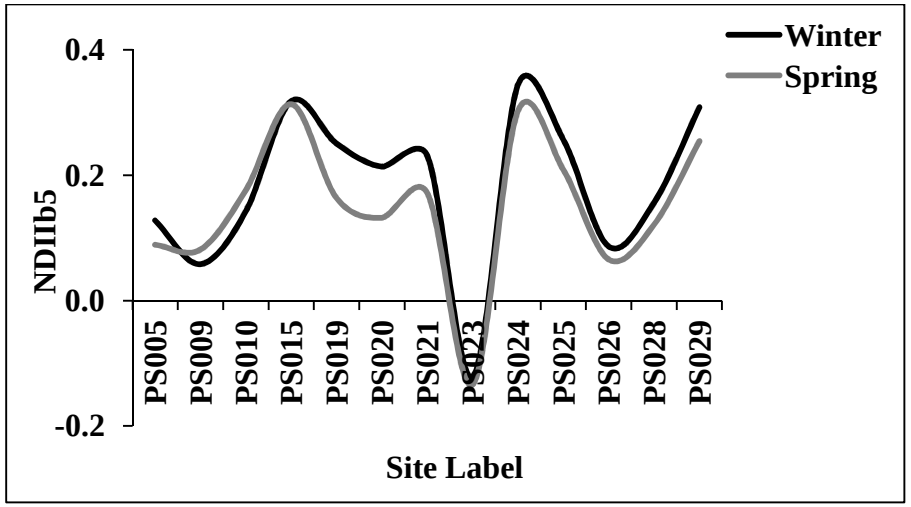
Winter
Spring
0.4
0.2
0.0
-0.2
NDIIb5
PS005
PS009
PS010
PS015
PS019
PS020
PS021
PS023
PS024
PS025
PS026
PS028
PS029
Site Label

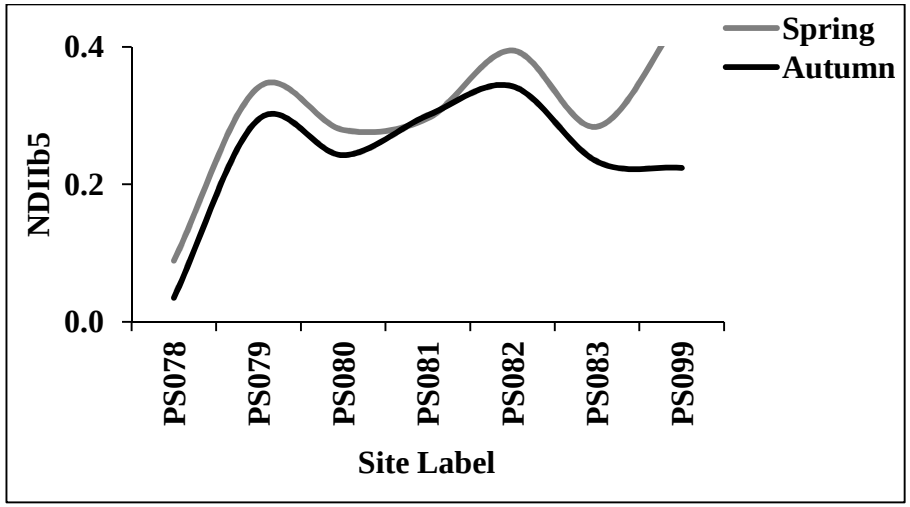
Spring
Autumn
0.4
0.2
0.0
NDIIb5
PS078
PS079
PS080
PS081
PS082
PS083
PS099
Site Label

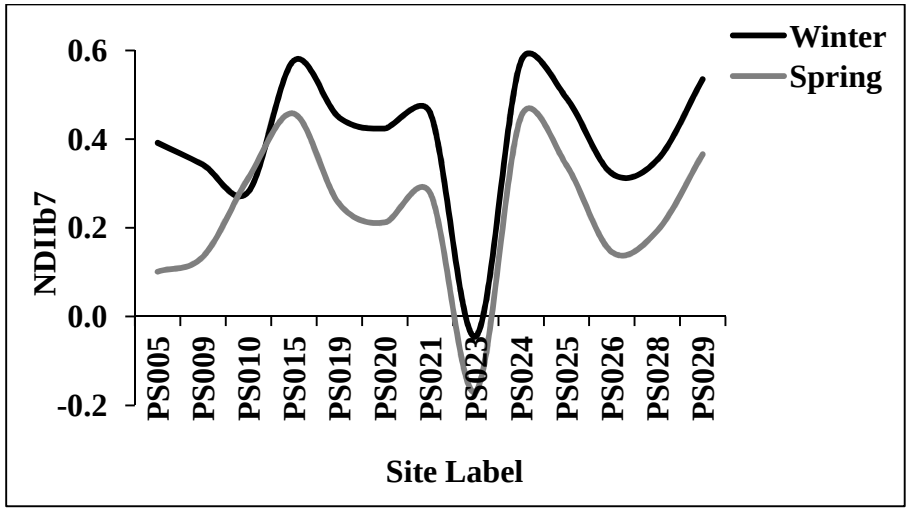
Winter
Spring
0.6
0.4
0.2
0.0
-0.2
NDIIb7
PS005
PS009
PS010
PS015
PS019
PS020
PS021
PS023
PS024
PS025
PS026
PS028
PS029
Site Label

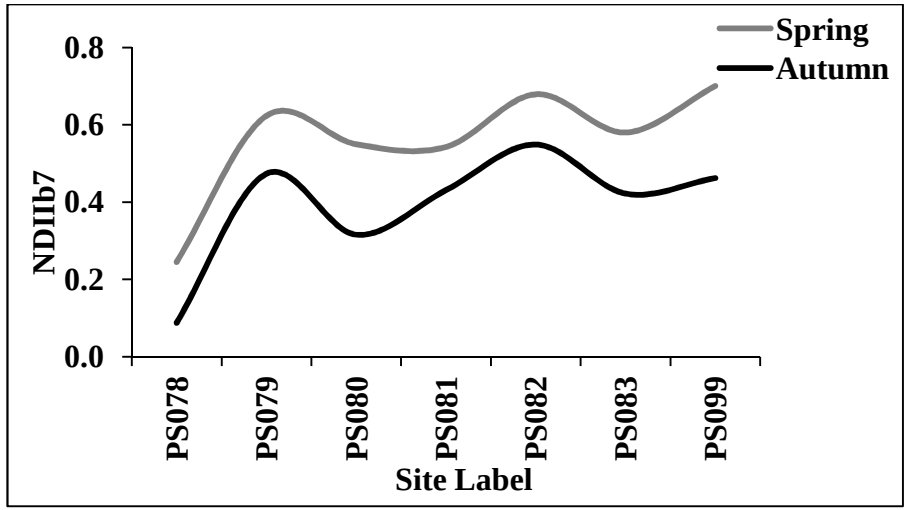
Spring
Autumn
0.8
0.6
0.4
0.2
0.0
NDIIb7
PS078
PS079
PS080
PS081
PS082
PS083
PS099
Site Label

Appendix D: Scatterplots for all analyses

Relationships between fuel cover layers and litter cover

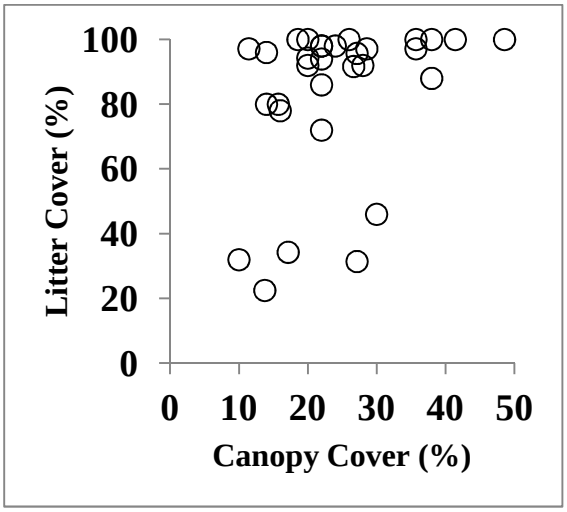

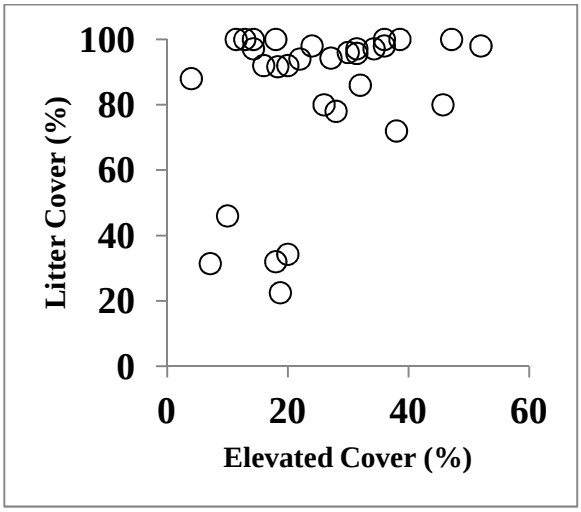

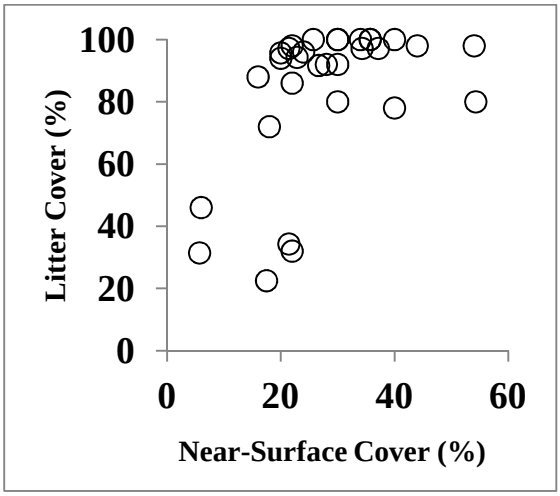

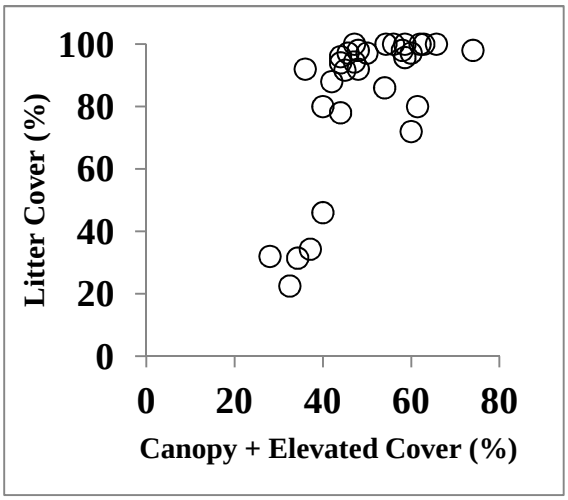

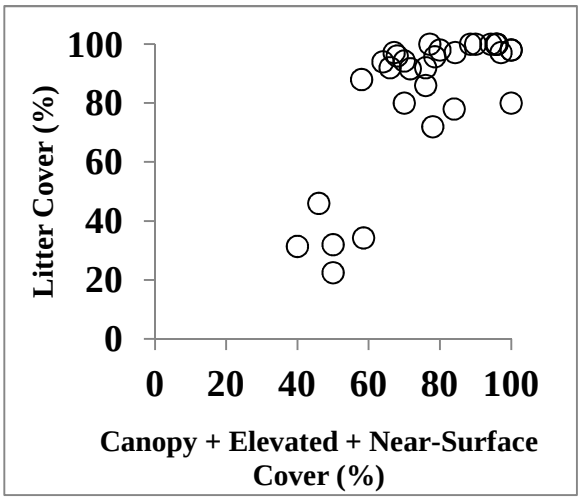

Approach 1: Live and Dead Fuel

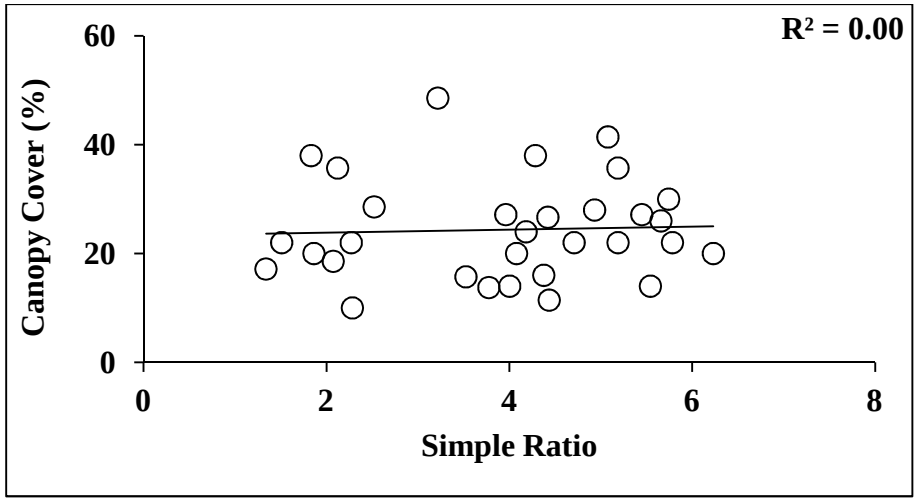

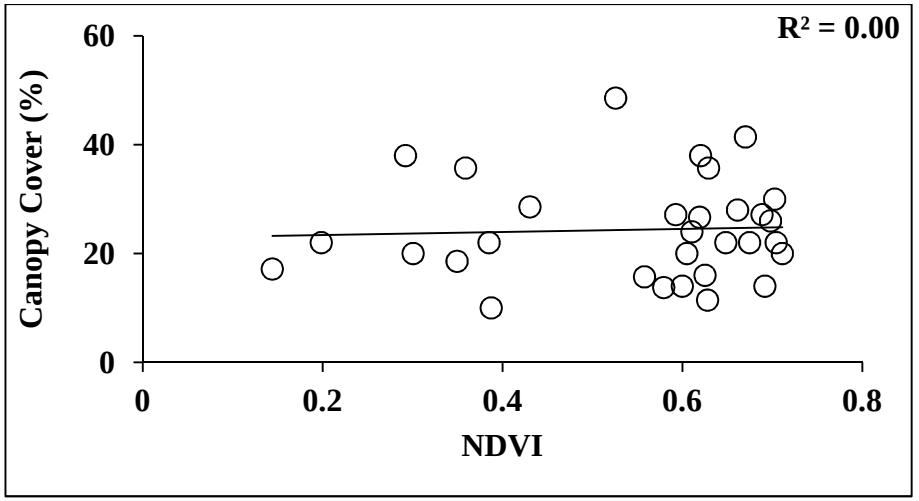

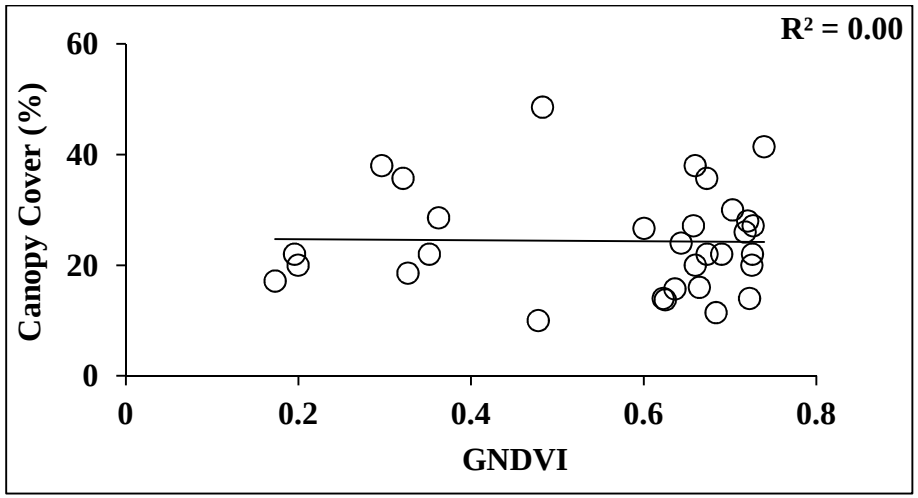

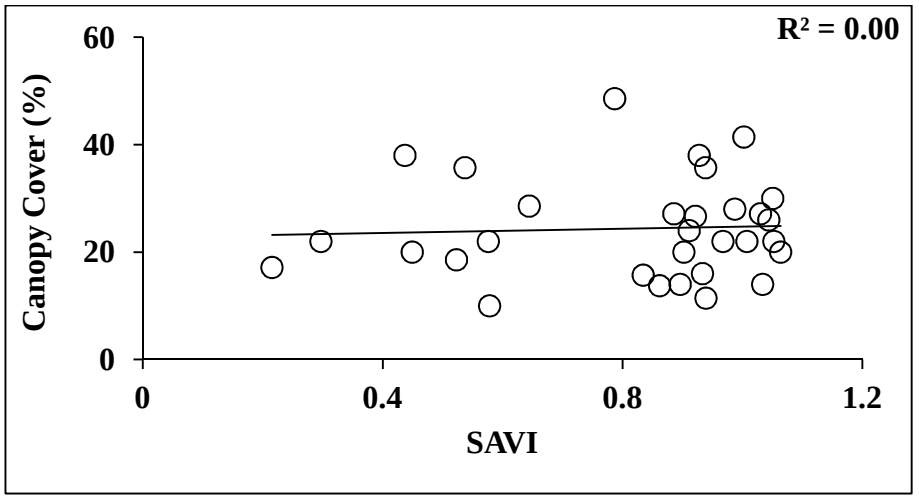

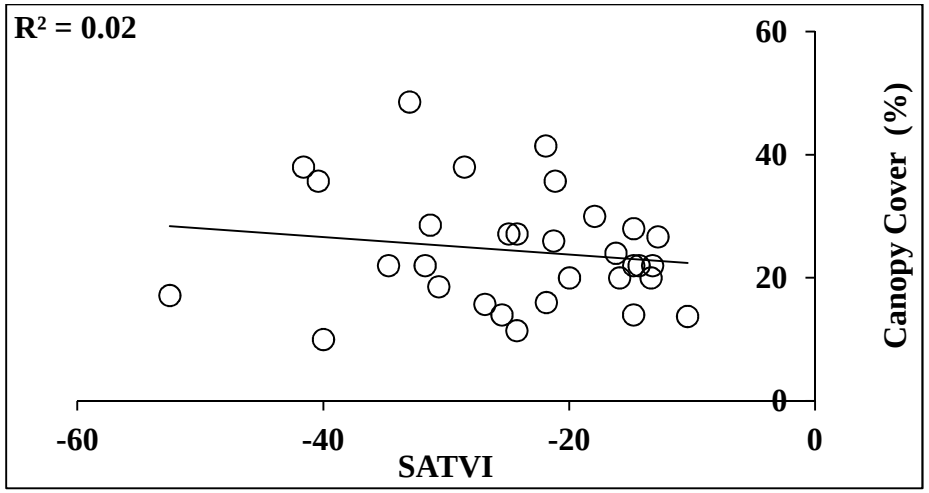
R² = 0.02
60
40
20
0
Canopy Cover (%)
-60
-40
-20
0
SATVI

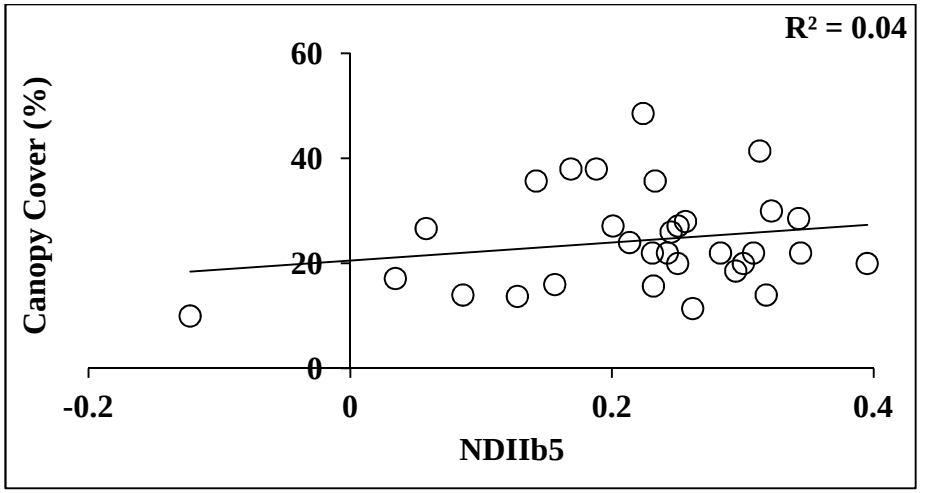
R² = 0.04
60
40
20
0
Canopy Cover (%)
-0.2
0
0.2
0.4
NDIIb5

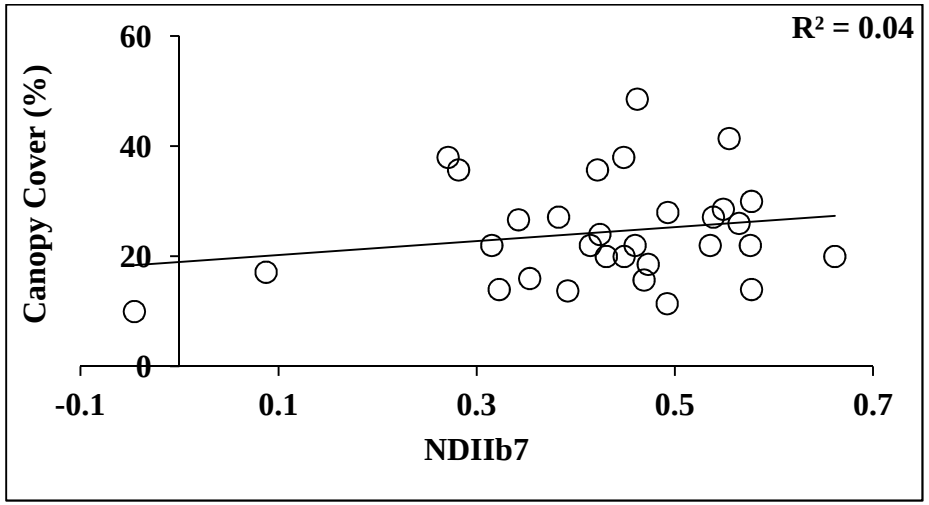
R² = 0.04
60
40
20
0
Canopy Cover (%)
-0.1
0.1
0.3
0.5
0.7
NDIIb7

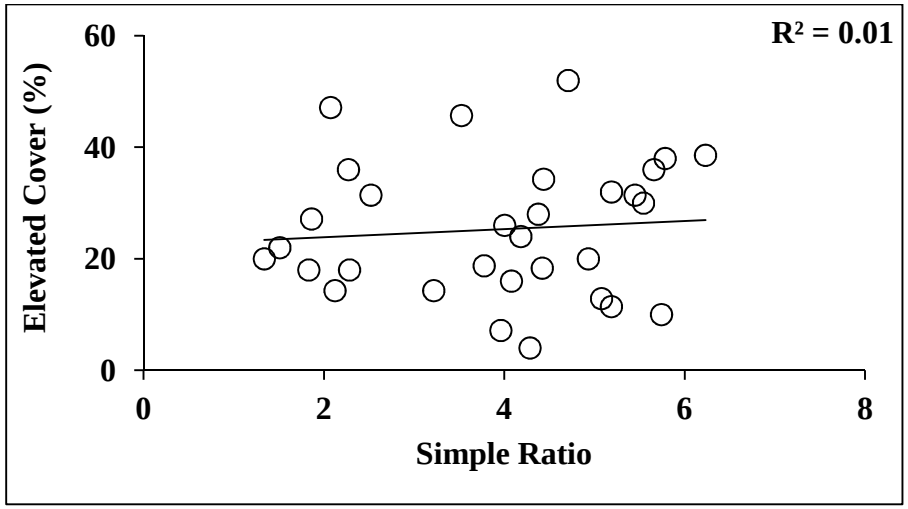
R² = 0.01
Elevated Cover (%)
60
40
20
0
0
2
4
6
8
Simple Ratio

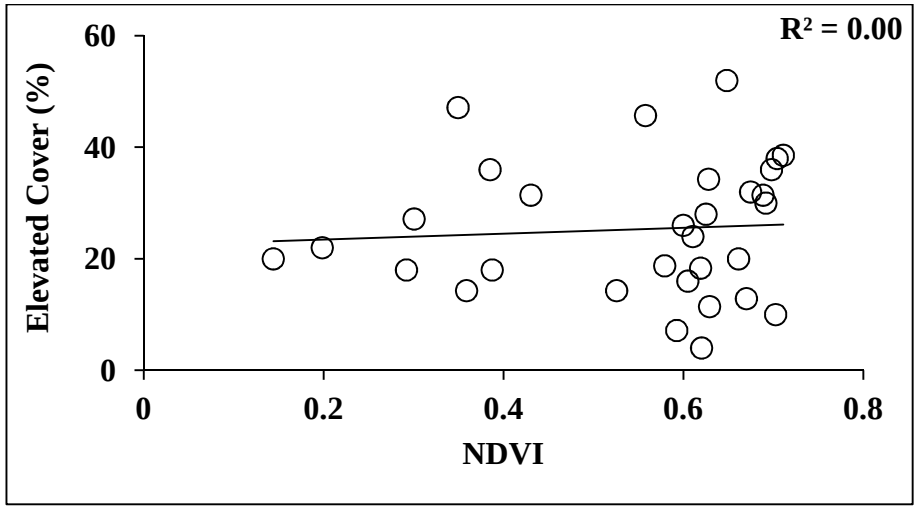
R² = 0.00
Elevated Cover (%)
60
40
20
0
0
0.2
0.4
0.6
0.8
NDVI

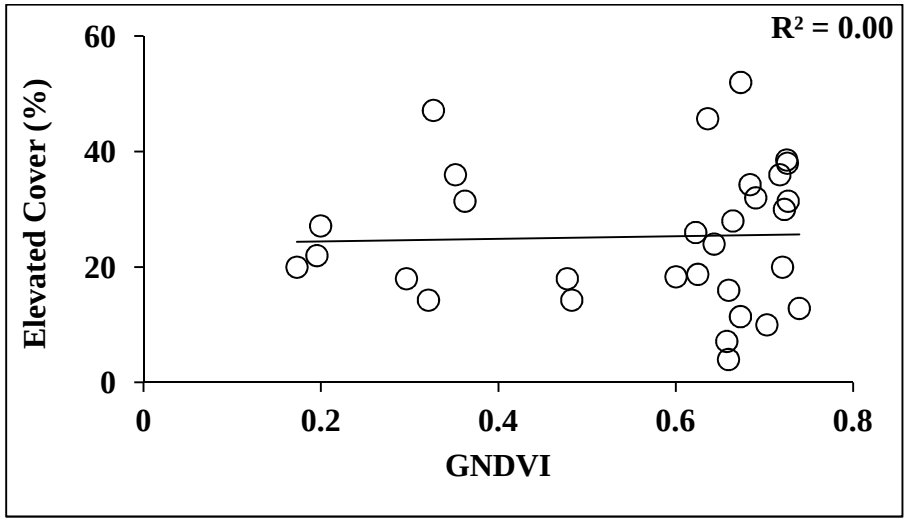
R² = 0.00
Elevated Cover (%)
60
40
20
0
0
0.2
0.4
0.6
0.8
GNDVI

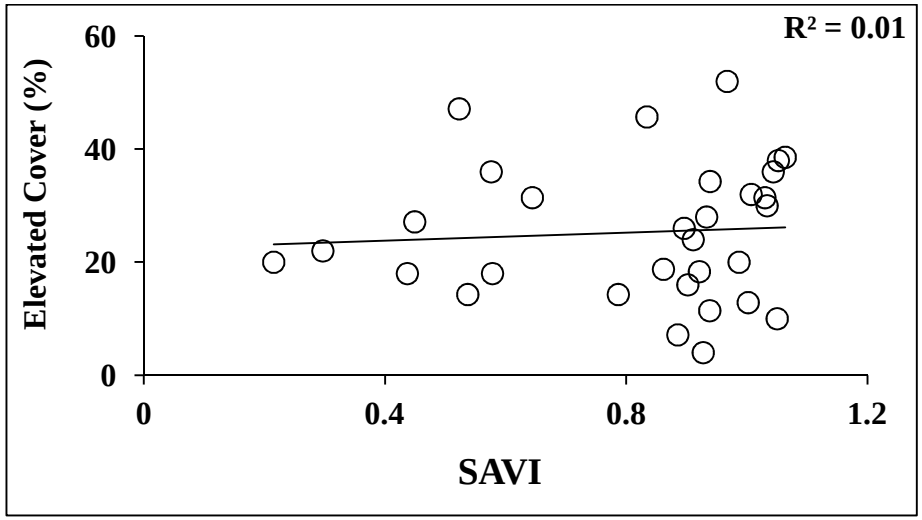
R² = 0.01
Elevated Cover (%)
60
40
20
0
0
0.4
0.8
1.2
SAVI

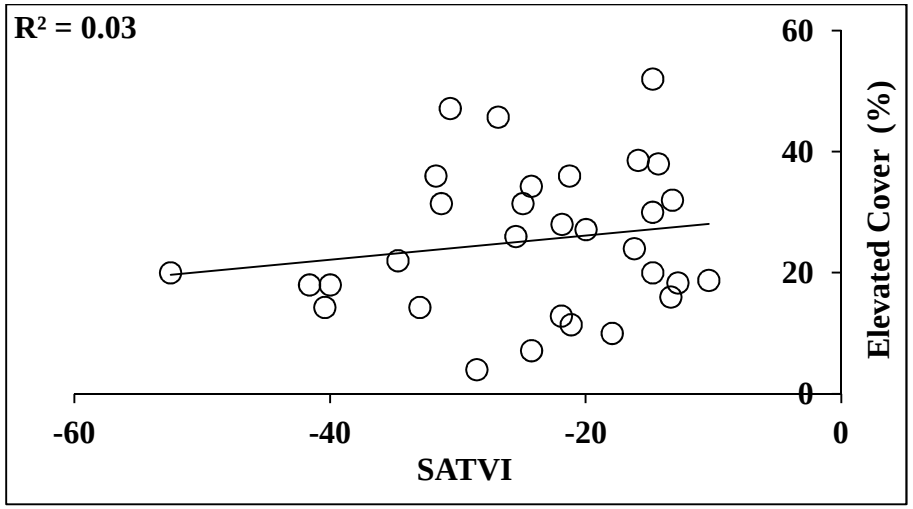
R² = 0.03
60
40
20
0
Elevated Cover (%)
-60
-40
-20
0
SATVI

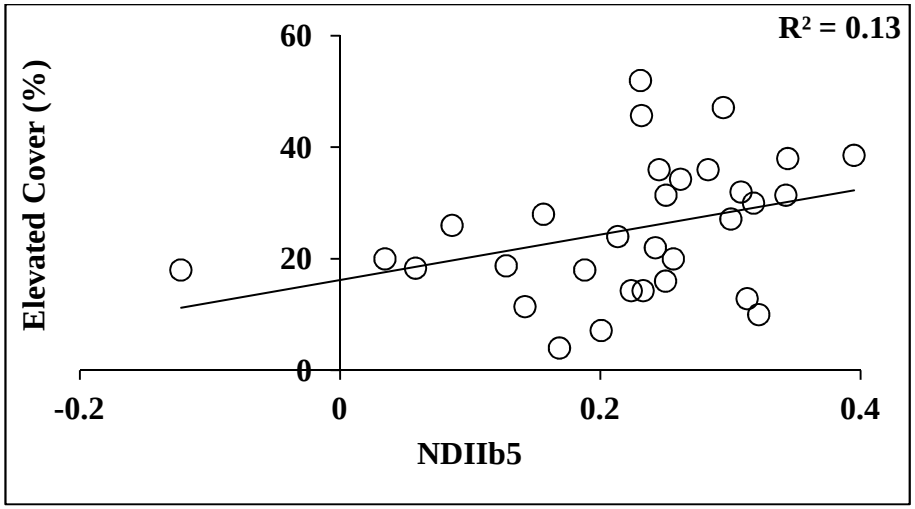
R² = 0.13
60
40
20
0
Elevated Cover (%)
-0.2
0
0.2
0.4
NDIIb5

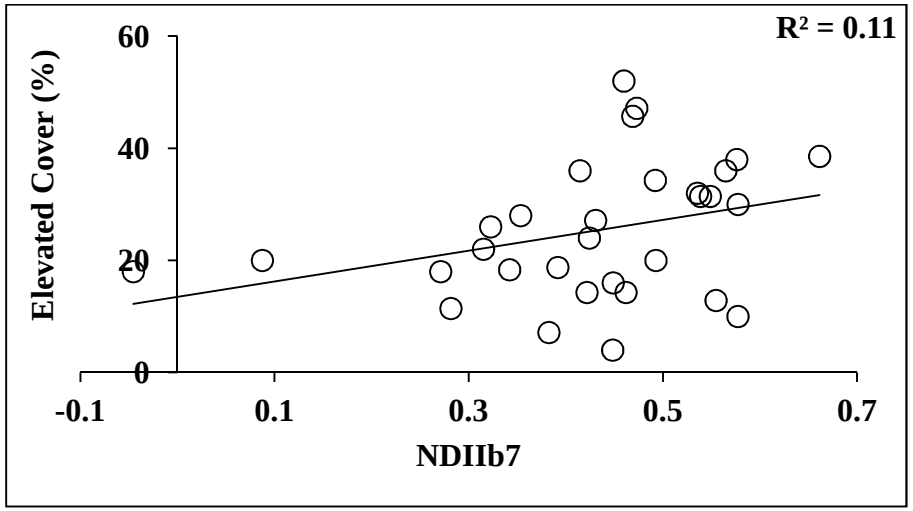
R² = 0.11
60
40
20
0
Elevated Cover (%)
-0.1
0.1
0.3
0.5
0.7
NDIIb7

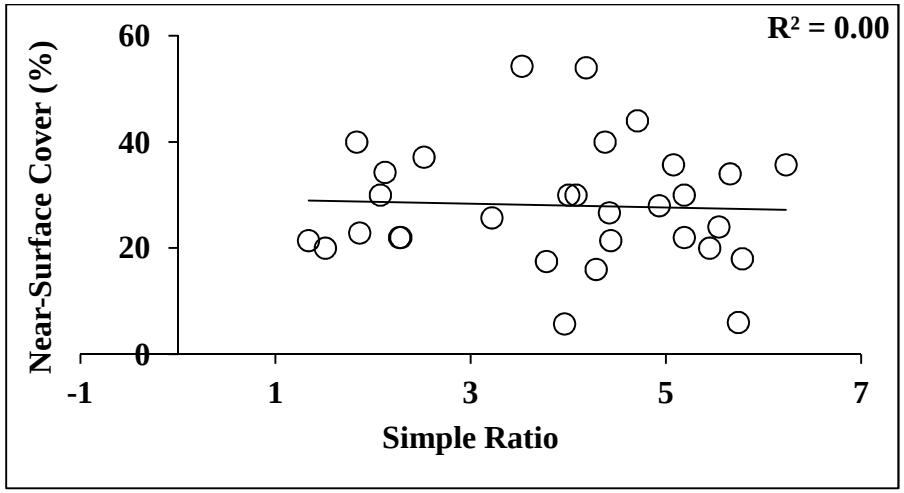
R² = 0.00
Near-Surface Cover (%)
60
40
20
0
-1
1
3
5
7
Simple Ratio

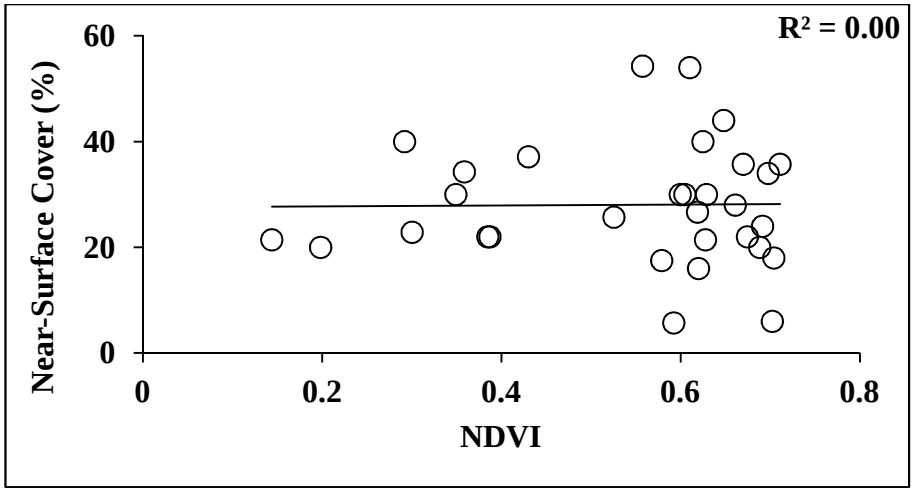
R² = 0.00
Near-Surface Cover (%)
60
40
20
0
0
0.2
0.4
0.6
0.8
NDVI

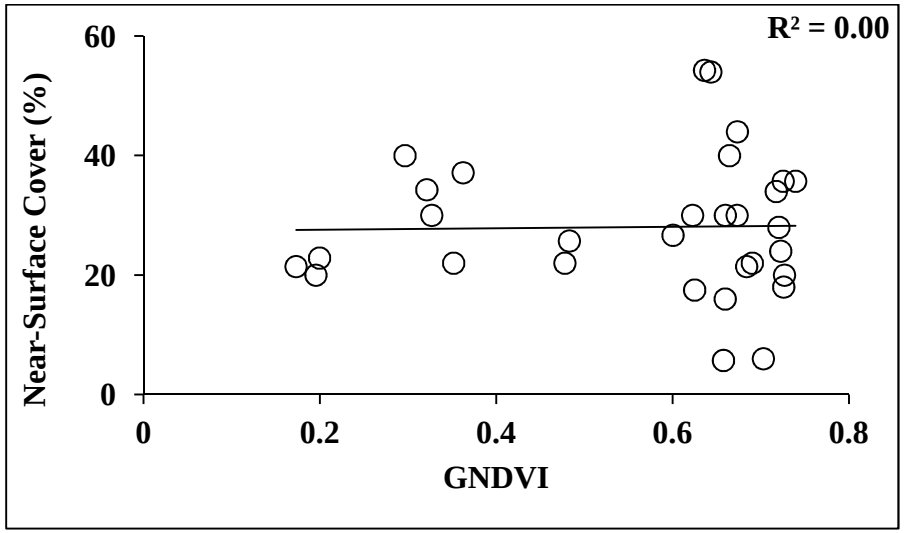
R² = 0.00
Near-Surface Cover (%)
60
40
20
0
0
0.2
0.4
0.6
0.8
GNDVI

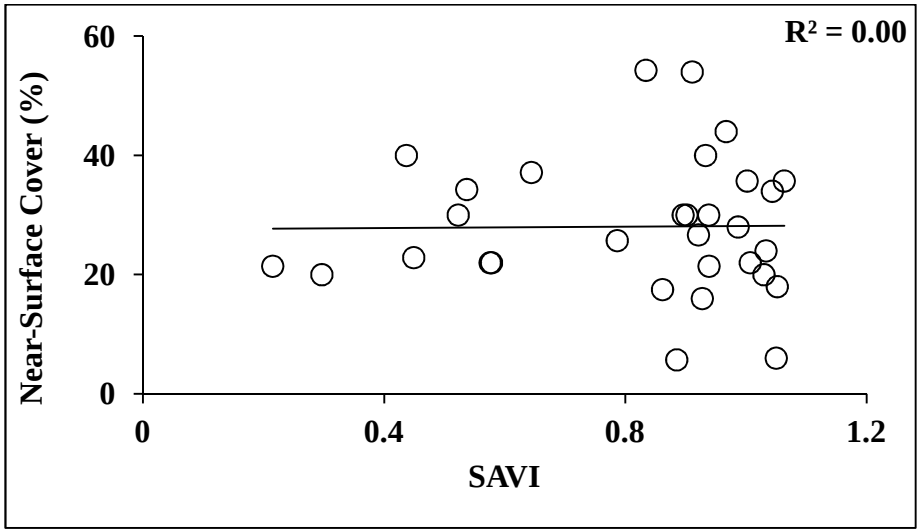
R² = 0.00
Near-Surface Cover (%)
60
40
20
0
0
0.4
0.8
1.2
SAVI

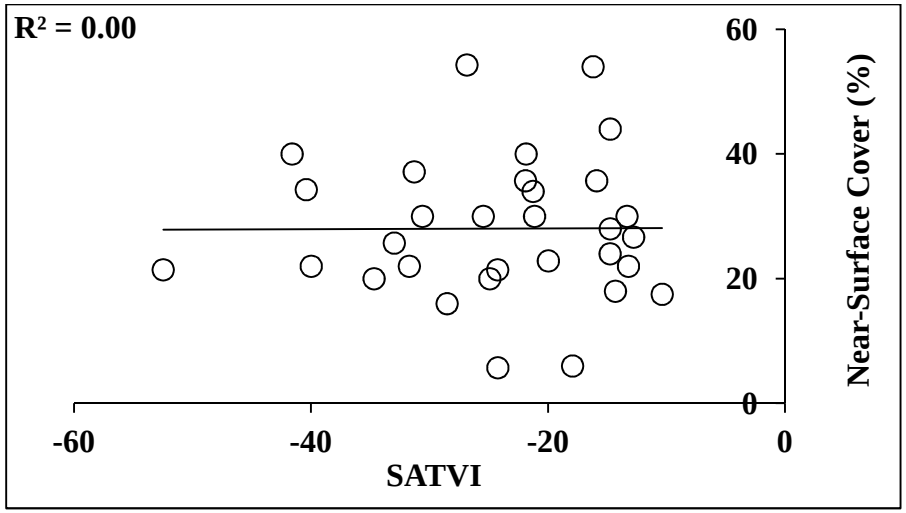
R² = 0.00
60
40
20
0
-60
-40
-20
0
SATVI
Near-Surface Cover (%)

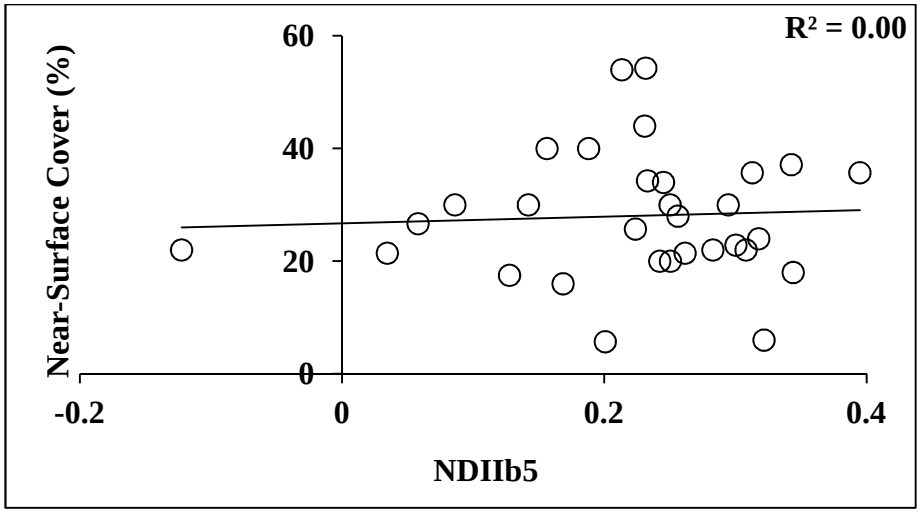
R² = 0.00
60
40
20
0
-0.2
0
0.2
0.4
NDIIb5
Near-Surface Cover (%)

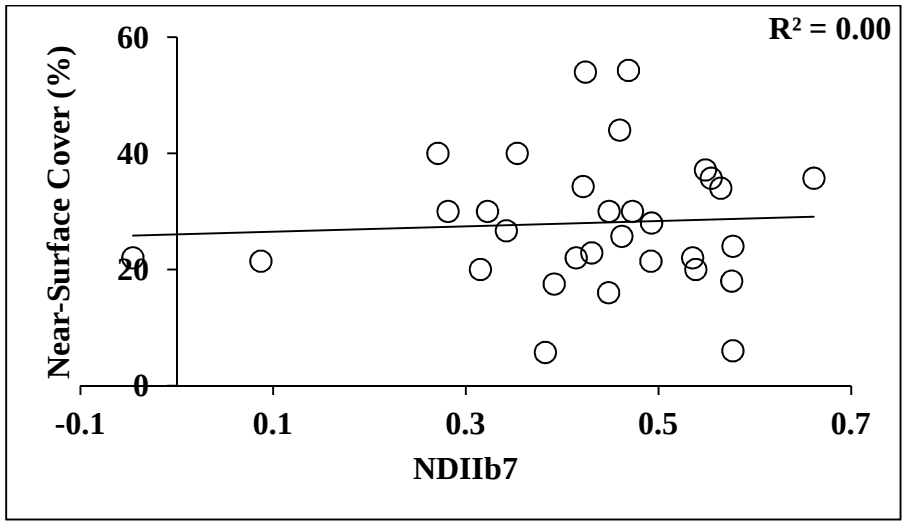
R² = 0.00
60
40
20
0
-0.1
0.1
0.3
0.5
0.7
NDIIb7
Near-Surface Cover (%)

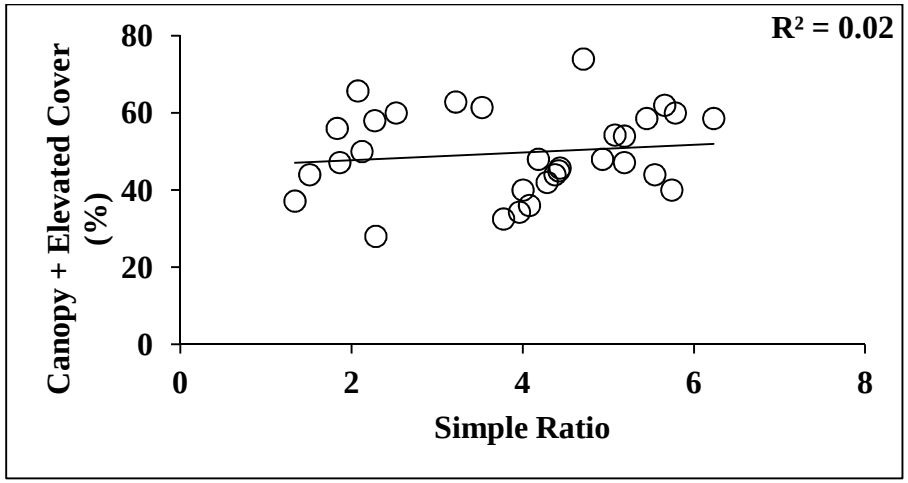
R² = 0.02
Canopy + Elevated Cover (%)
80
60
40
20
0
0
2
4
6
8
Simple Ratio

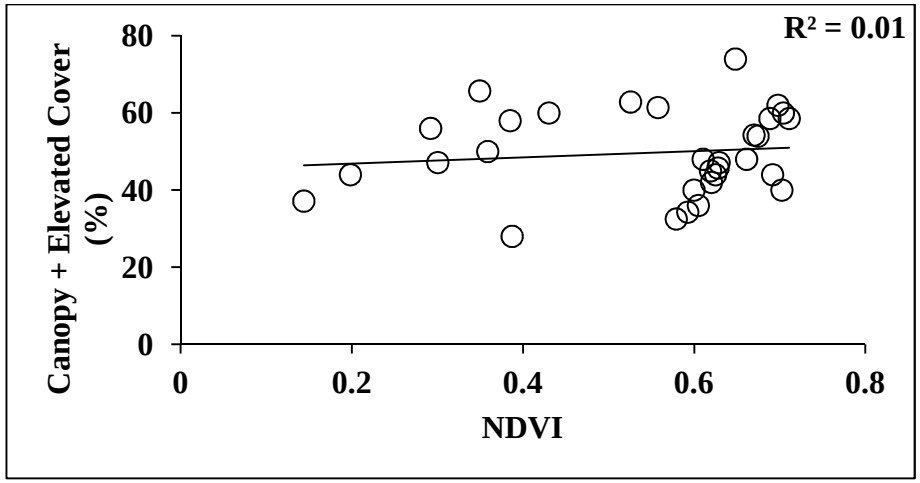
R² = 0.01
Canopy + Elevated Cover (%)
80
60
40
20
0
0
0.2
0.4
0.6
0.8
NDVI

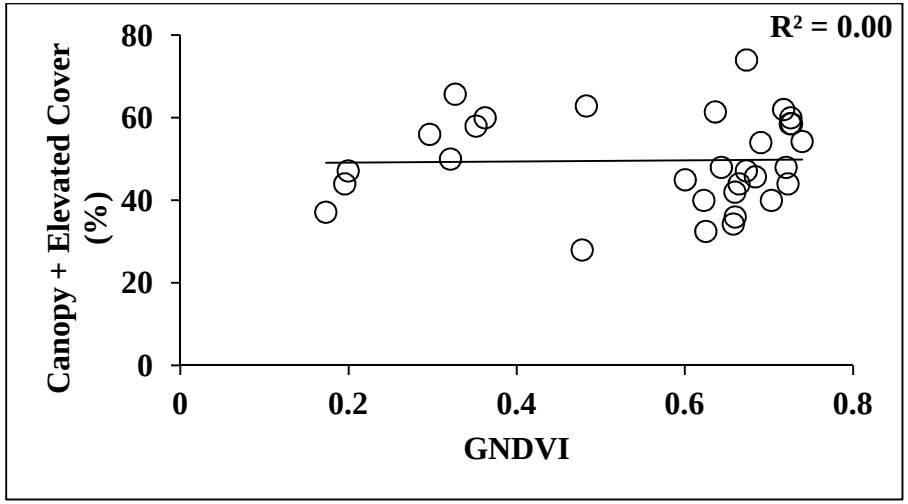
R² = 0.00
Canopy + Elevated Cover (%)
80
60
40
20
0
0
0.2
0.4
0.6
0.8
GNDVI

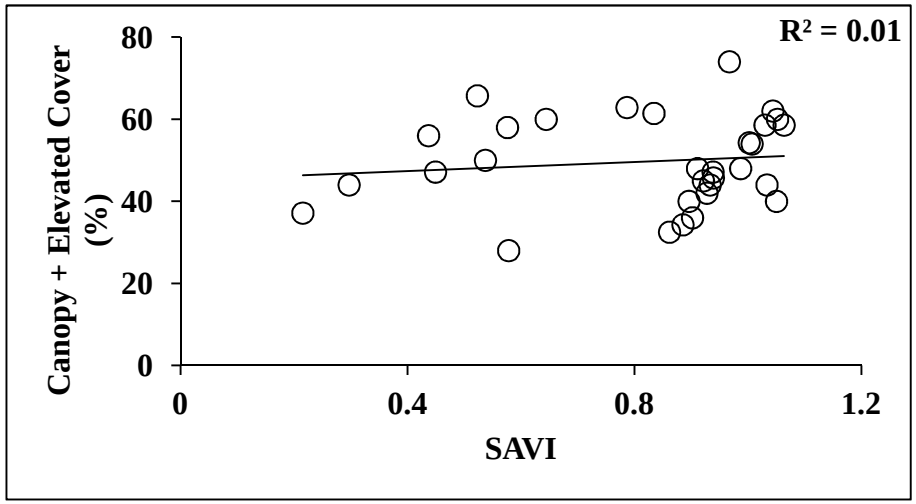
R² = 0.01
Canopy + Elevated Cover (%)
80
60
40
20
0
0
0.4
0.8
1.2
SAVI

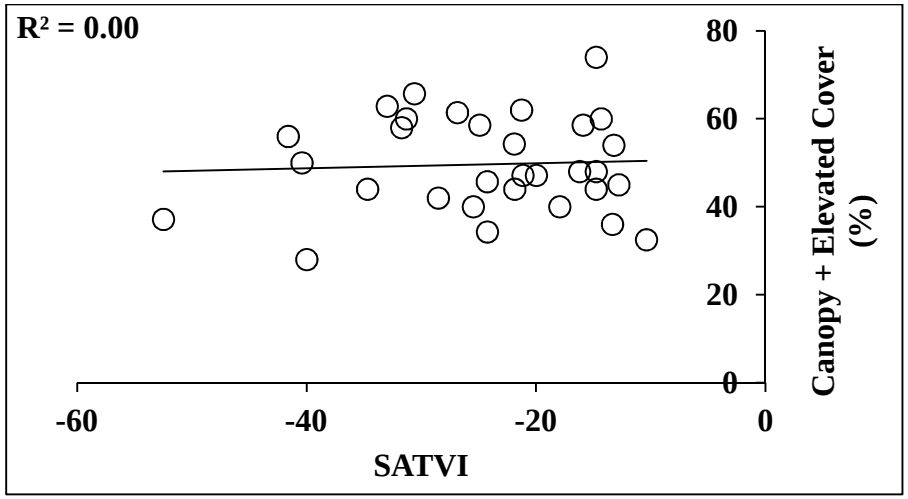
R² = 0.00
80
60
40
20
0
Canopy + Elevated Cover (%)
-60
-40
-20
0
SATVI

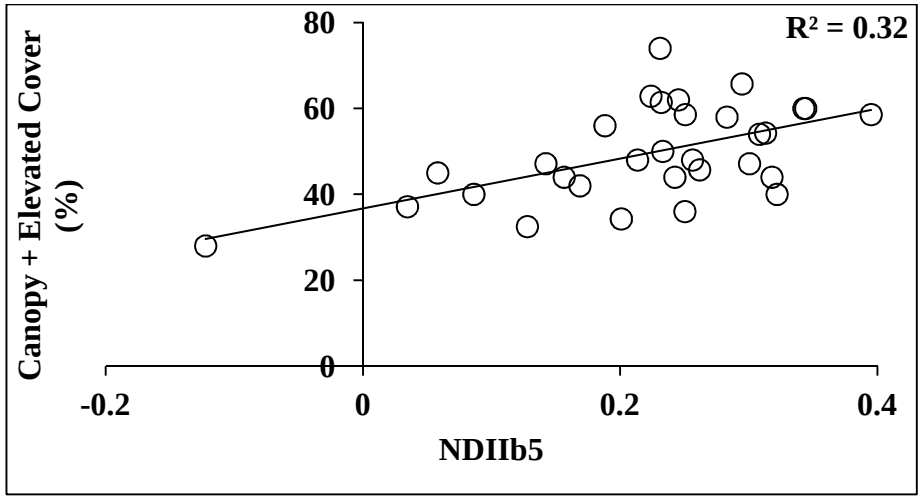
R² = 0.32
80
60
40
20
0
Canopy + Elevated Cover (%)
-0.2
0
0.2
0.4
NDIIb5

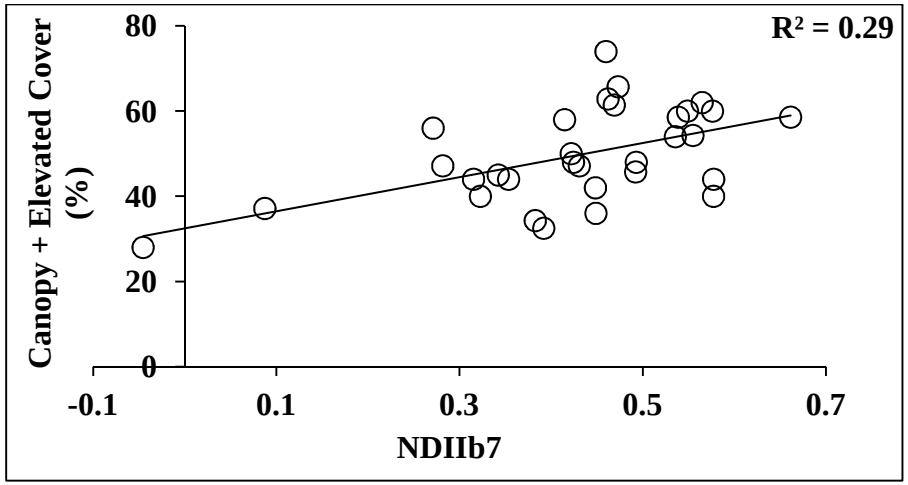
R² = 0.29
80
60
40
20
0
Canopy + Elevated Cover (%)
-0.1
0.1
0.3
0.5
0.7
NDIIb7

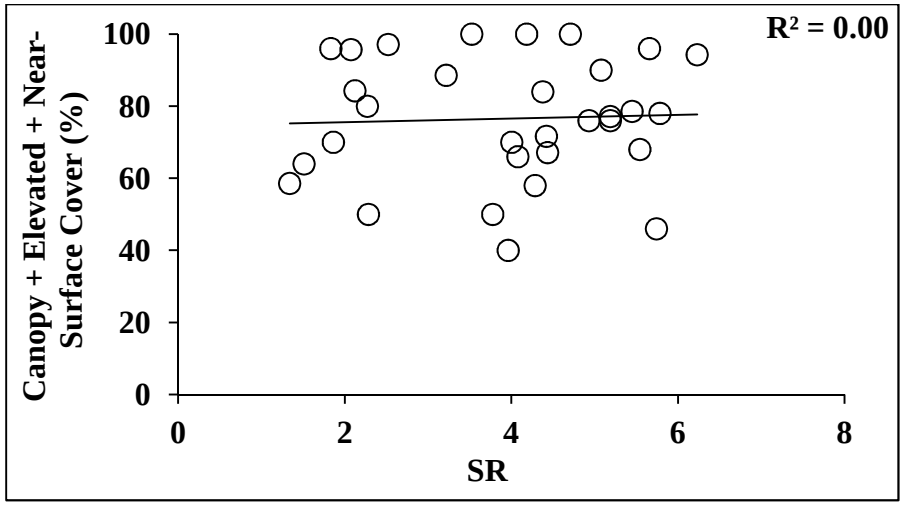
R² = 0.00
Canopy + Elevated + Near-Surface Cover (%)
100
80
60
40
20
0
0
2
4
6
8
SR

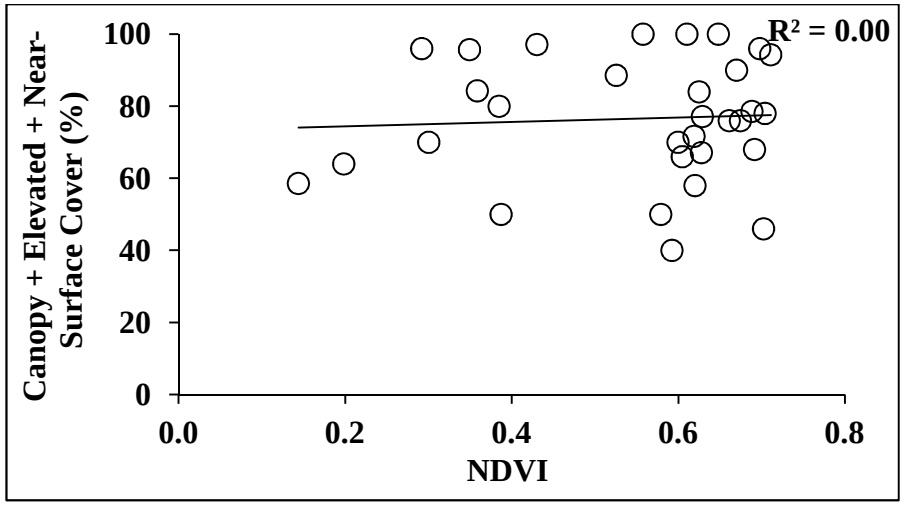
R² = 0.00
Canopy + Elevated + Near-Surface Cover (%)
100
80
60
40
20
0
0.0
0.2
0.4
0.6
0.8
NDVI

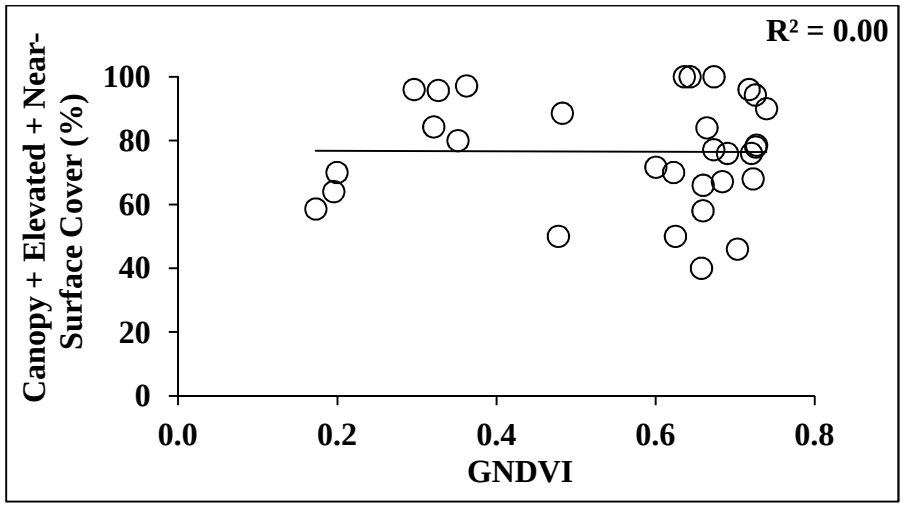
R² = 0.00
Canopy + Elevated + Near-Surface Cover (%)
100
80
60
40
20
0
0.0
0.2
0.4
0.6
0.8
GNDVI

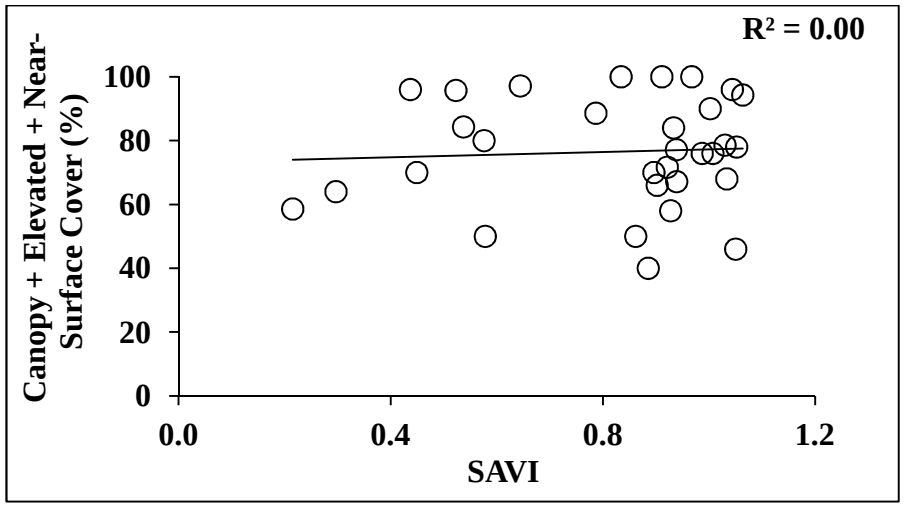
R² = 0.00
Canopy + Elevated + Near-Surface Cover (%)
100
80
60
40
20
0
0.0
0.4
0.8
1.2
SAVI

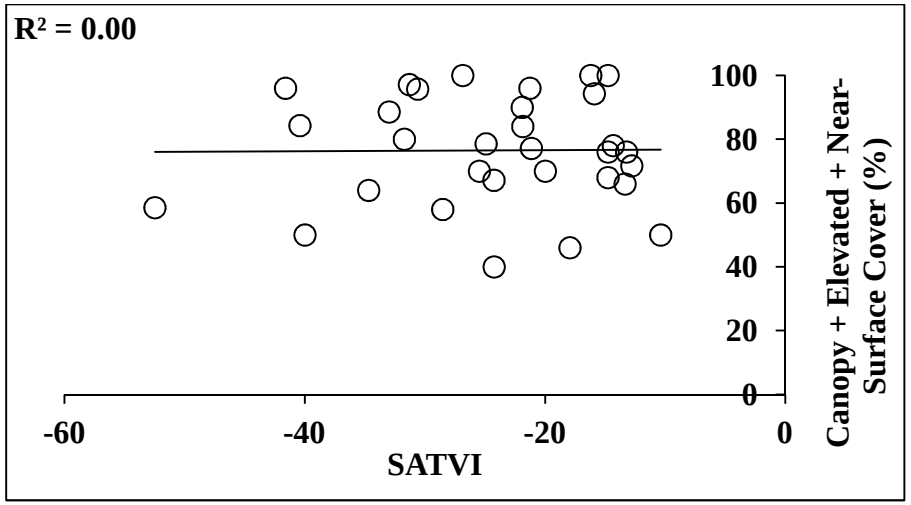
R² = 0.00
100
80
60
40
20
0
-60
-40
-20
0
SATVI
Canopy + Elevated + Near-Surface Cover (%)

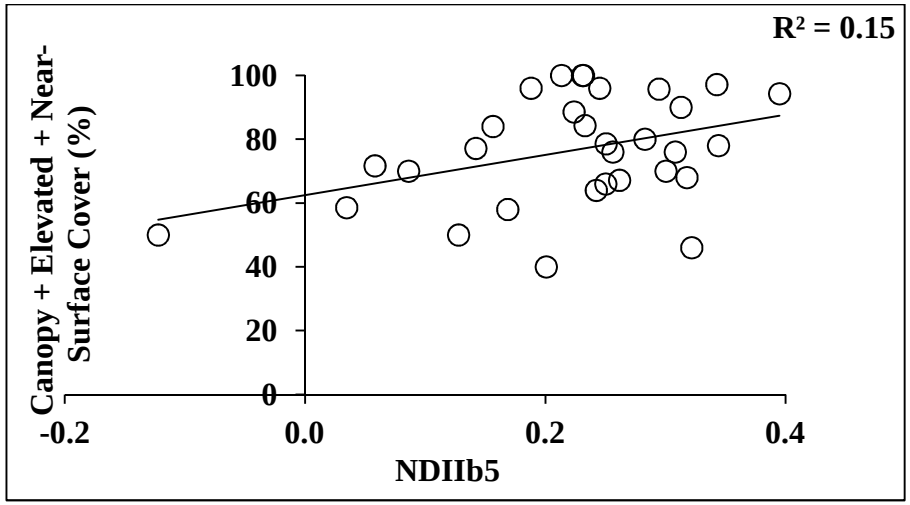
R² = 0.15
100
80
60
40
20
0
-0.2
0.0
0.2
0.4
NDIIb5
Canopy + Elevated + Near-Surface Cover (%)

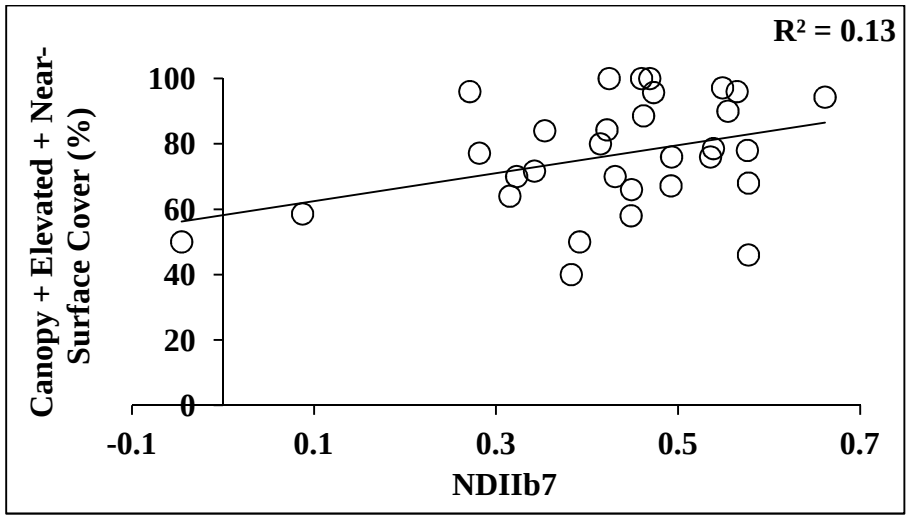
R² = 0.13
100
80
60
40
20
0
-0.1
0.1
0.3
0.5
0.7
NDIIb7
Canopy + Elevated + Near-Surface Cover (%)

Approach 1: Live Fuel Only

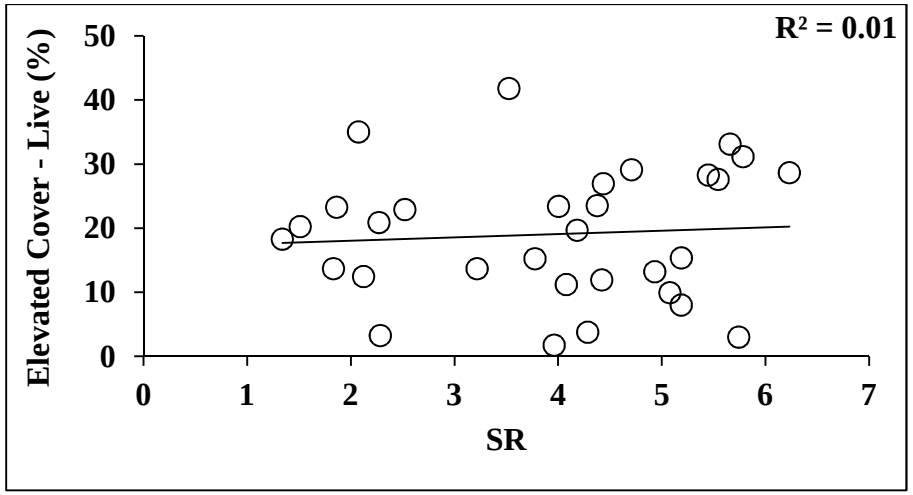

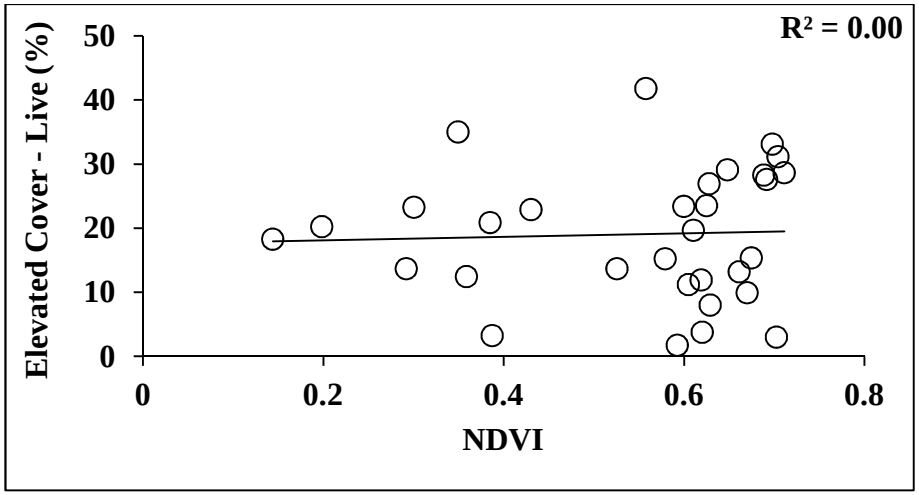

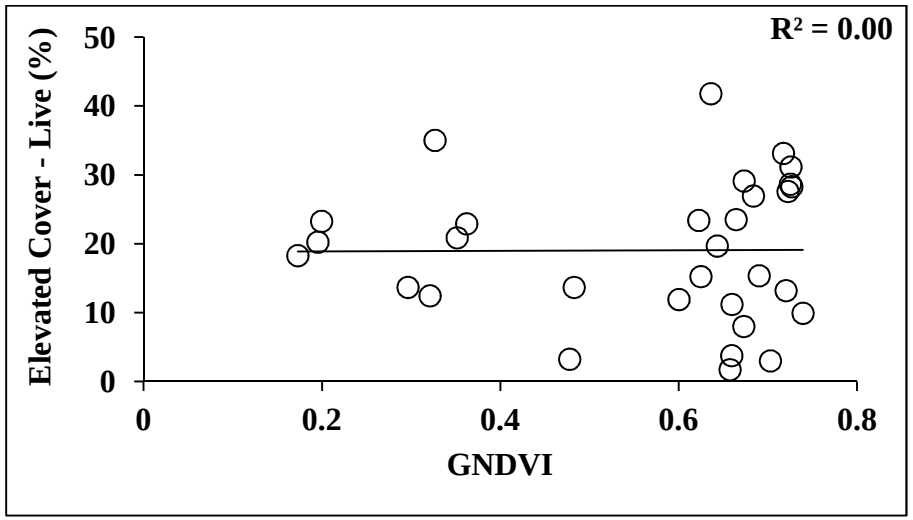

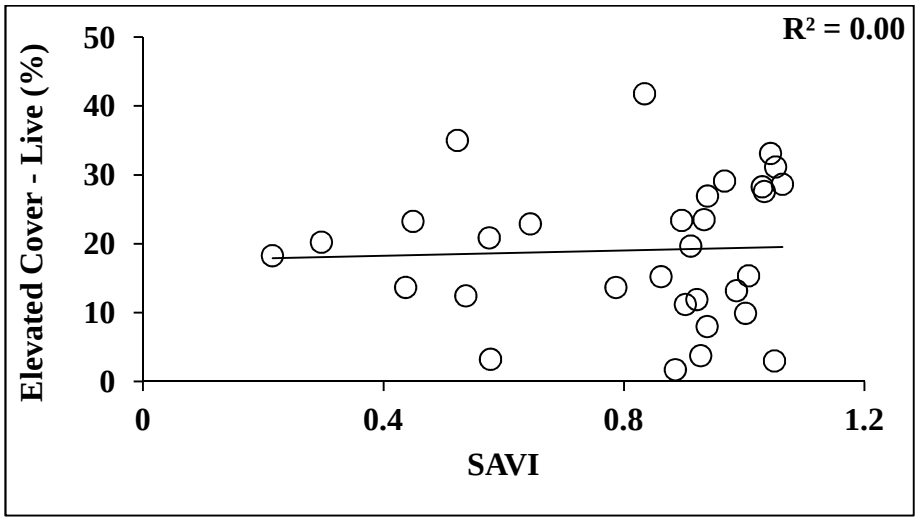

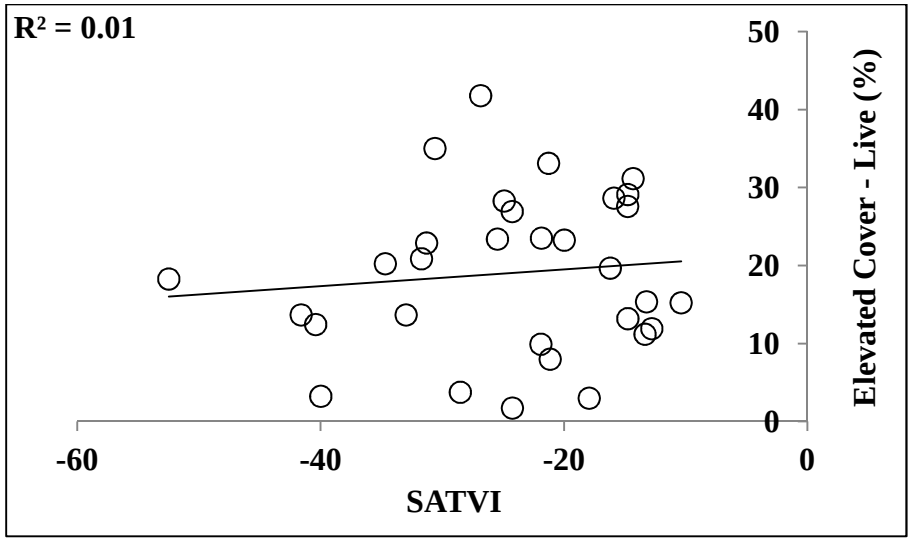
R² = 0.01
50
40
30
20
10
0
Elevated Cover - Live (%)
-60
-40
-20
0
SATVI

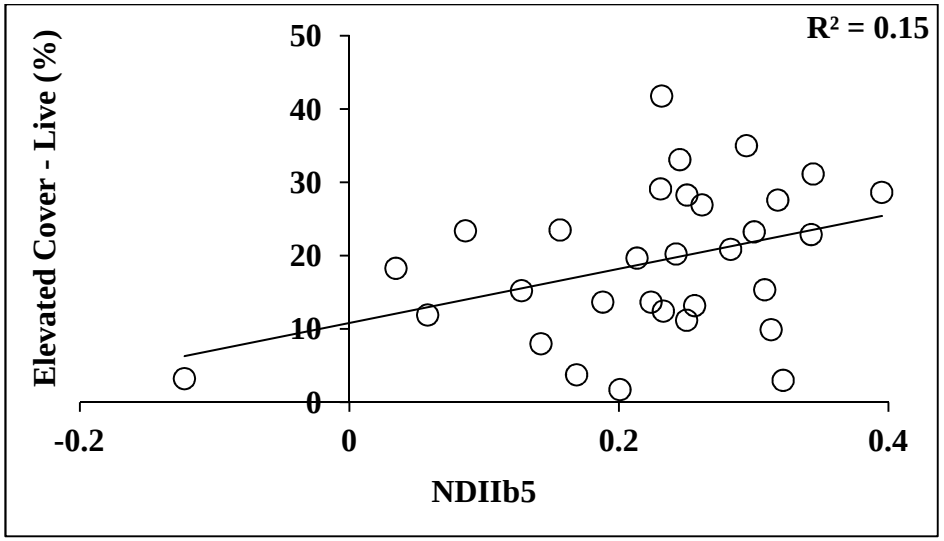
R² = 0.15
50
40
30
20
10
0
Elevated Cover - Live (%)
-0.2
0
0.2
0.4
NDIIb5

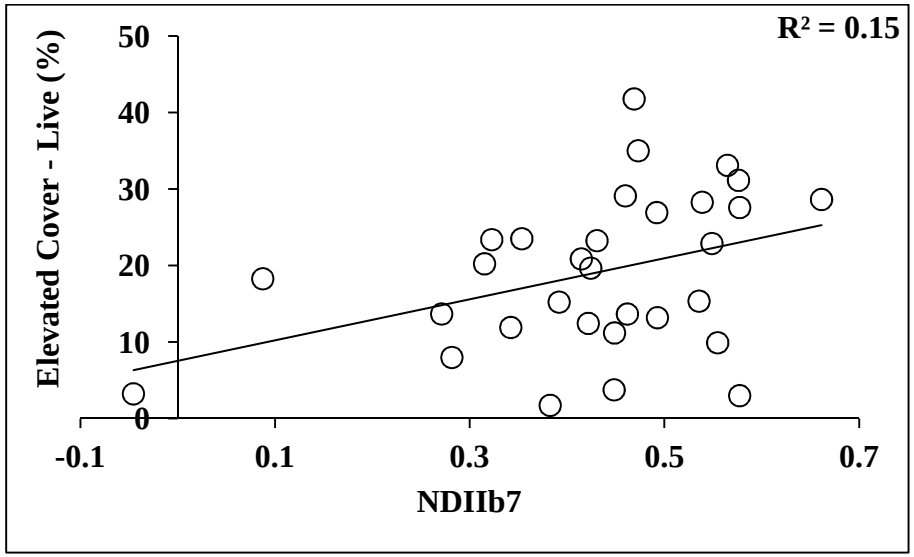
R² = 0.15
50
40
30
20
10
0
Elevated Cover - Live (%)
-0.1
0.1
0.3
0.5
0.7
NDIIb7

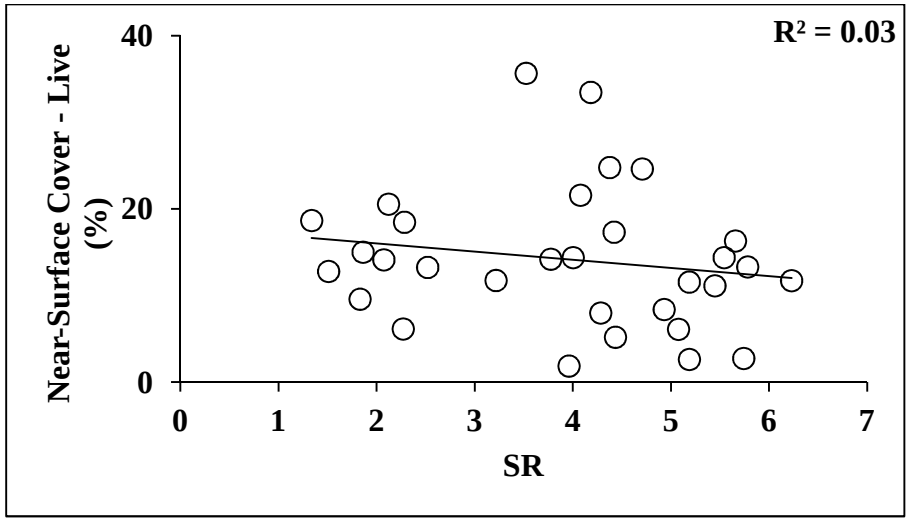
R² = 0.03
Near-Surface Cover - Live (%)
40
20
0
0
1
2
3
4
5
6
7
SR

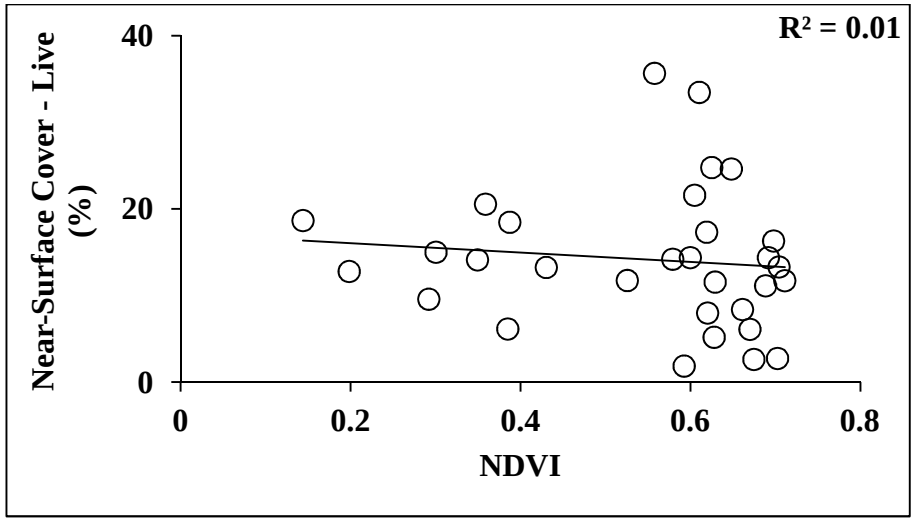
R² = 0.01
Near-Surface Cover - Live (%)
40
20
0
0
0.2
0.4
0.6
0.8
NDVI

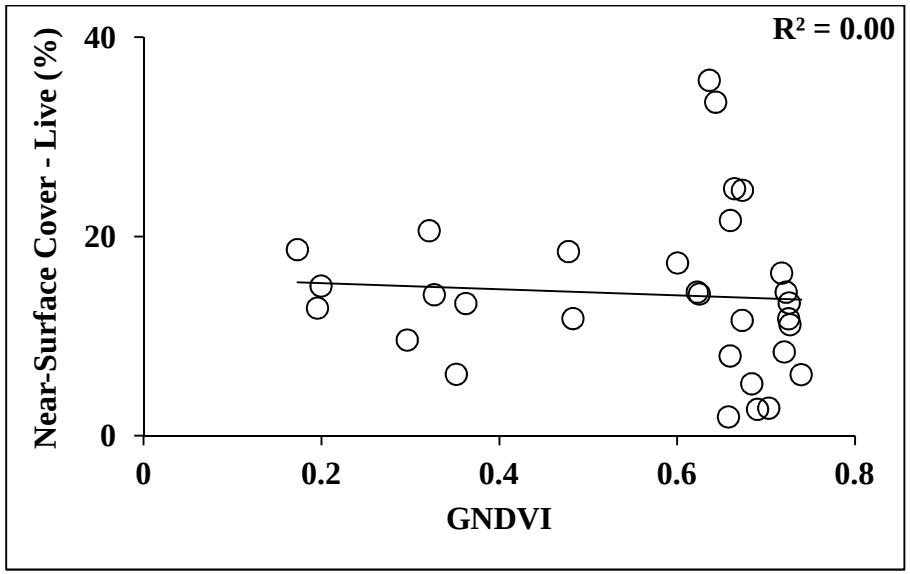
R² = 0.00
Near-Surface Cover - Live (%)
40
20
0
0
0.2
0.4
0.6
0.8
GNDVI

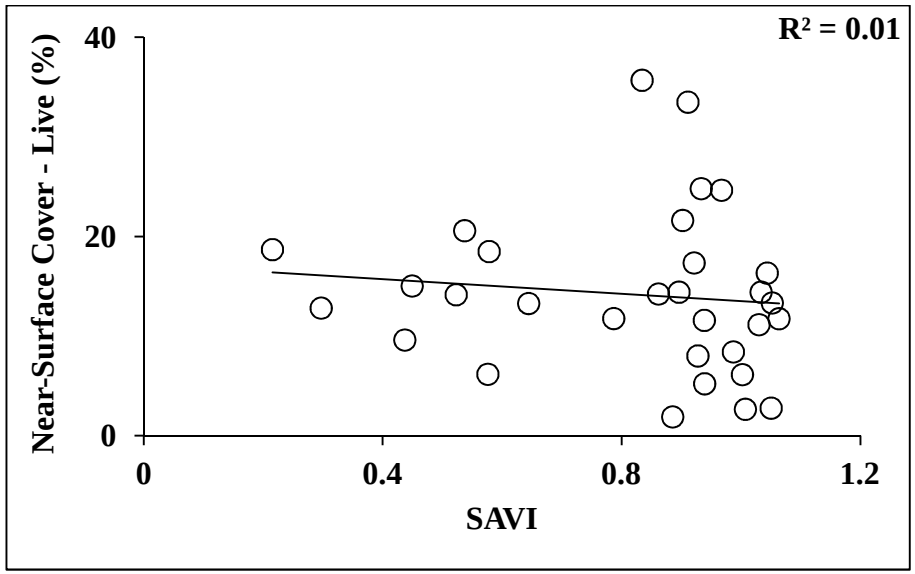
R² = 0.01
Near-Surface Cover - Live (%)
40
20
0
0
0.4
0.8
1.2
SAVI

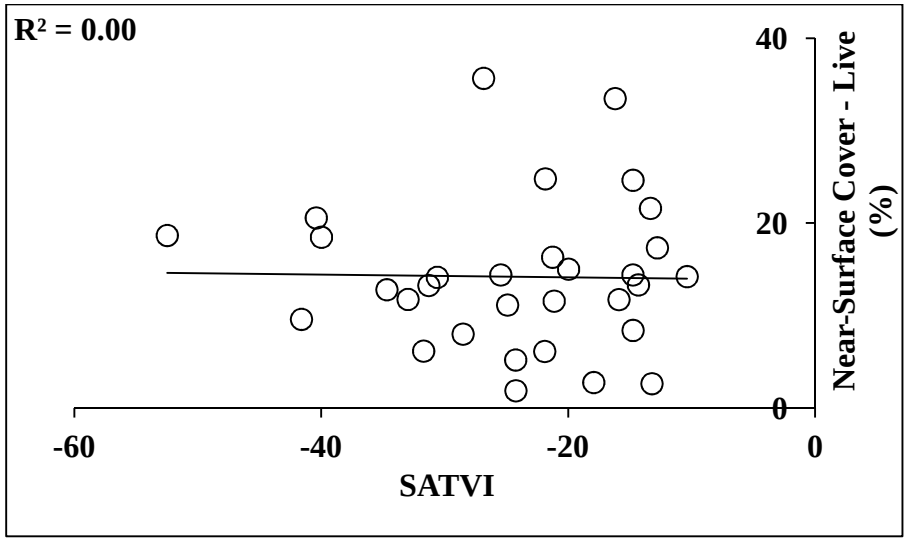
R² = 0.00
40
20
0
Near-Surface Cover - Live (%)
-60
-40
-20
0
SATVI

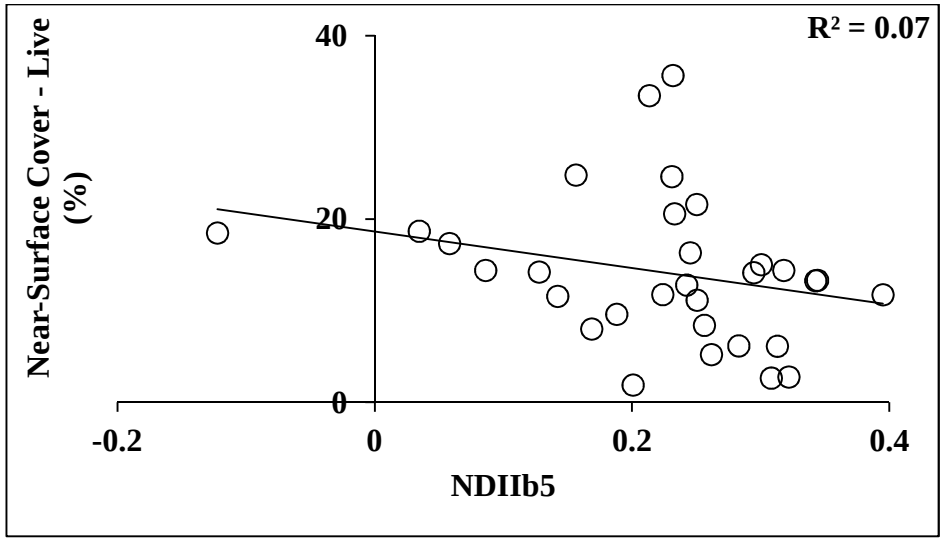
R² = 0.07
40
20
0
Near-Surface Cover - Live (%)
-0.2
0
0.2
0.4
NDIIb5

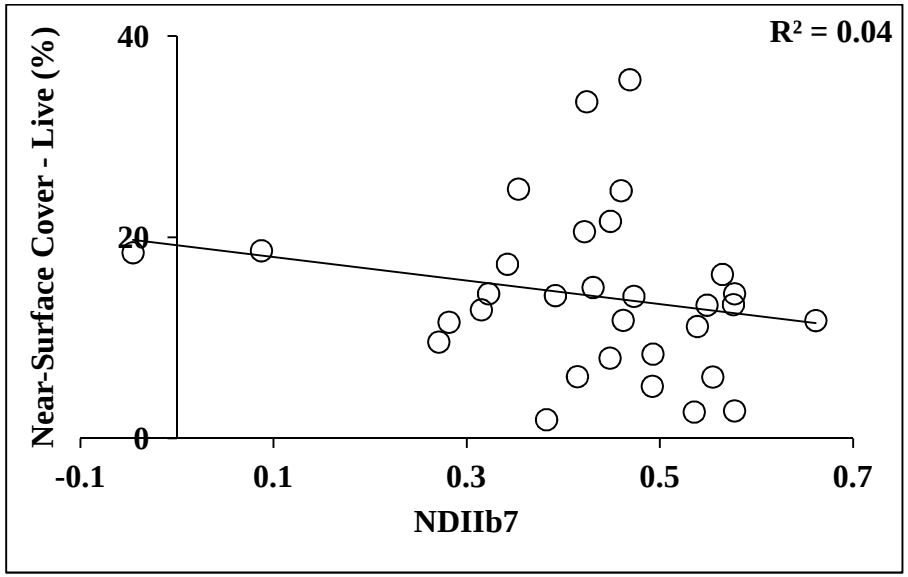
R² = 0.04
40
20
0
Near-Surface Cover - Live (%)
-0.1
0.1
0.3
0.5
0.7
NDIIb7

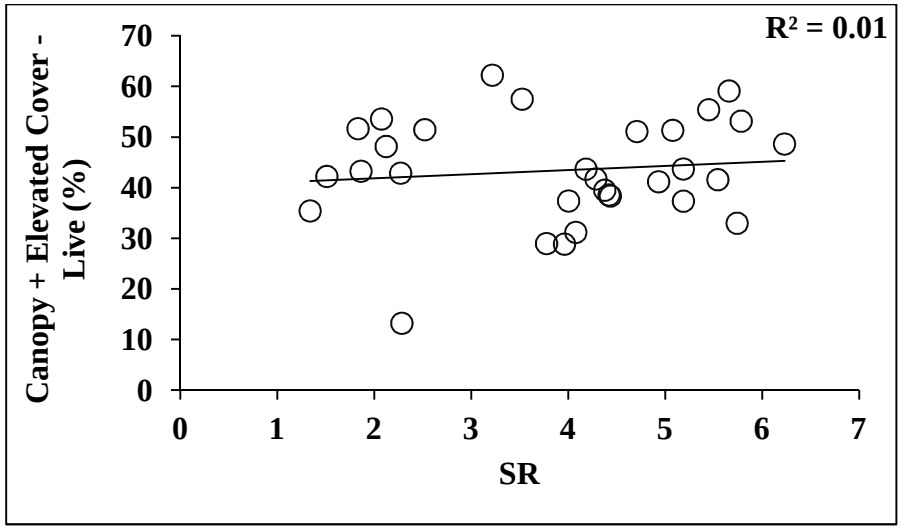
R² = 0.01
Canopy + Elevated Cover - Live (%)
70
60
50
40
30
20
10
0
0
1
2
3
4
5
6
7
SR

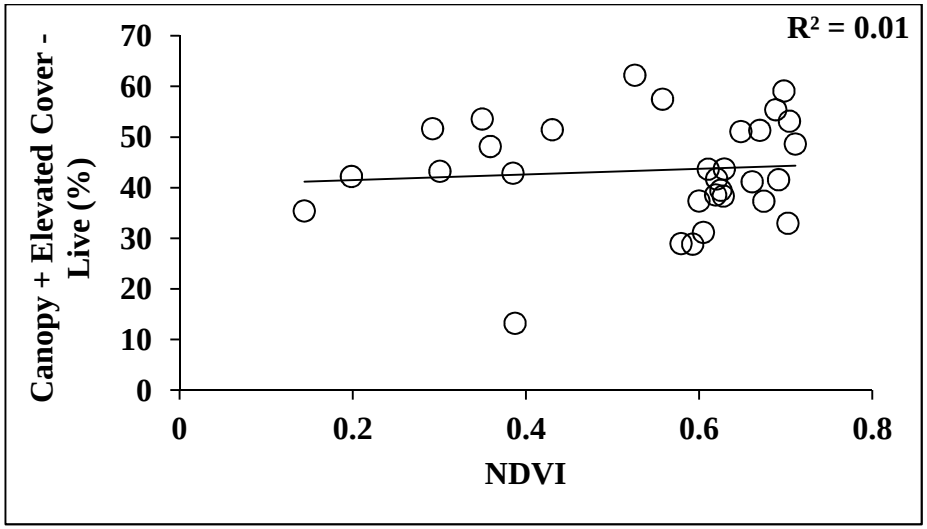
R² = 0.01
Canopy + Elevated Cover - Live (%)
70
60
50
40
30
20
10
0
0
0.2
0.4
0.6
0.8
NDVI

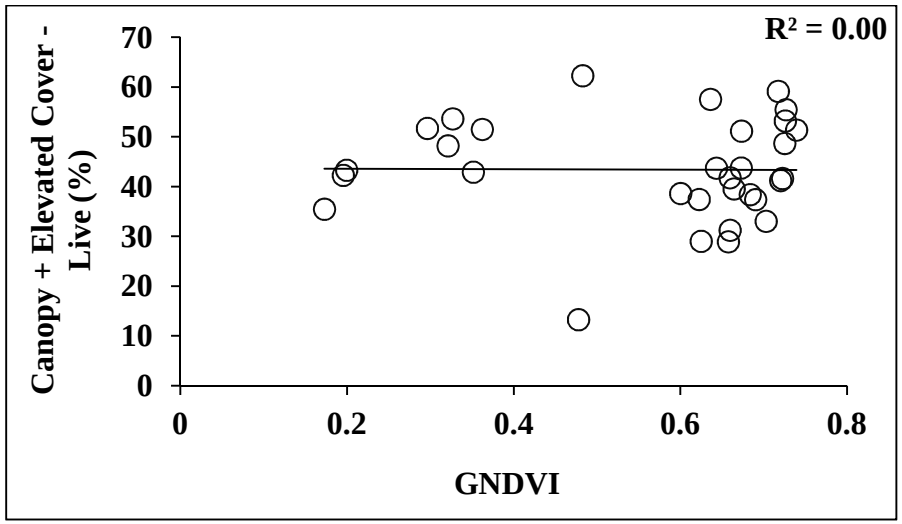
R² = 0.00
Canopy + Elevated Cover - Live (%)
70
60
50
40
30
20
10
0
0
0.2
0.4
0.6
0.8
GNDVI

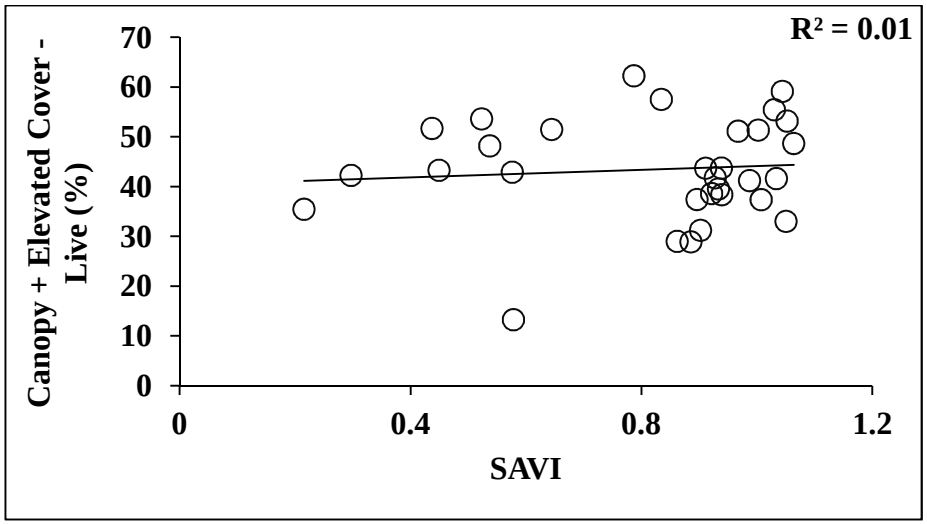
R² = 0.01
Canopy + Elevated Cover - Live (%)
70
60
50
40
30
20
10
0
0
0.4
0.8
1.2
SAVI

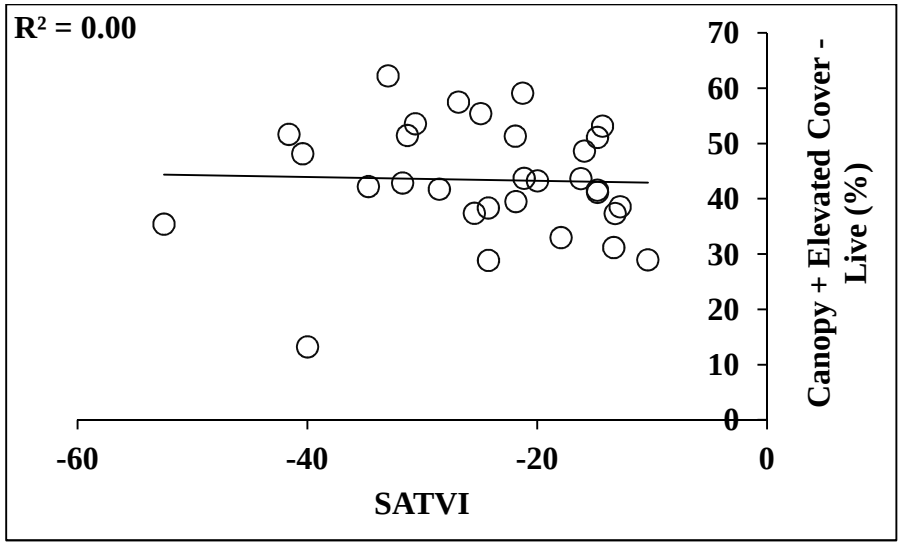
R² = 0.00
70
60
50
40
30
20
10
0
-60
-40
-20
0
SATVI
Canopy + Elevated Cover - Live (%)

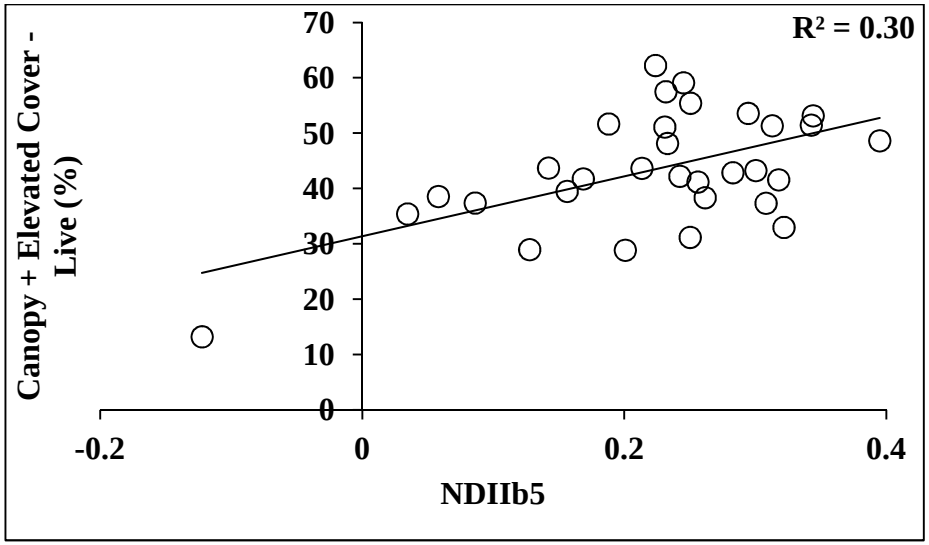
R² = 0.30
70
60
50
40
30
20
10
0
-0.2
0
0.2
0.4
NDIIb5
Canopy + Elevated Cover - Live (%)

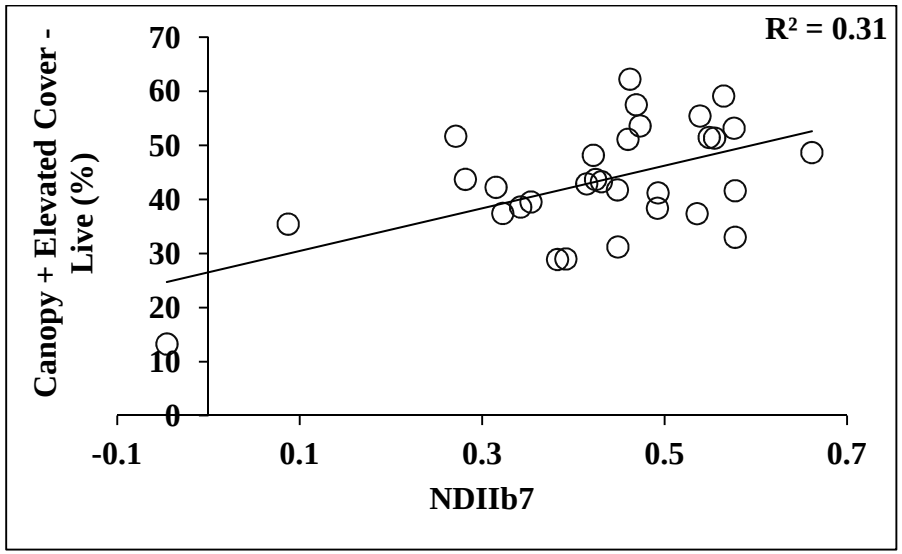
R² = 0.31
70
60
50
40
30
20
10
0
-0.1
0.1
0.3
0.5
0.7
NDIIb7
Canopy + Elevated Cover - Live (%)

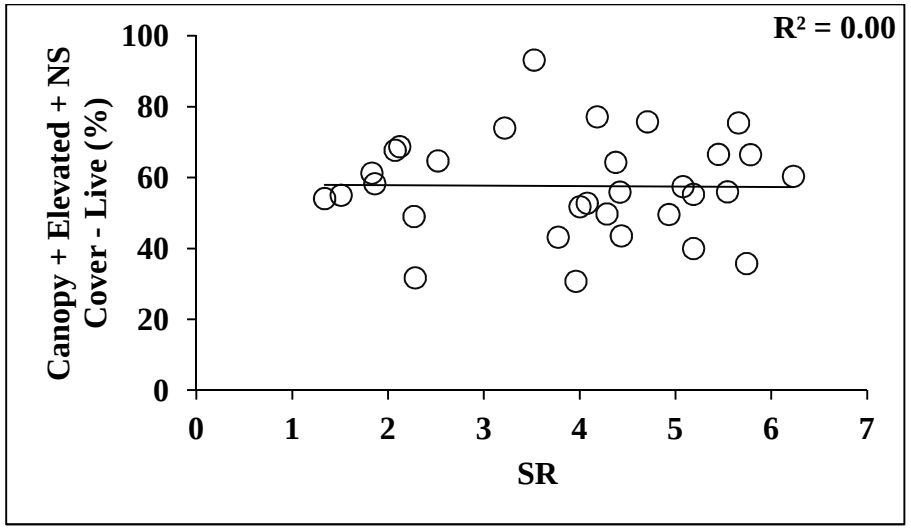
R² = 0.00
Canopy + Elevated + NS Cover - Live (%)
100
80
60
40
20
0
0
1
2
3
4
5
6
7
SR

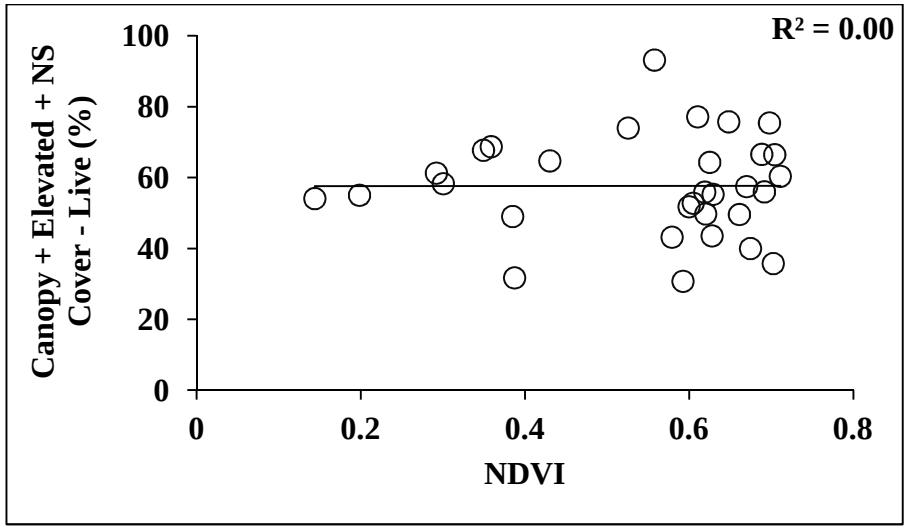
R² = 0.00
Canopy + Elevated + NS Cover - Live (%)
100
80
60
40
20
0
0
0.2
0.4
0.6
0.8
NDVI

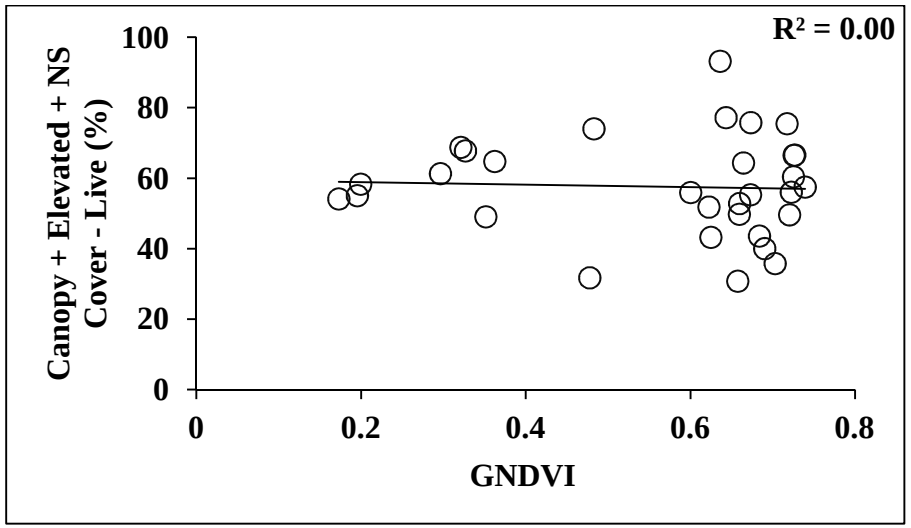
R² = 0.00
Canopy + Elevated + NS Cover - Live (%)
100
80
60
40
20
0
0
0.2
0.4
0.6
0.8
GNDVI

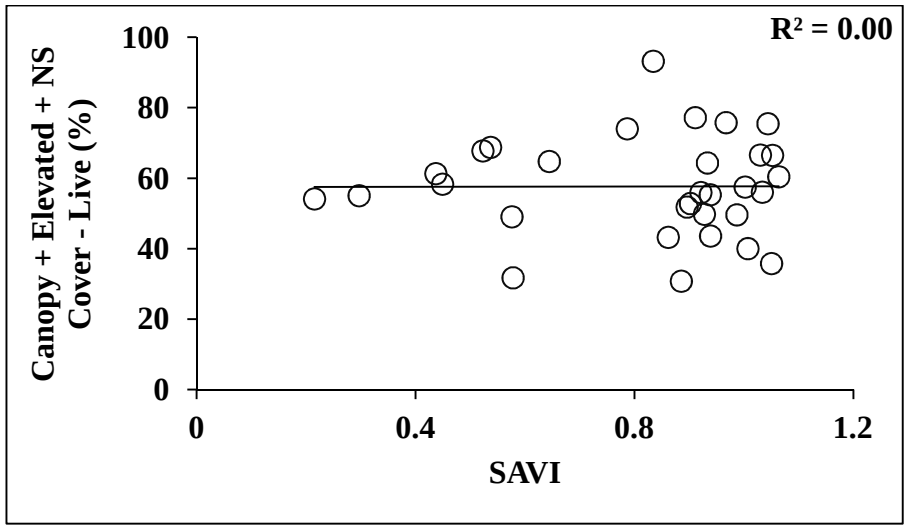
R² = 0.00
Canopy + Elevated + NS Cover - Live (%)
100
80
60
40
20
0
0
0.4
0.8
1.2
SAVI

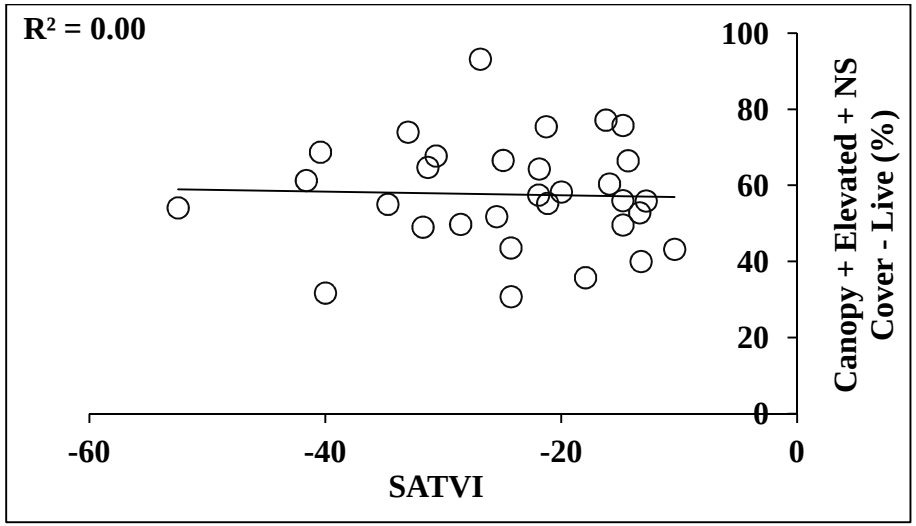
R² = 0.00
100
80
60
40
20
0
-60
-40
-20
0
SATVI
Canopy + Elevated + NS Cover - Live (%)

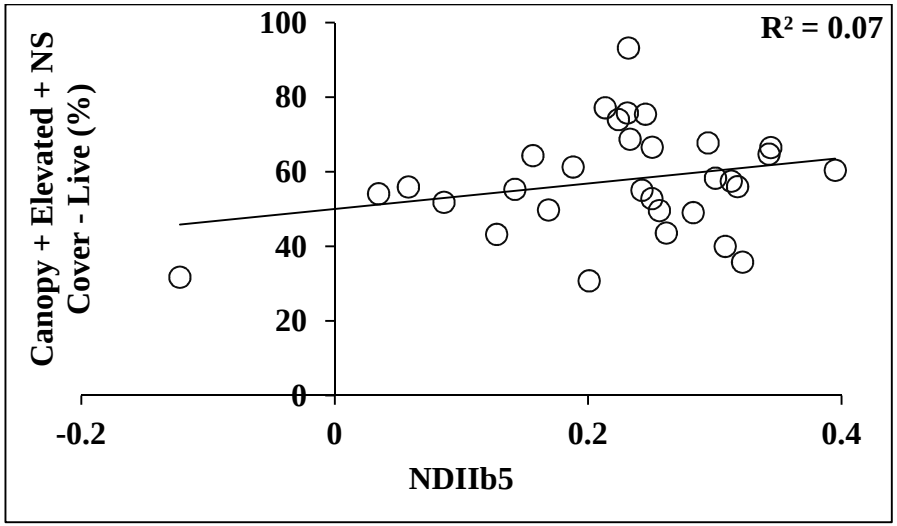
R² = 0.07
100
80
60
40
20
0
-0.2
0
0.2
0.4
NDIIb5
Canopy + Elevated + NS Cover - Live (%)

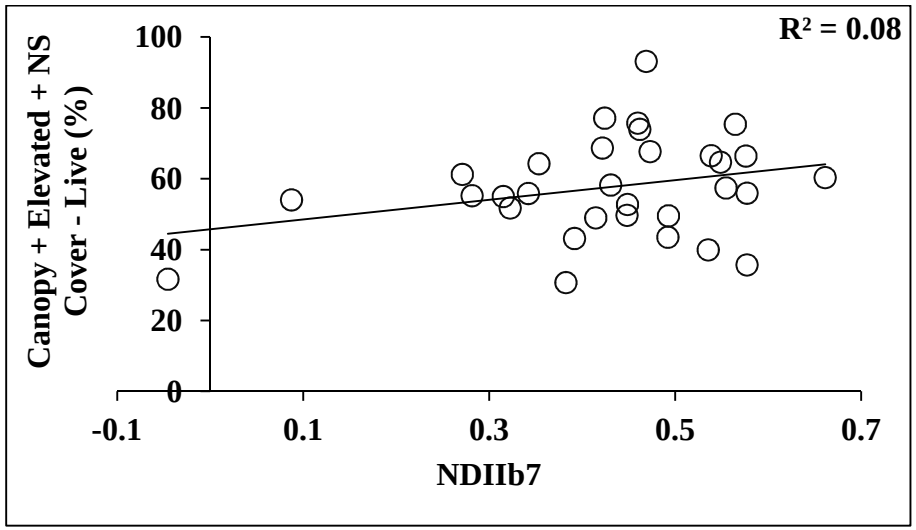
R² = 0.08
100
80
60
40
20
0
-0.1
0.1
0.3
0.5
0.7
NDIIb7
Canopy + Elevated + NS Cover - Live (%)

Approach 2: Live and Dead Fuel

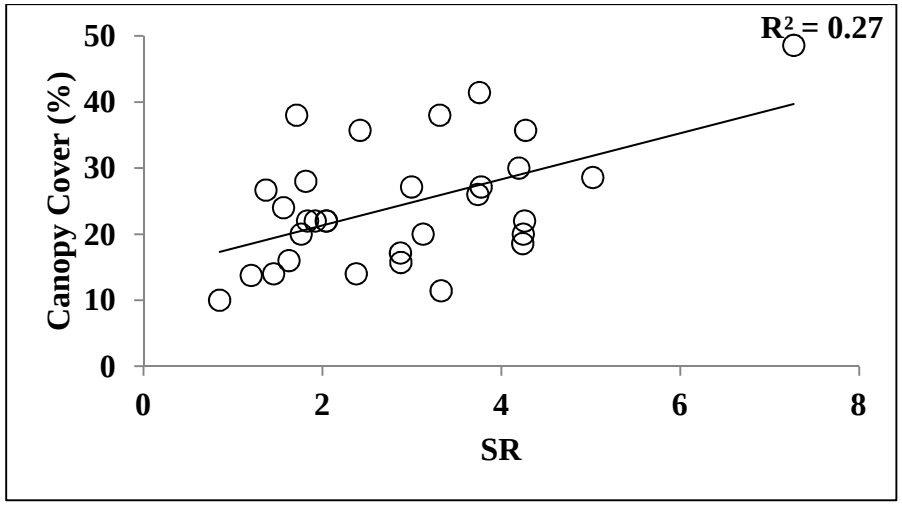

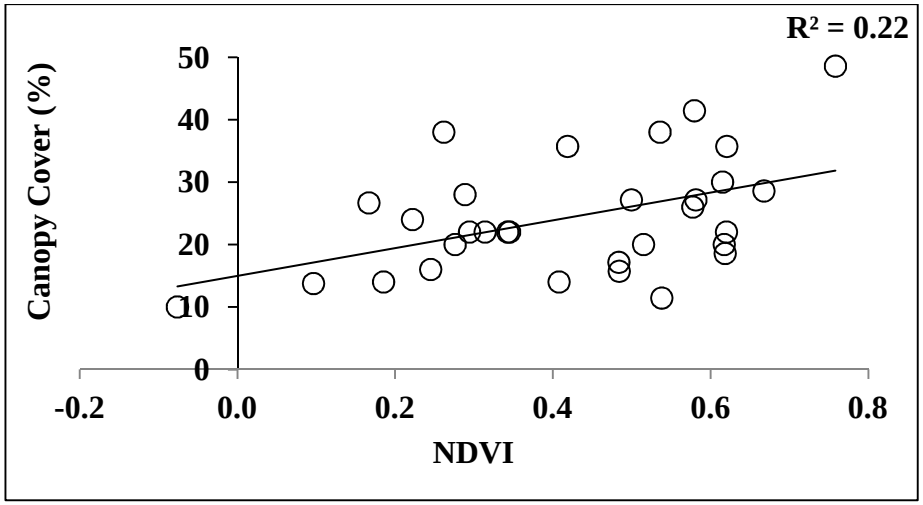

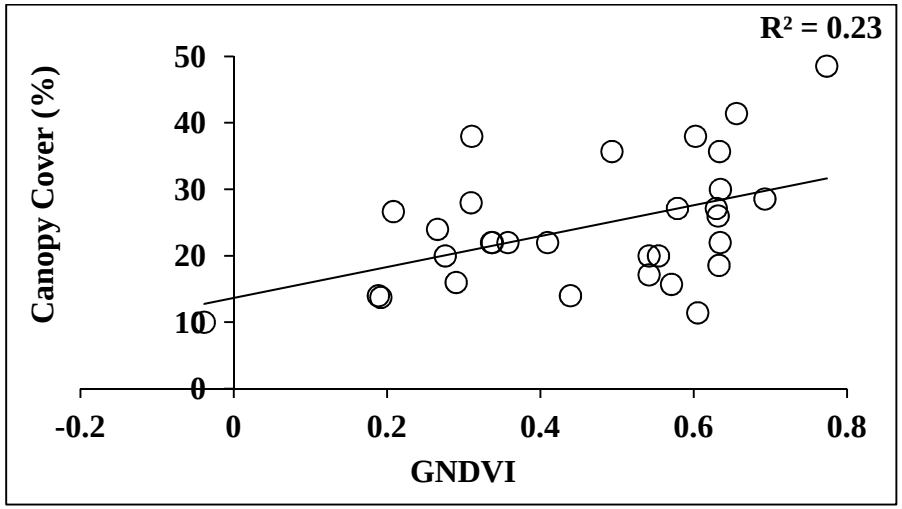

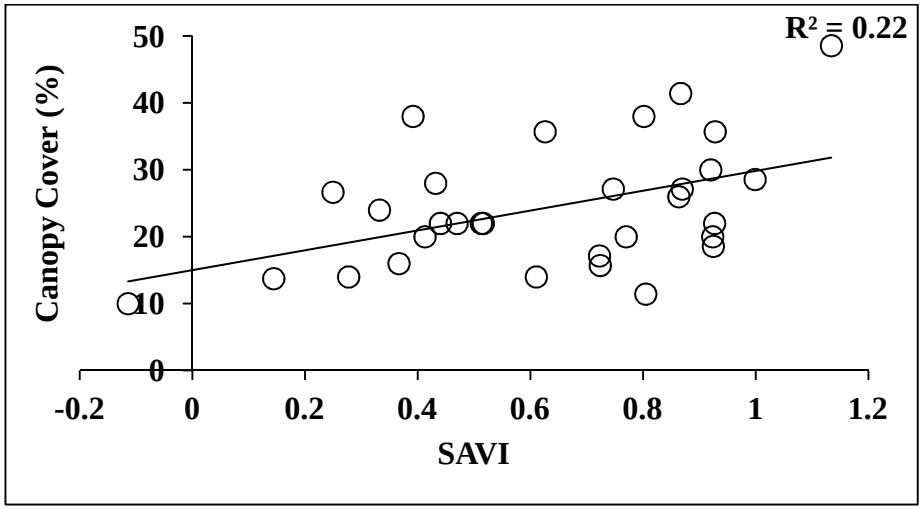

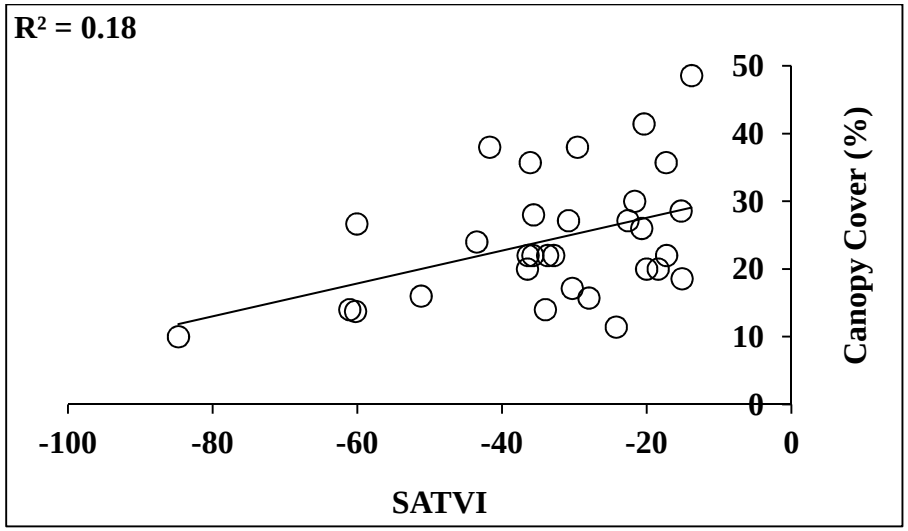
R² = 0.18
Canopy Cover (%)
50
40
30
20
10
0
-100
-80
-60
-40
-20
0
SATVI

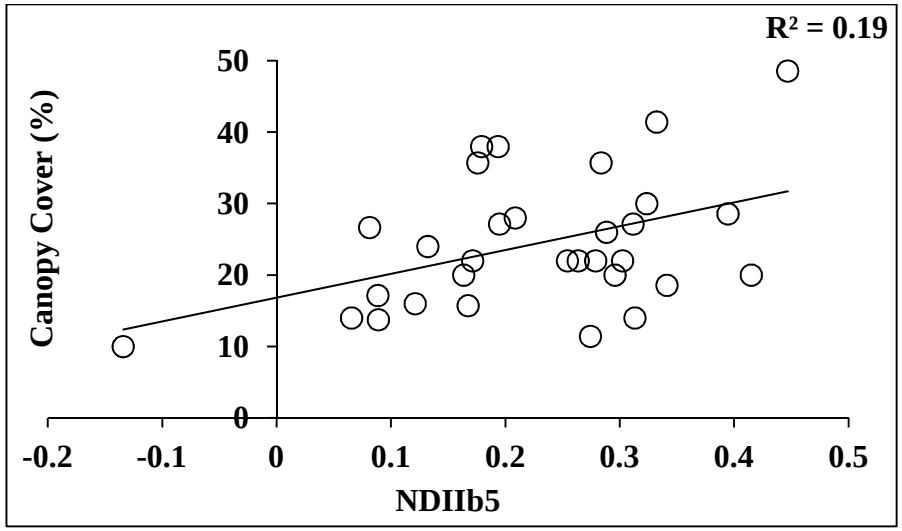
R² = 0.19
Canopy Cover (%)
50
40
30
20
10
0
-0.2
-0.1
0
0.1
0.2
0.3
0.4
0.5
NDIIb5

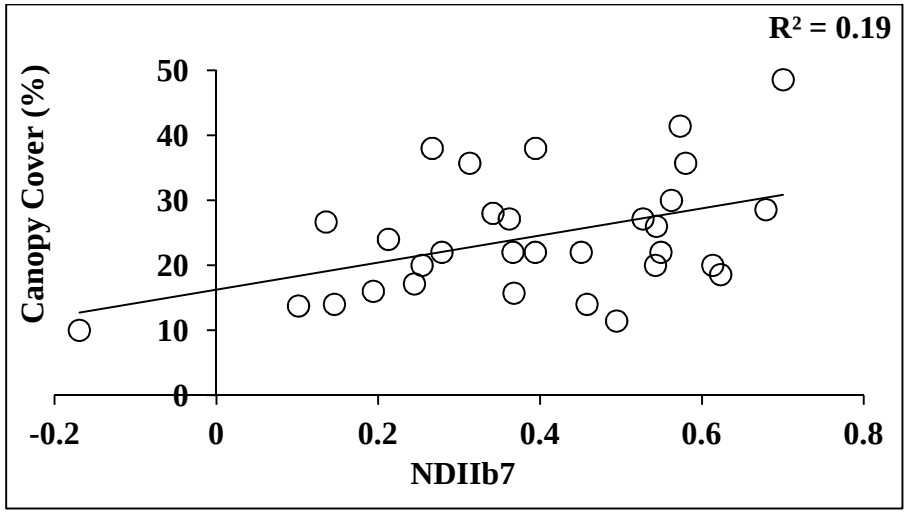
R² = 0.19
Canopy Cover (%)
50
40
30
20
10
0
-0.2
0
0.2
0.4
0.6
0.8
NDIIb7

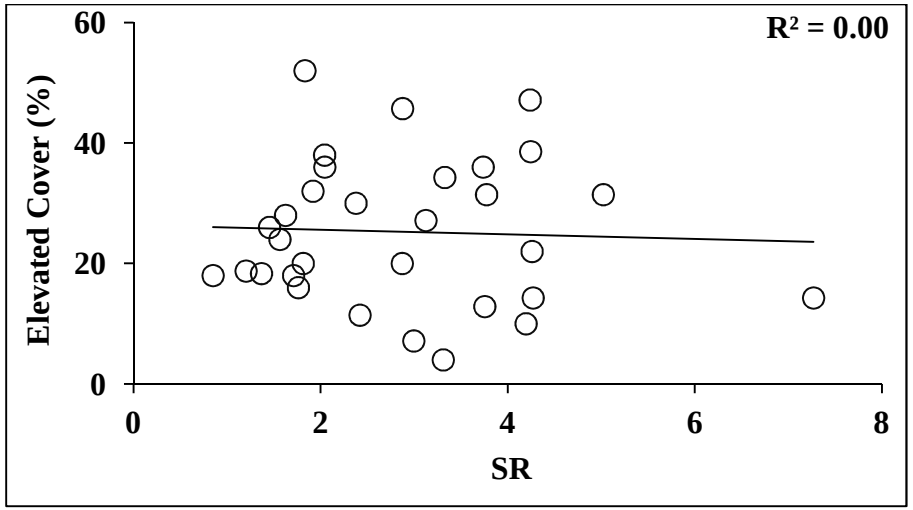
R² = 0.00
Elevated Cover (%)
60
40
20
0
0
2
4
6
8
SR

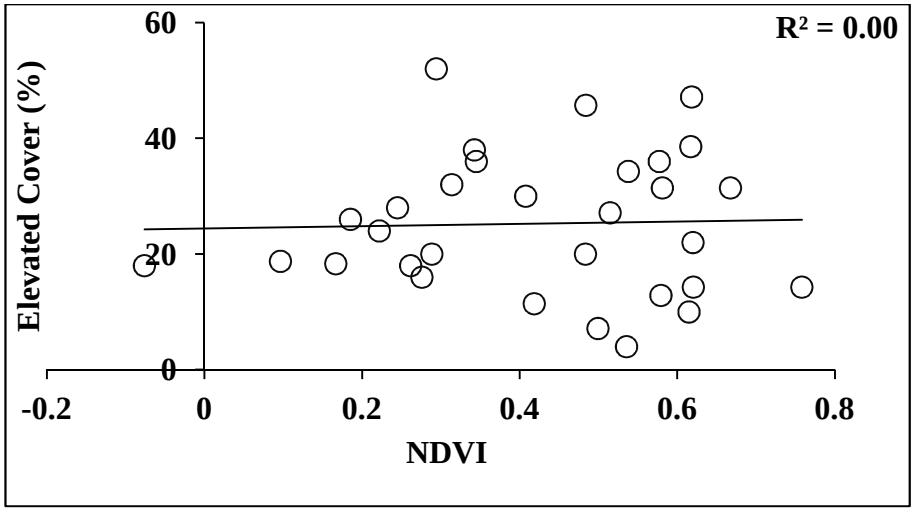
R² = 0.00
Elevated Cover (%)
60
40
20
0
-0.2
0
0.2
0.4
0.6
0.8
NDVI

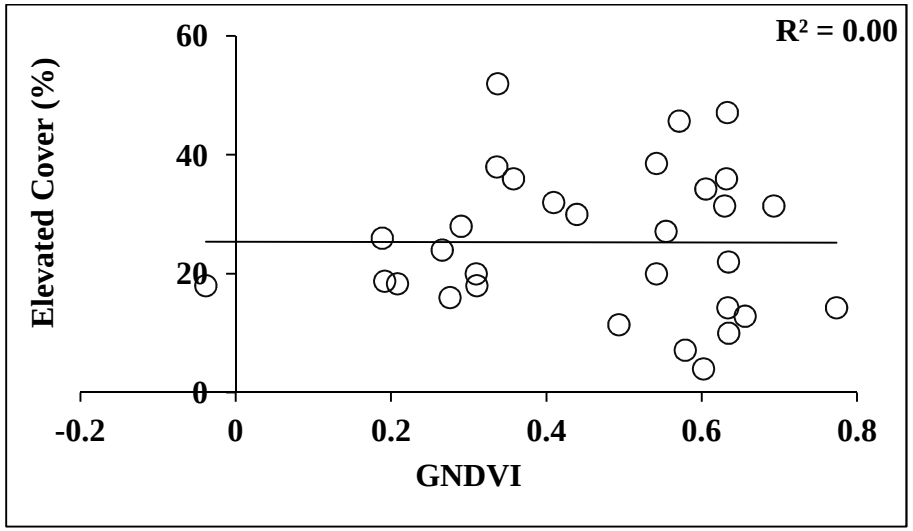
R² = 0.00
Elevated Cover (%)
60
40
20
0
-0.2
0
0.2
0.4
0.6
0.8
GNDVI

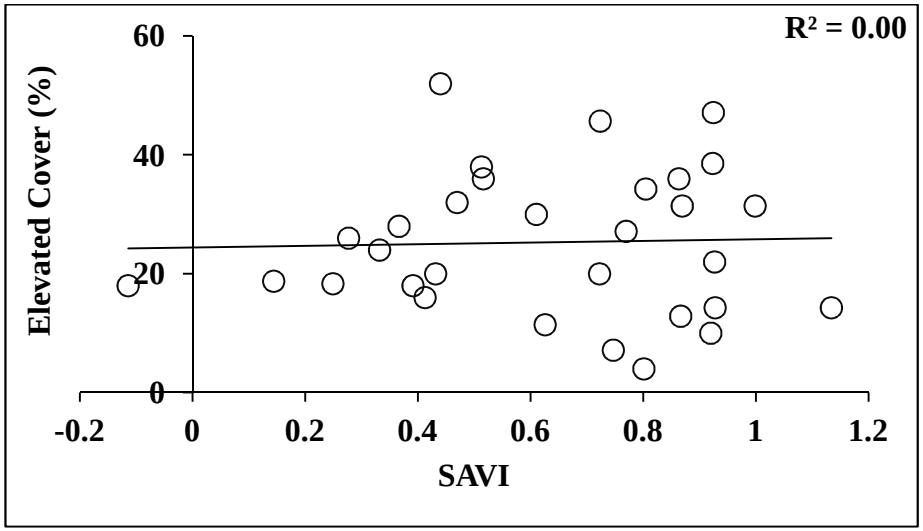
R² = 0.00
Elevated Cover (%)
60
40
20
0
-0.2
0
0.2
0.4
0.6
0.8
1
1.2
SAVI

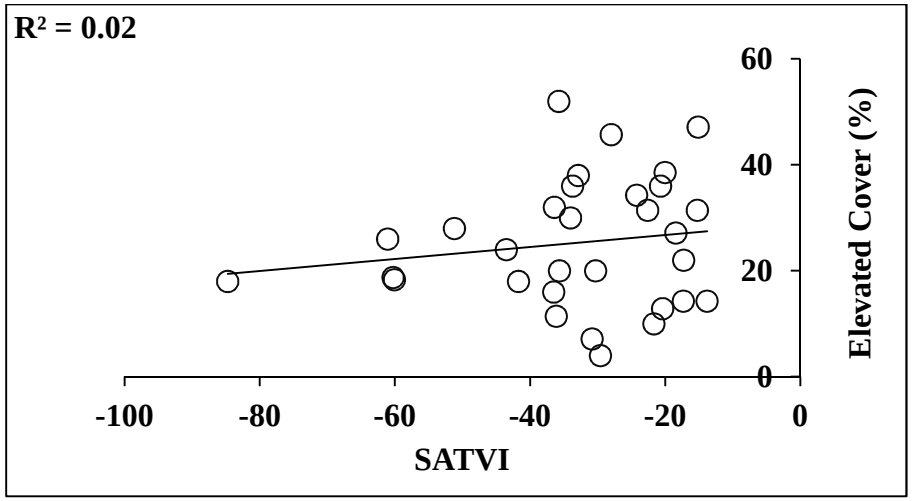
R² = 0.02
60
40
20
0
-100
-80
-60
-40
-20
0
SATVI
Elevated Cover (%)

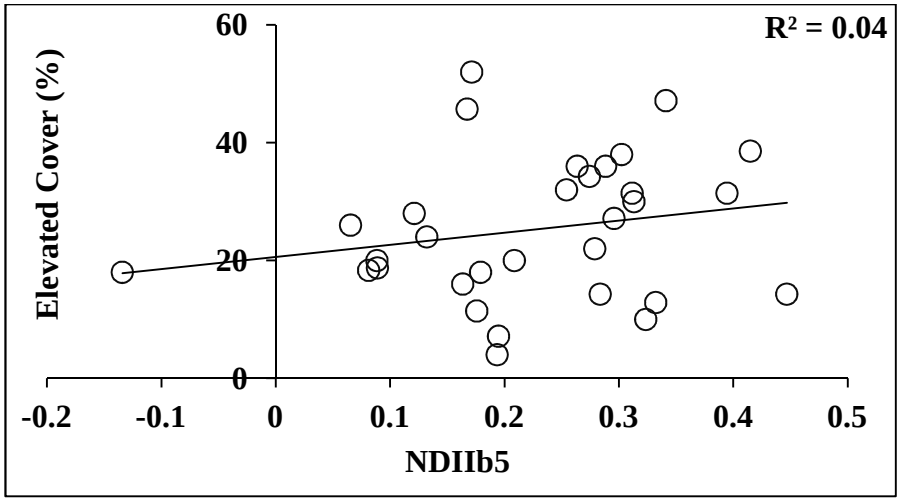
R² = 0.04
60
40
20
0
-0.2
-0.1
0
0.1
0.2
0.3
0.4
0.5
NDIIb5
Elevated Cover (%)

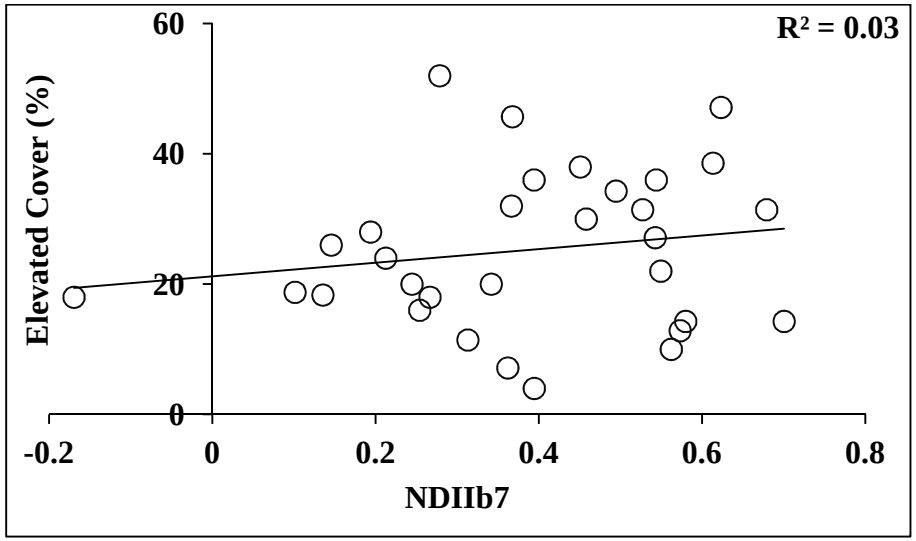
R² = 0.03
60
40
20
0
-0.2
0
0.2
0.4
0.6
0.8
NDIIb7
Elevated Cover (%)

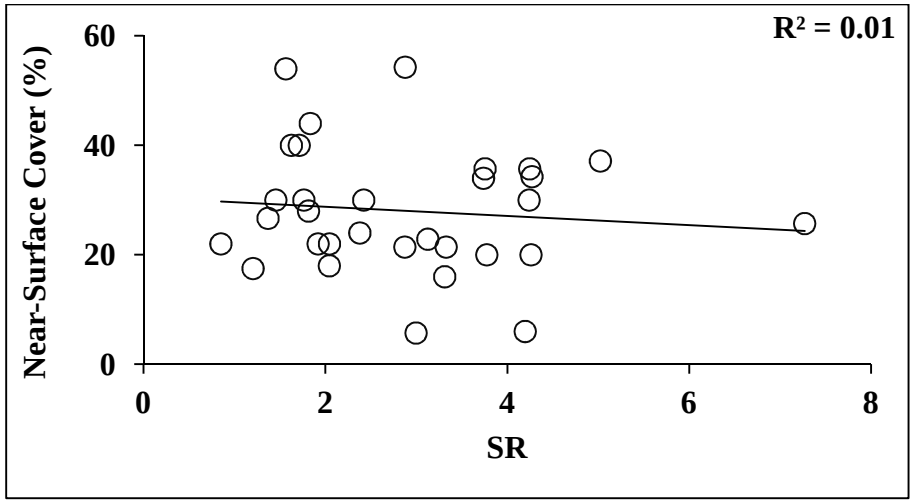
R² = 0.01
Near-Surface Cover (%)
60
40
20
0
0
2
4
6
8
SR

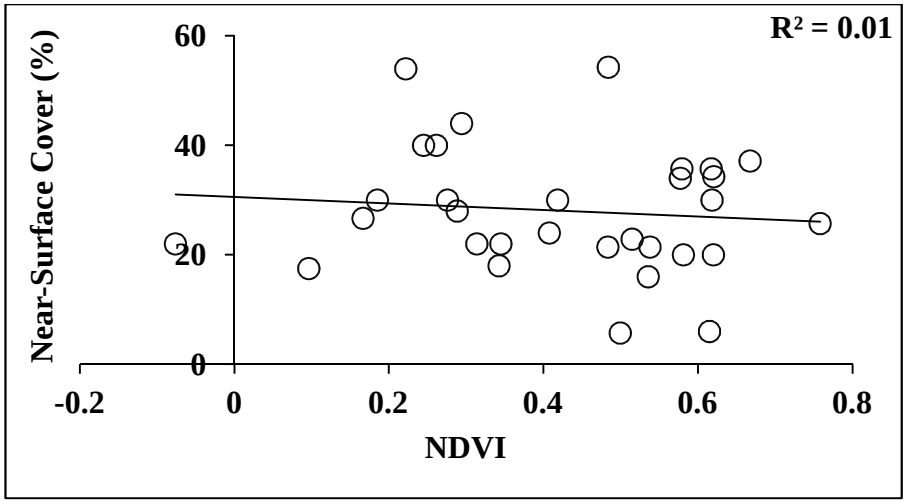
R² = 0.01
Near-Surface Cover (%)
60
40
20
0
-0.2
0
0.2
0.4
0.6
0.8
NDVI

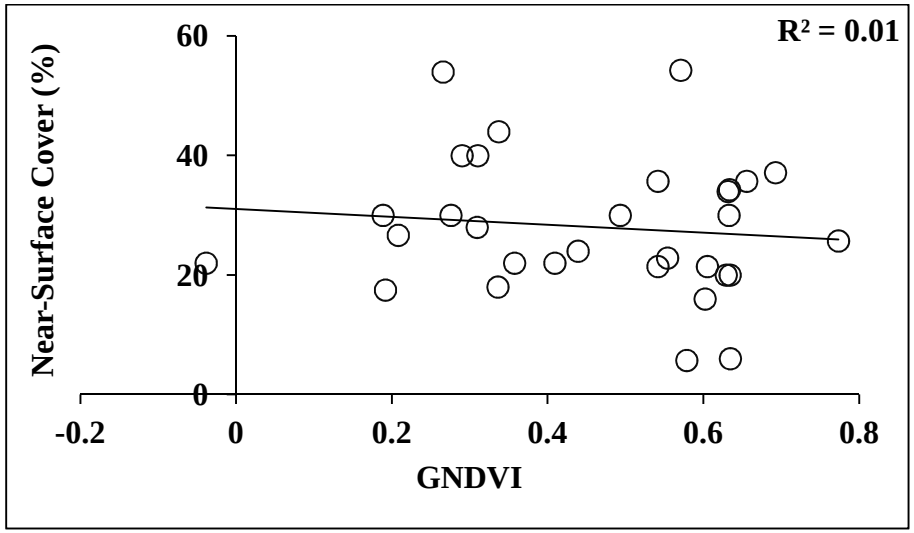
R² = 0.01
Near-Surface Cover (%)
60
40
20
0
-0.2
0
0.2
0.4
0.6
0.8
GNDVI

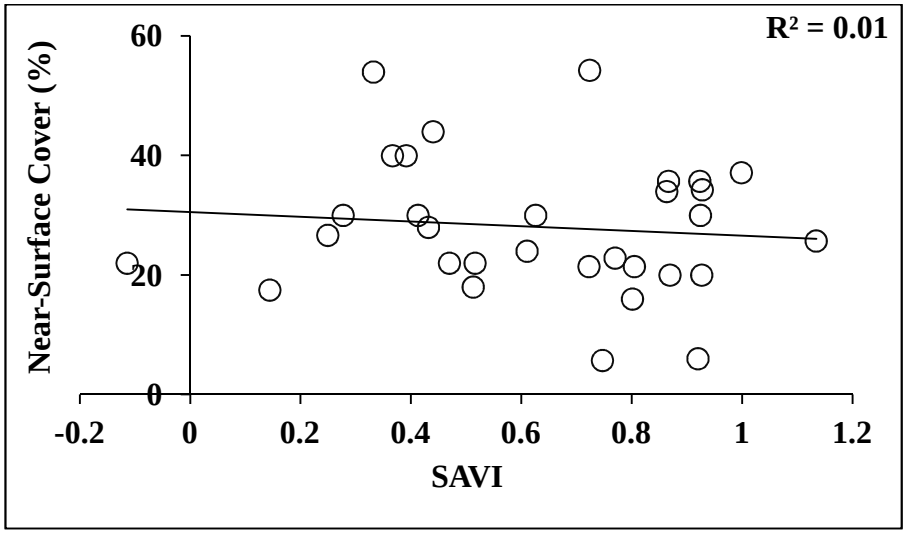
R² = 0.01
Near-Surface Cover (%)
60
40
20
0
-0.2
0
0.2
0.4
0.6
0.8
1
1.2
SAVI

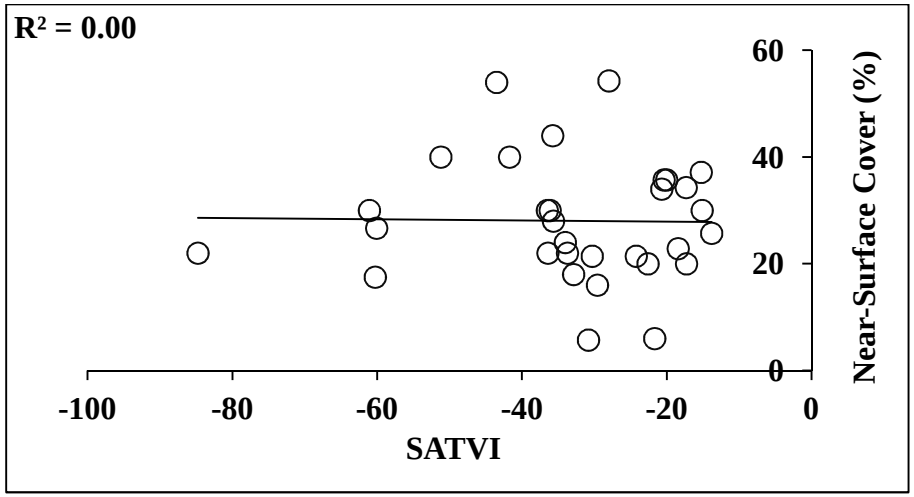
R² = 0.00
60
40
20
0
Near-Surface Cover (%)
-100
-80
-60
-40
-20
0
SATVI

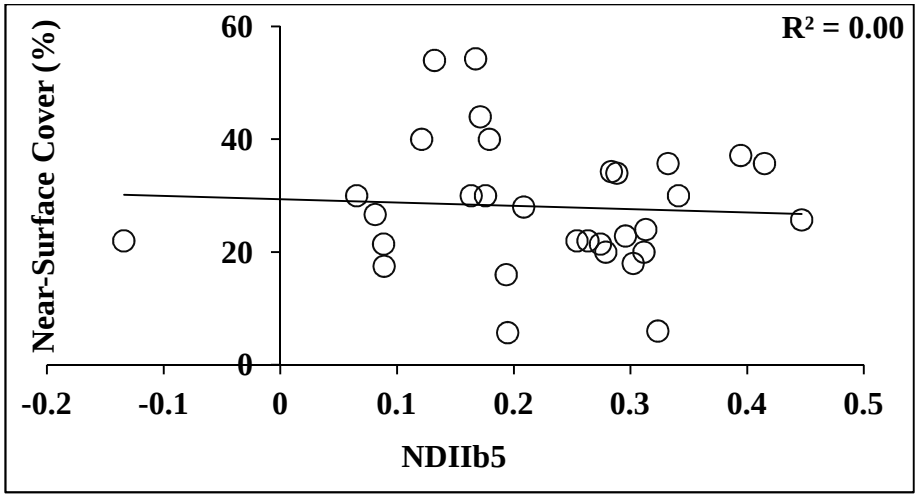
R² = 0.00
60
40
20
0
Near-Surface Cover (%)
-0.2
-0.1
0
0.1
0.2
0.3
0.4
0.5
NDIIb5

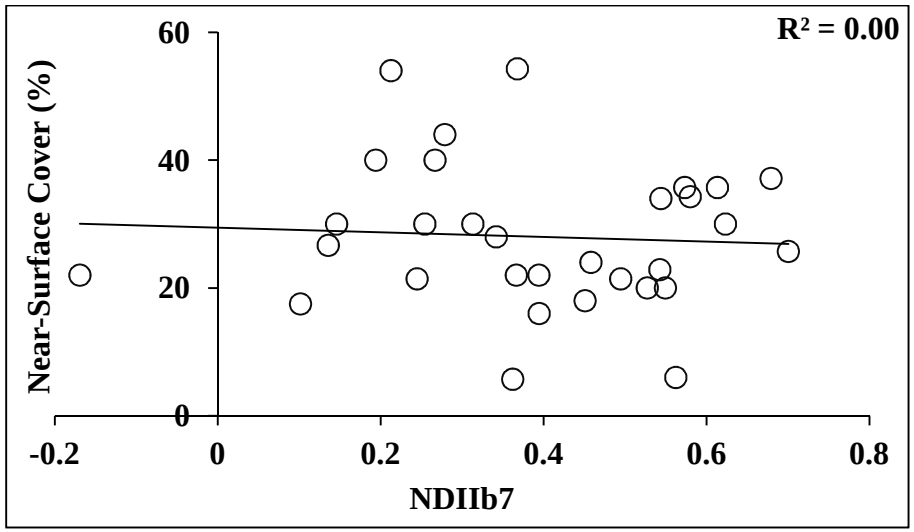
R² = 0.00
60
40
20
0
Near-Surface Cover (%)
-0.2
0
0.2
0.4
0.6
0.8
NDIIb7

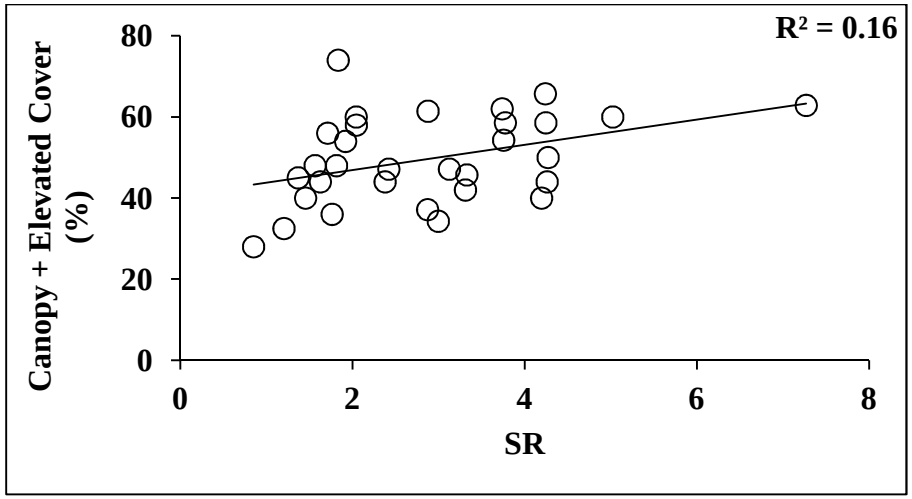
R² = 0.16
Canopy + Elevated Cover (%)
80
60
40
20
0
0
2
4
6
8
SR

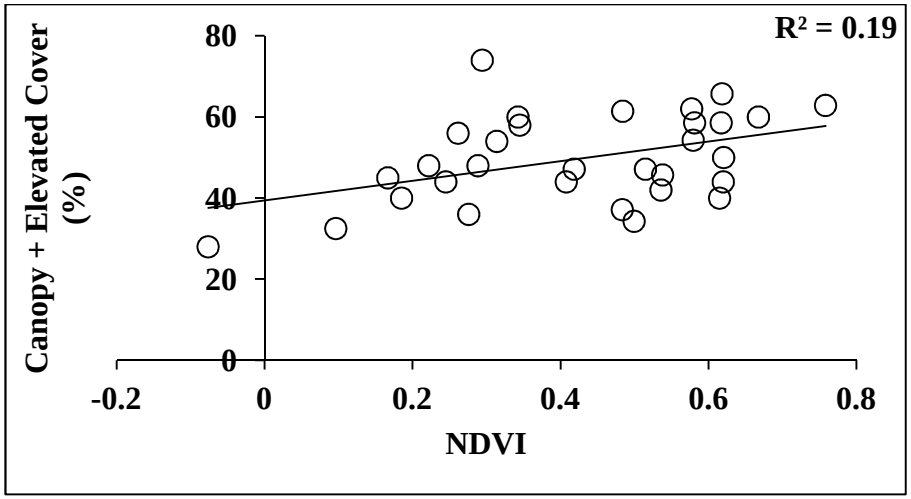
R² = 0.19
Canopy + Elevated Cover (%)
80
60
40
20
0
-0.2
0
0.2
0.4
0.6
0.8
NDVI

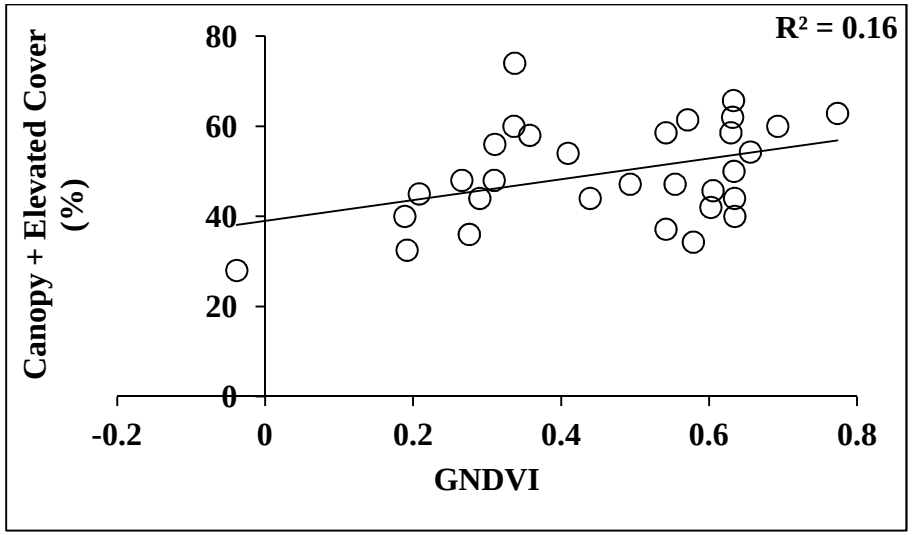
R² = 0.16
Canopy + Elevated Cover (%)
80
60
40
20
0
-0.2
0
0.2
0.4
0.6
0.8
GNDVI

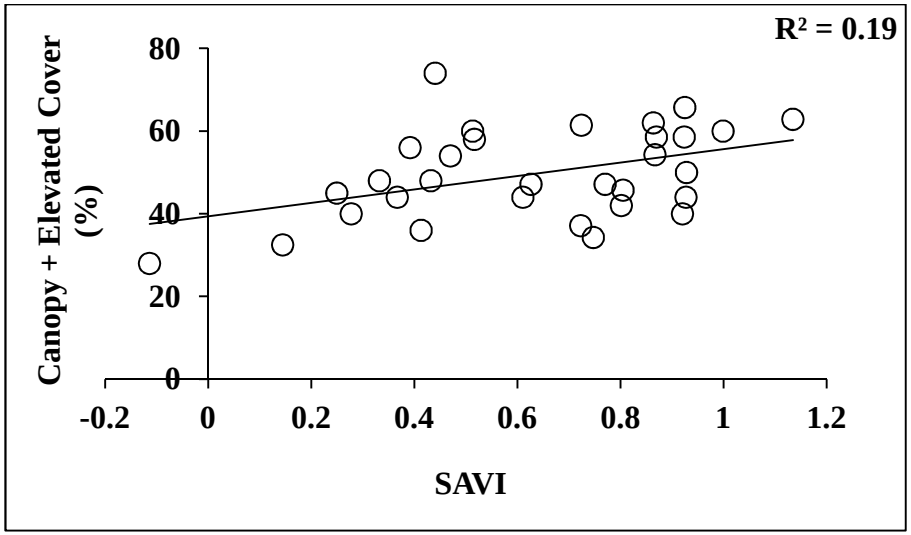
R² = 0.19
Canopy + Elevated Cover (%)
80
60
40
20
0
-0.2
0
0.2
0.4
0.6
0.8
1
1.2
SAVI

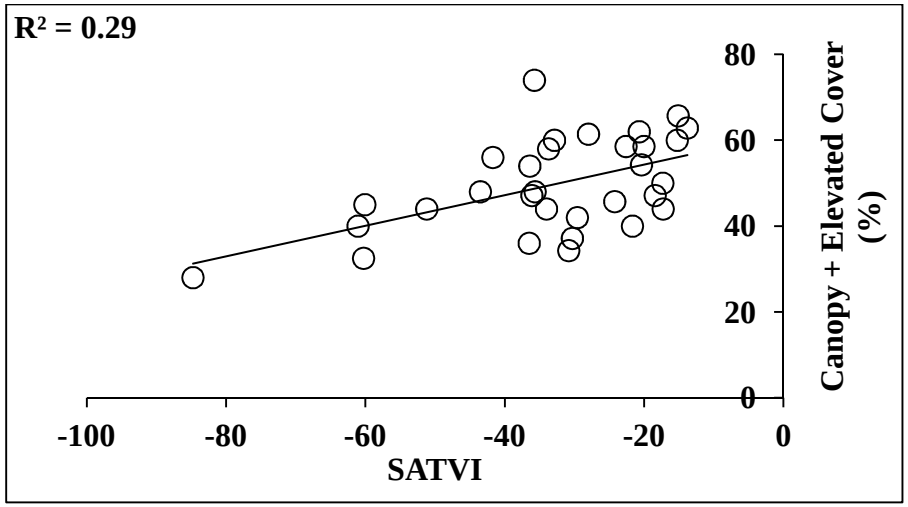
R² = 0.29
80
60
40
20
0
Canopy + Elevated Cover (%)
-100
-80
-60
-40
-20
0
SATVI

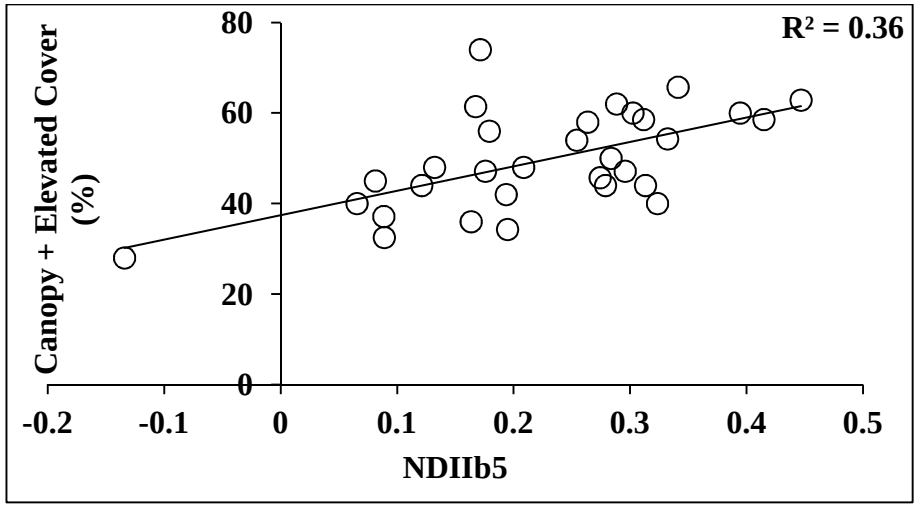
R² = 0.36
80
60
40
20
0
Canopy + Elevated Cover (%)
-0.2
-0.1
0
0.1
0.2
0.3
0.4
0.5
NDIIb5

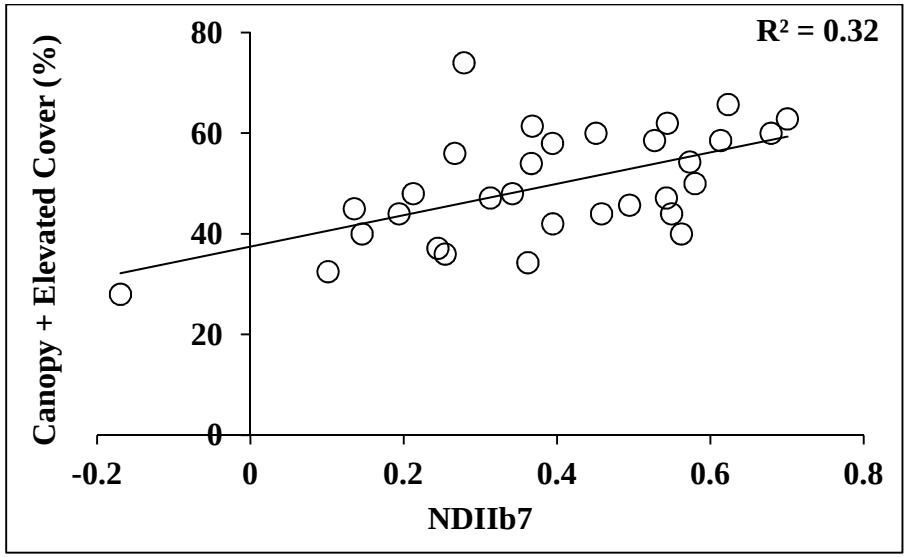
R² = 0.32
80
60
40
20
0
Canopy + Elevated Cover (%)
-0.2
0
0.2
0.4
0.6
0.8
NDIIb7

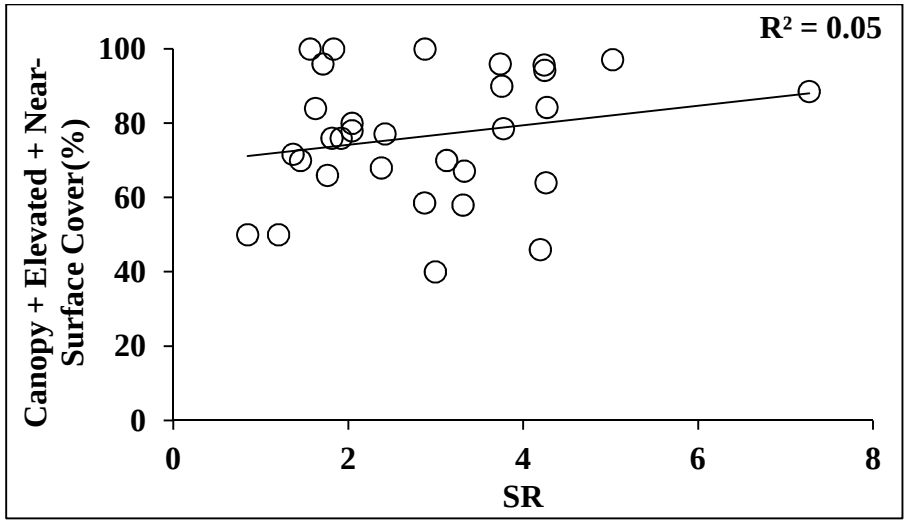
R² = 0.05
Canopy + Elevated + Near-Surface Cover(%)
100
80
60
40
20
0
0
2
4
6
8
SR

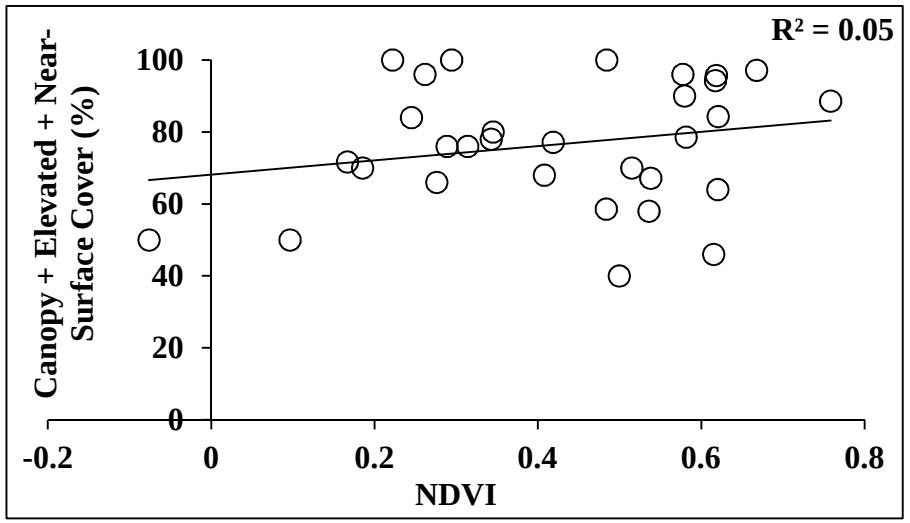
R² = 0.05
Canopy + Elevated + Near-Surface Cover (%)
100
80
60
40
20
0
-0.2
0
0.2
0.4
0.6
0.8
NDVI

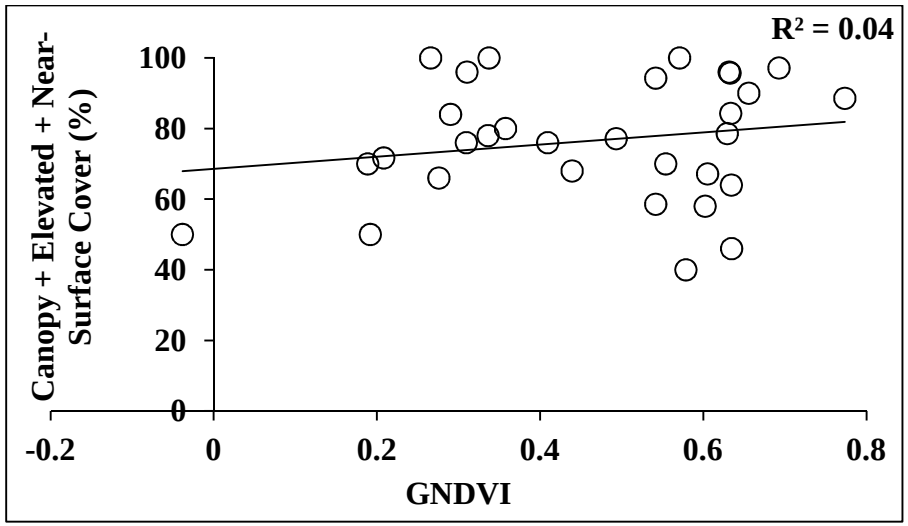
R² = 0.04
Canopy + Elevated + Near-Surface Cover (%)
100
80
60
40
20
0
-0.2
0
0.2
0.4
0.6
0.8
GNDVI

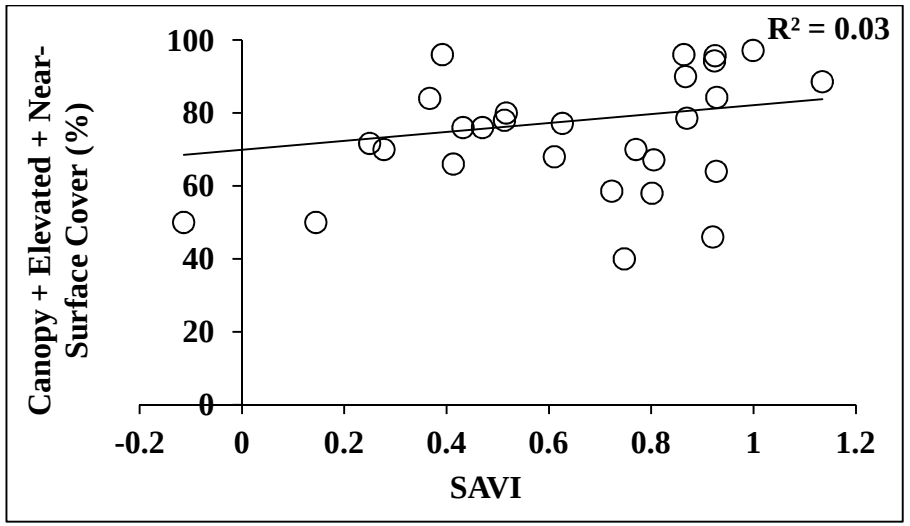
R² = 0.03
Canopy + Elevated + Near-Surface Cover (%)
100
80
60
40
20
0
-0.2
0
0.2
0.4
0.6
0.8
1
1.2
SAVI

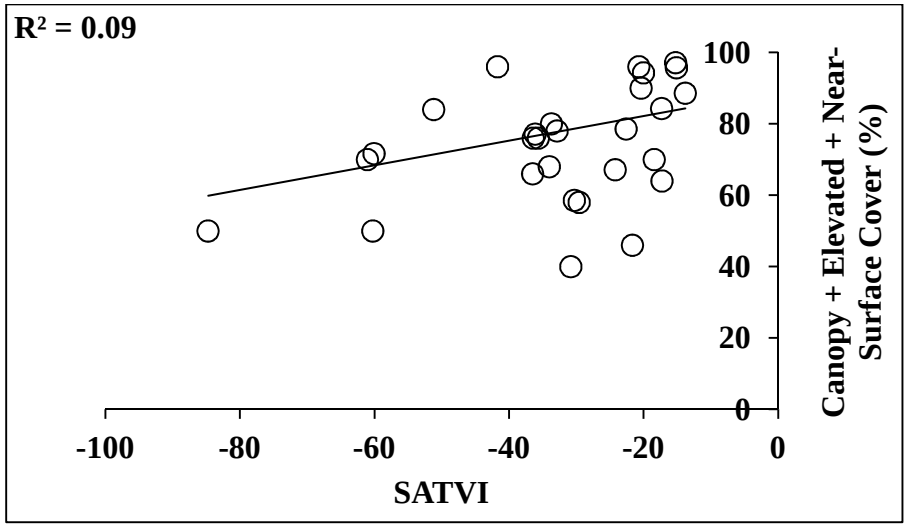
R² = 0.09
Canopy + Elevated + Near-Surface Cover (%)
100
80
60
40
20
0
-100
-80
-60
-40
-20
0
SATVI

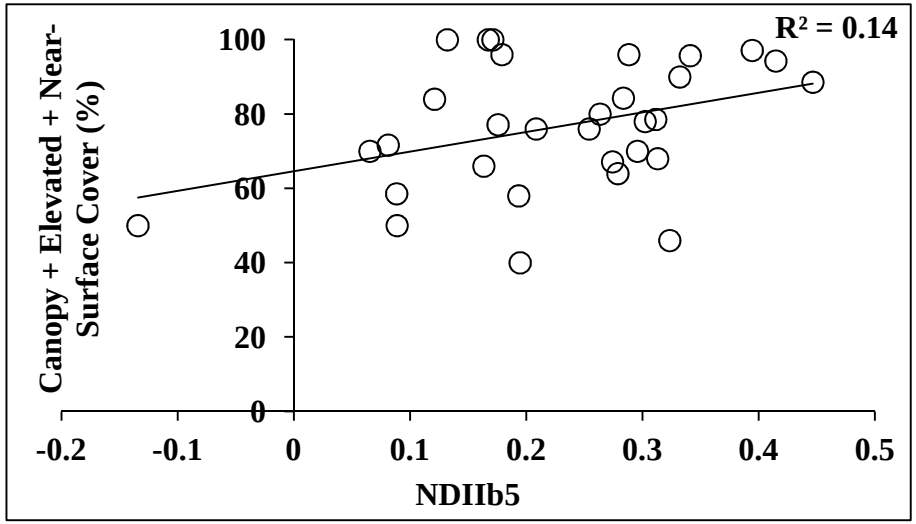
R² = 0.14
Canopy + Elevated + Near-Surface Cover (%)
100
80
60
40
20
0
-0.2
-0.1
0
0.1
0.2
0.3
0.4
0.5
NDIIb5

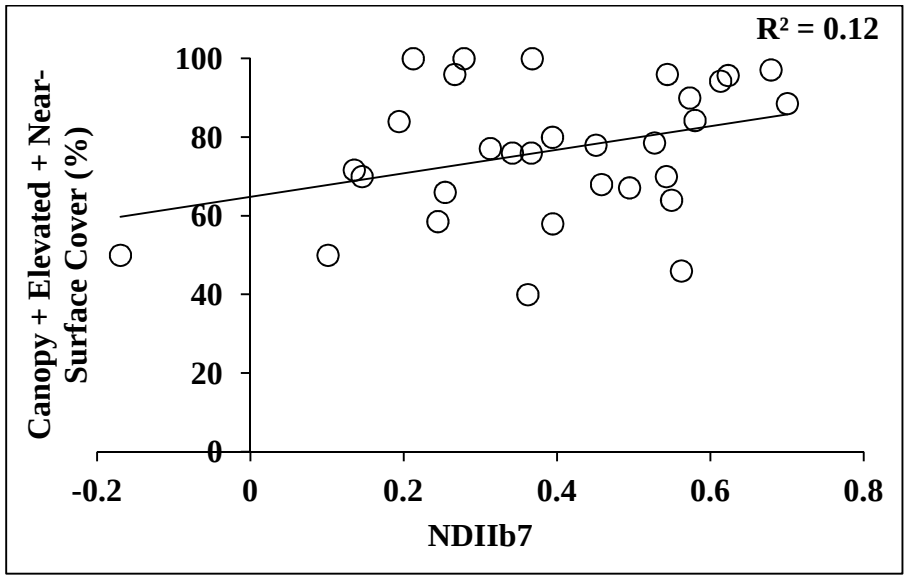
R² = 0.12
Canopy + Elevated + Near-Surface Cover (%)
100
80
60
40
20
0
-0.2
0
0.2
0.4
0.6
0.8
NDIIb7

Approach 2: Live fuel only

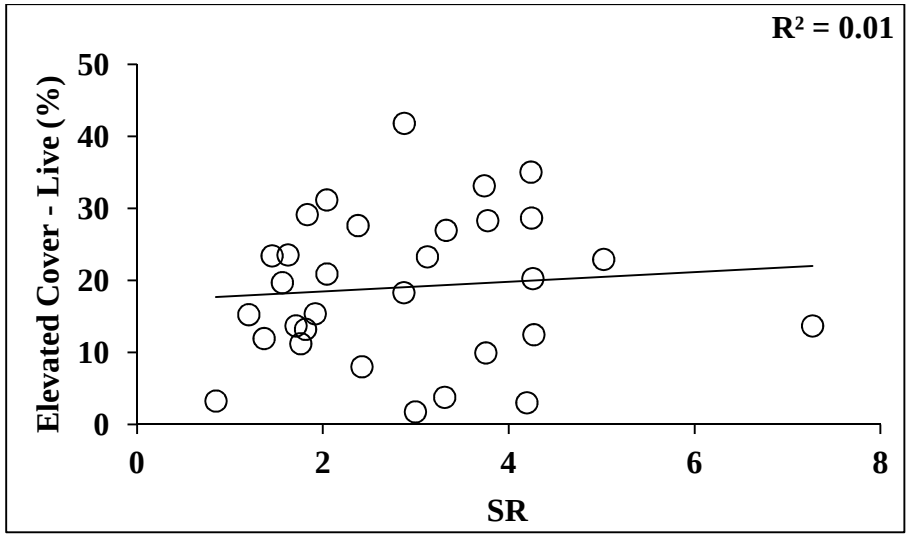

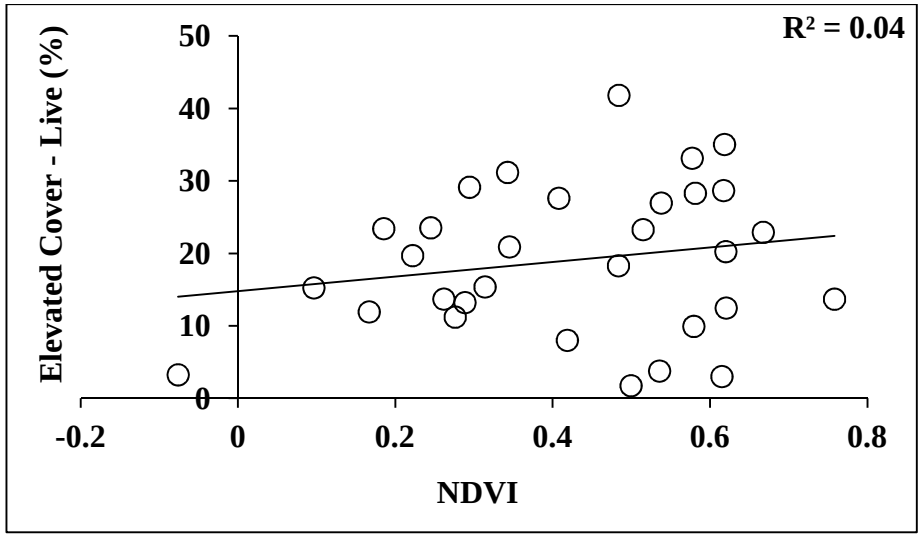

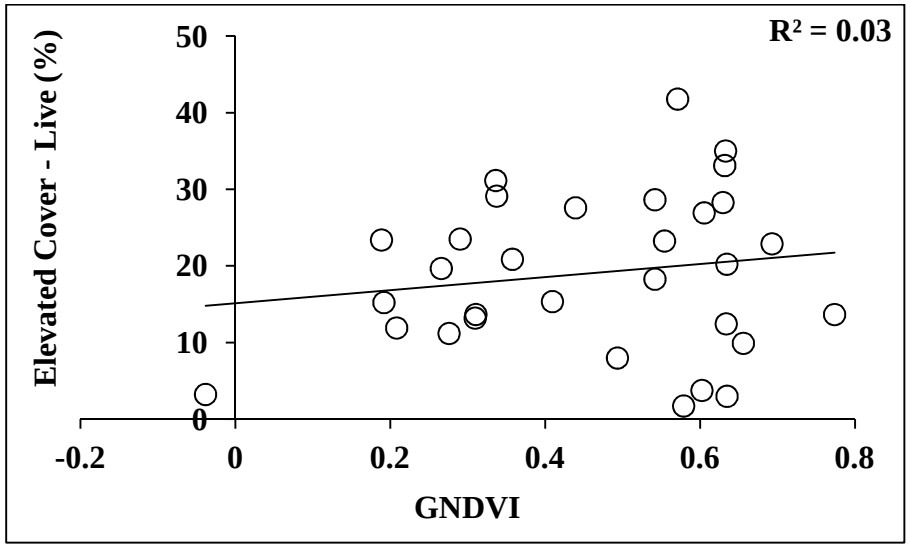

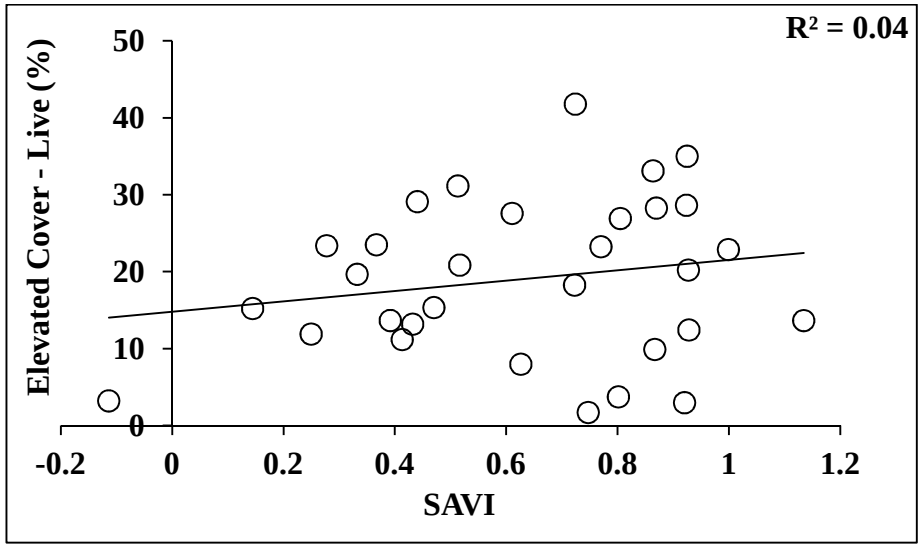

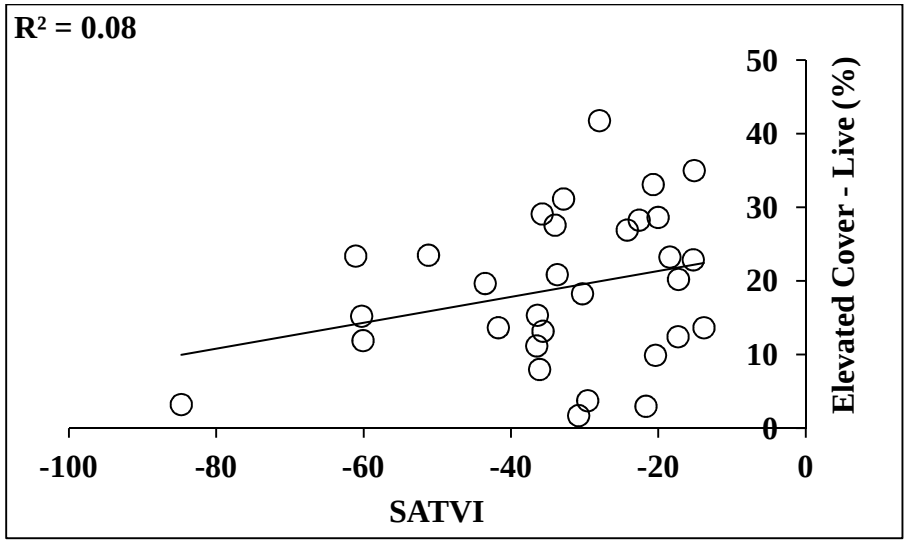
R² = 0.08
Elevated Cover - Live (%)
SATVI
50
40
30
20
10
0
-100
-80
-60
-40
-20
0

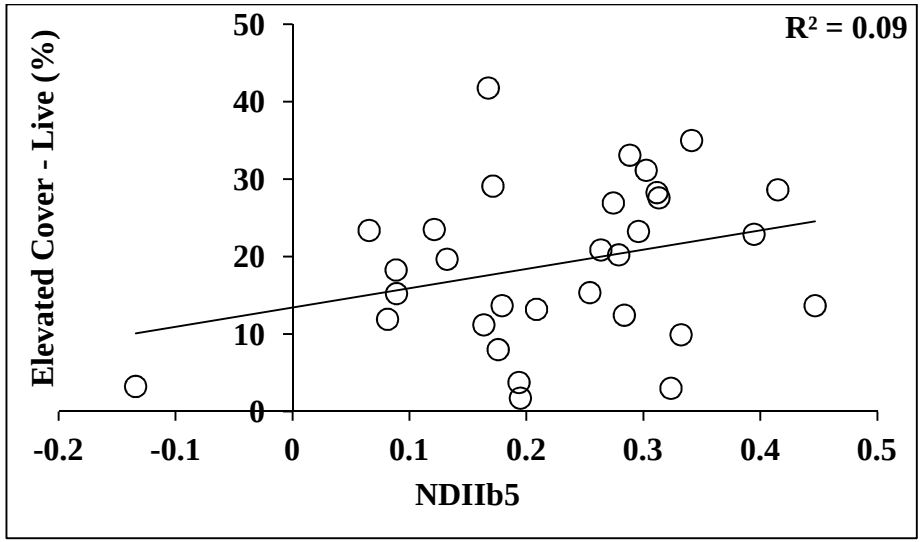
R² = 0.09
Elevated Cover - Live (%)
NDIIb5
50
40
30
20
10
0
-0.2
-0.1
0
0.1
0.2
0.3
0.4
0.5

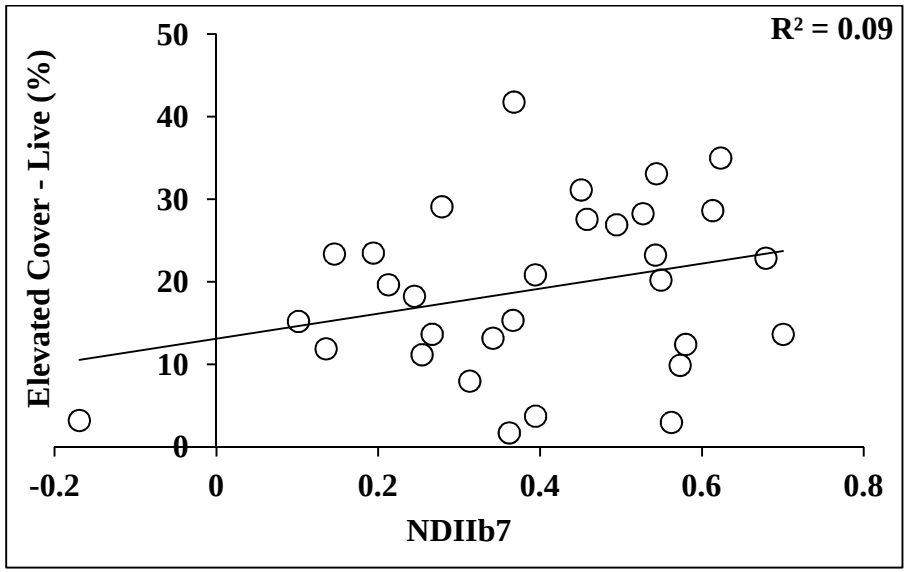
R² = 0.09
Elevated Cover - Live (%)
NDIIb7
50
40
30
20
10
0
-0.2
0
0.2
0.4
0.6
0.8

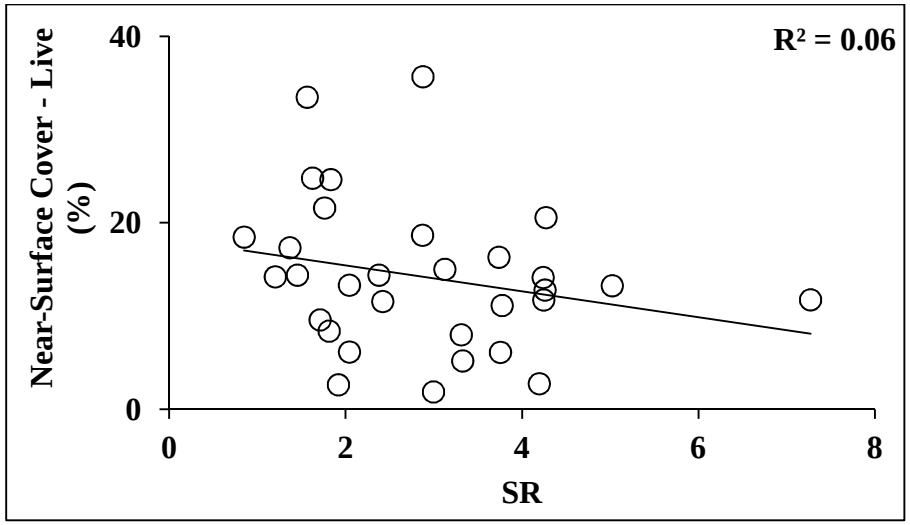
Near-Surface Cover - Live (%)
R² = 0.06
40
20
0
0
2
4
6
8
SR

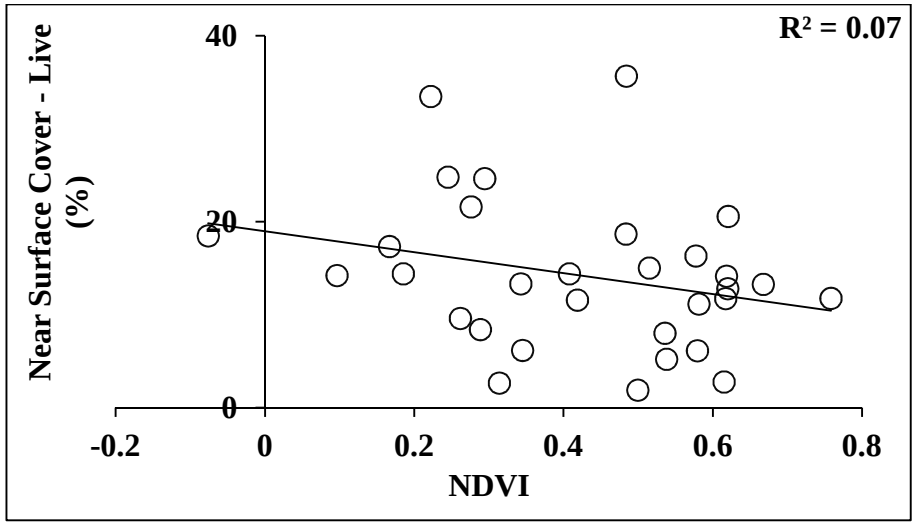
Near Surface Cover - Live (%)
R² = 0.07
40
20
0
-0.2
0
0.2
0.4
0.6
0.8
NDVI

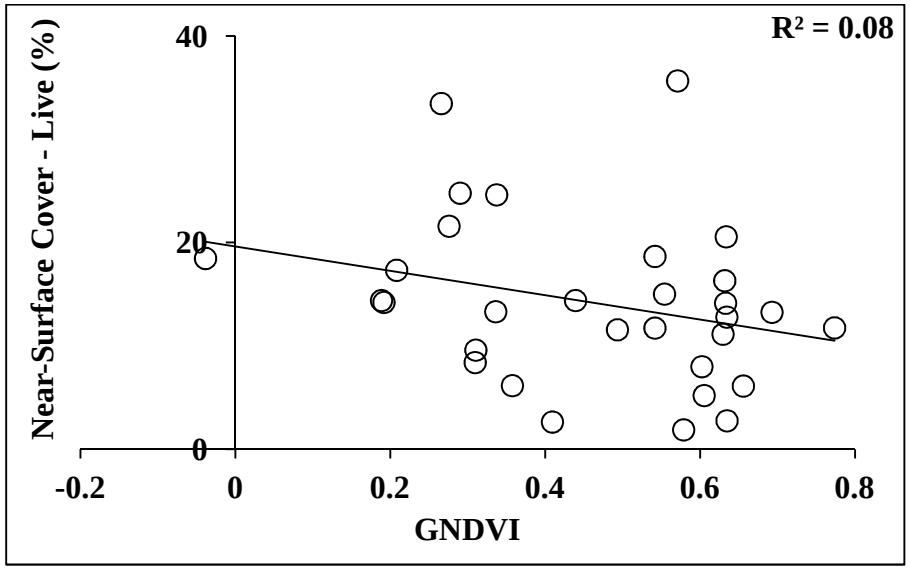
Near-Surface Cover - Live (%)
R² = 0.08
40
20
0
-0.2
0
0.2
0.4
0.6
0.8
GNDVI

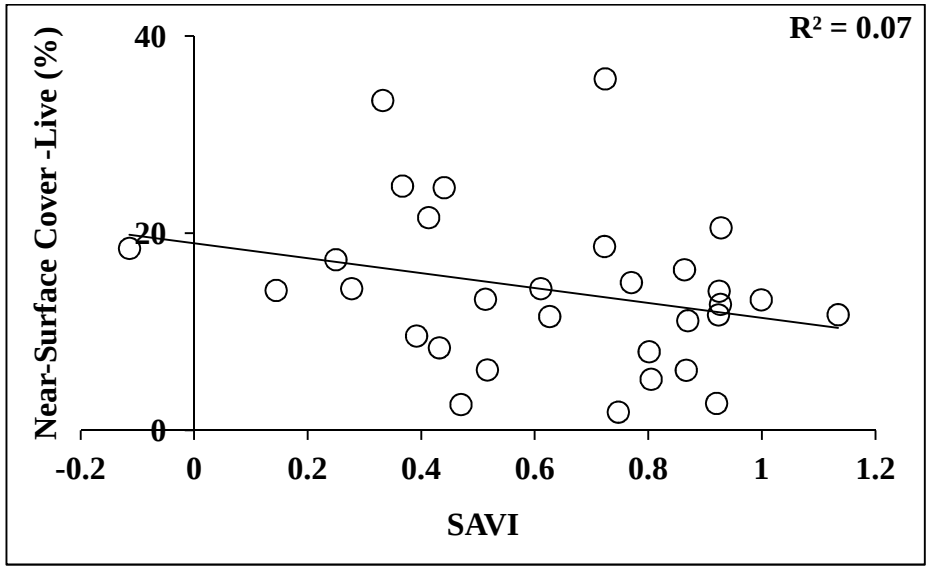
Near-Surface Cover -Live (%)
R² = 0.07
40
20
0
-0.2
0
0.2
0.4
0.6
0.8
1
1.2
SAVI

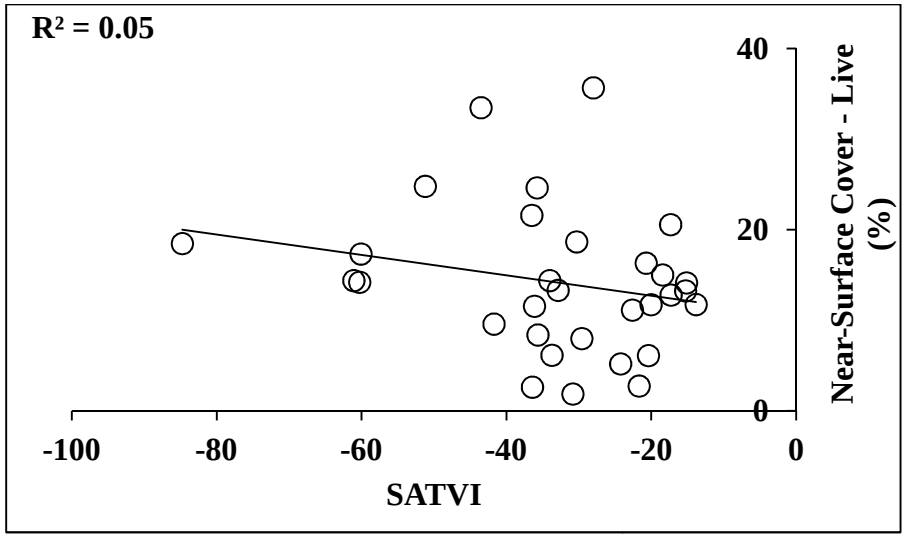
R² = 0.05
40
20
0
-100
-80
-60
-40
-20
0
SATVI
Near-Surface Cover - Live (%)

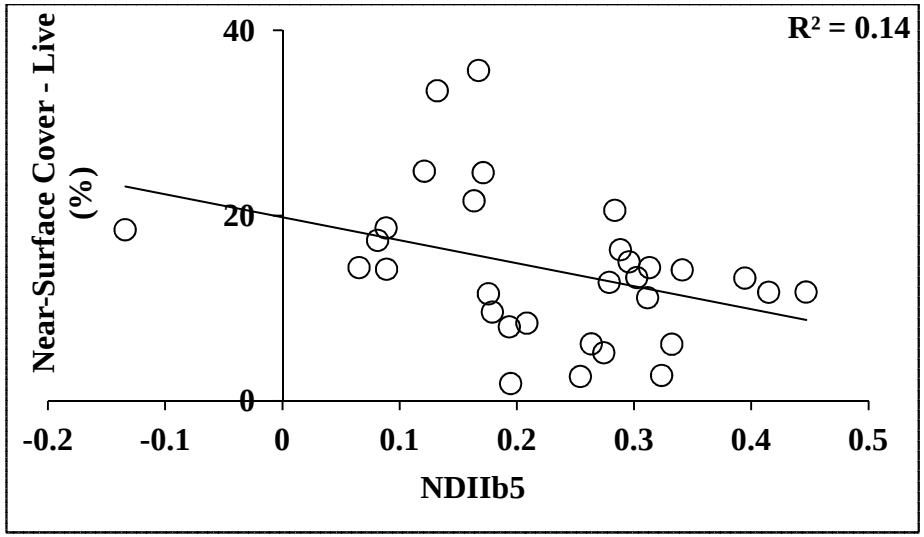
R² = 0.14
40
20
0
-0.2
-0.1
0
0.1
0.2
0.3
0.4
0.5
NDIIb5
Near-Surface Cover - Live (%)

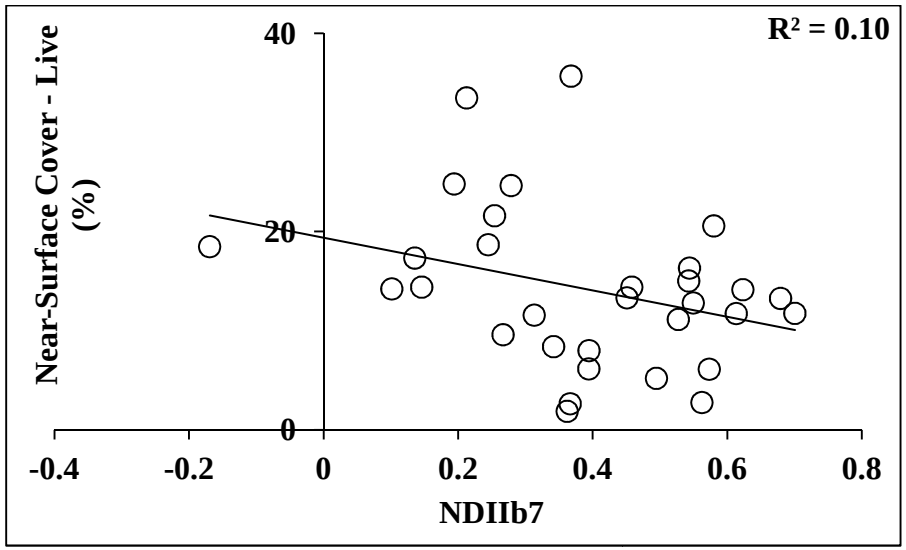
R² = 0.10
40
20
0
-0.4
-0.2
0
0.2
0.4
0.6
0.8
NDIIb7
Near-Surface Cover - Live (%)

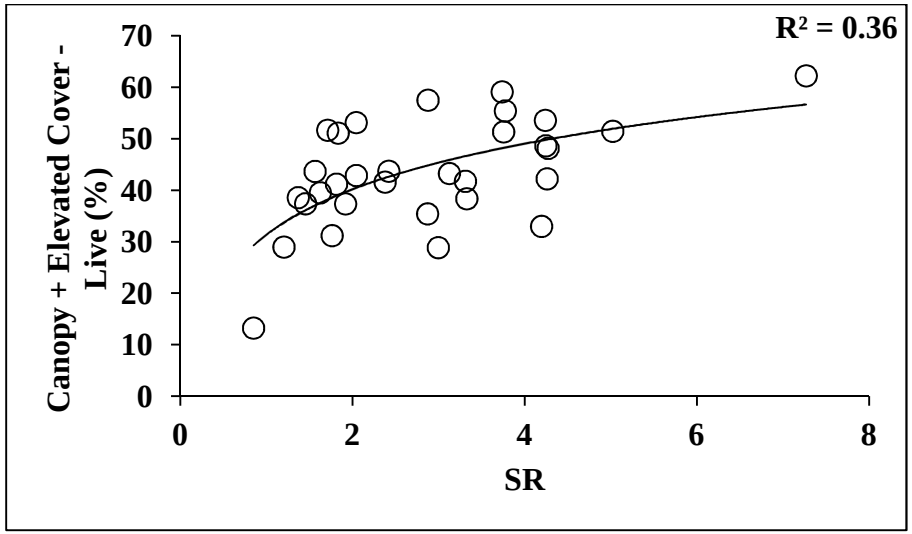
R² = 0.36
Canopy + Elevated Cover - Live (%)
SR
0
10
20
30
40
50
60
70
0
2
4
6
8

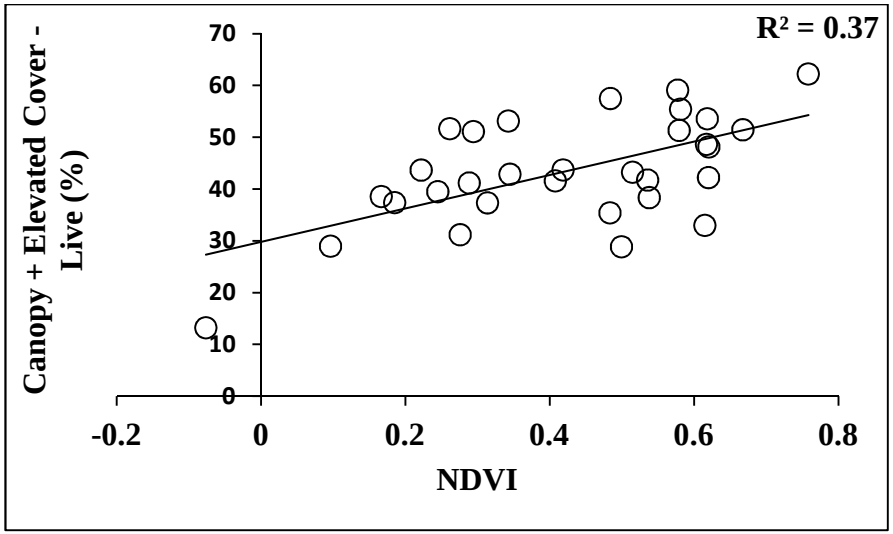
R² = 0.37
Canopy + Elevated Cover - Live (%)
NDVI
0
10
20
30
40
50
60
70
-0.2
0
0.2
0.4
0.6
0.8

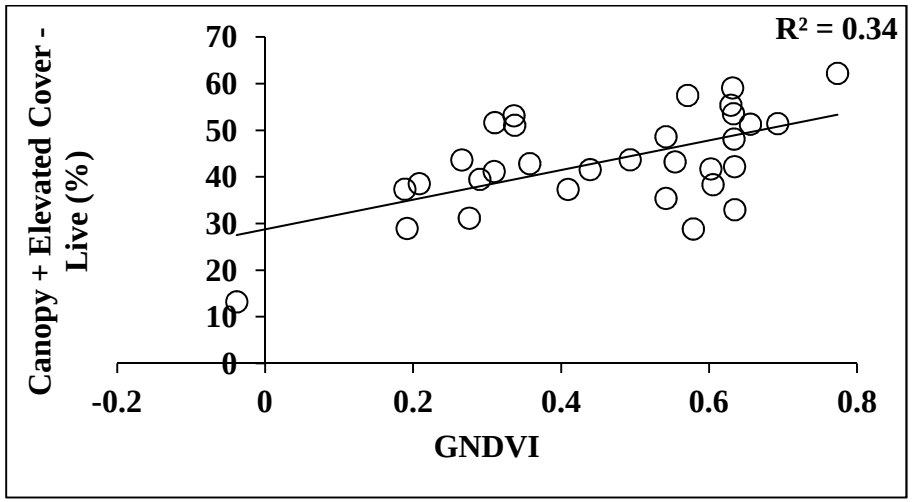
R² = 0.34
Canopy + Elevated Cover - Live (%)
GNDVI
0
10
20
30
40
50
60
70
-0.2
0
0.2
0.4
0.6
0.8

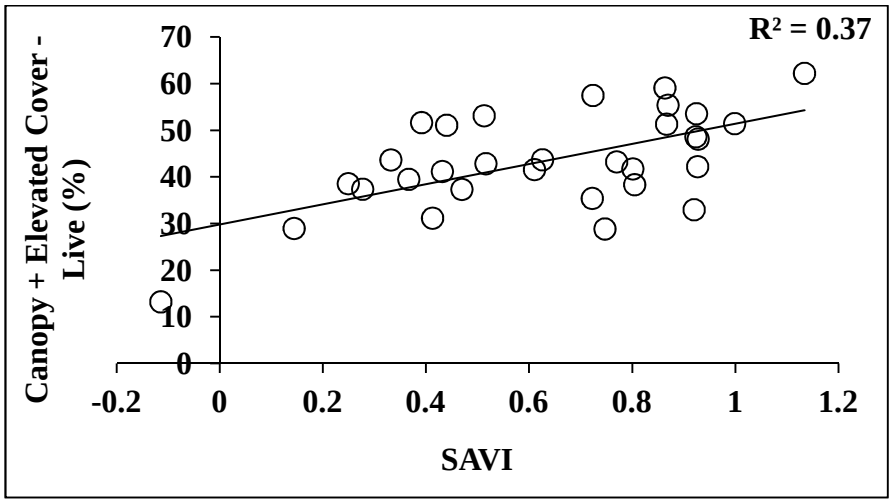
R² = 0.37
Canopy + Elevated Cover - Live (%)
SAVI
0
10
20
30
40
50
60
70
-0.2
0
0.2
0.4
0.6
0.8
1
1.2

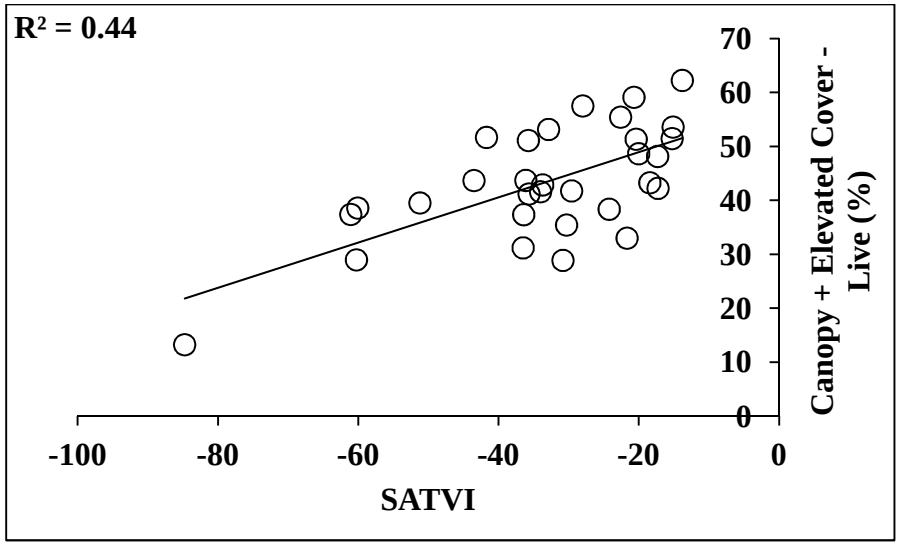
R² = 0.44
70
60
50
40
30
20
10
0
-100
-80
-60
-40
-20
0
SATVI
Canopy + Elevated Cover - Live (%)

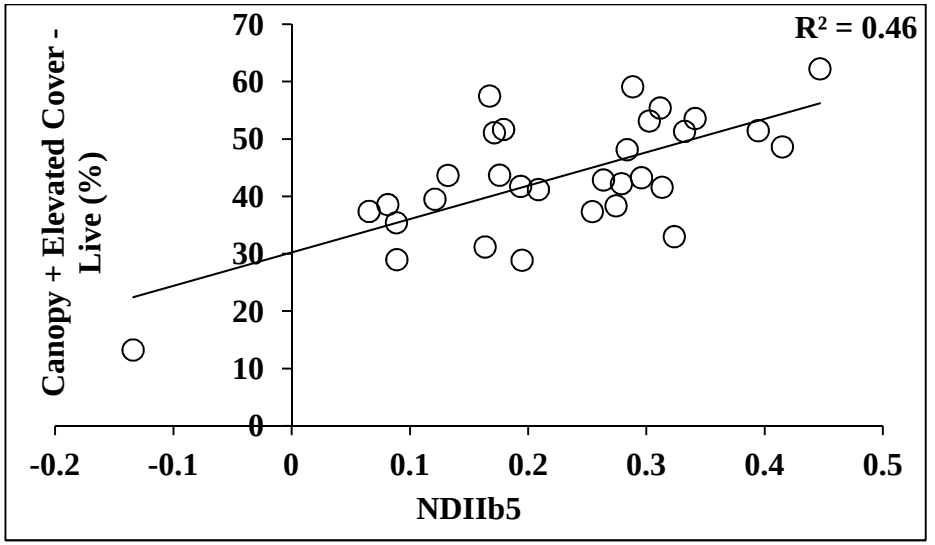
R² = 0.46
70
60
50
40
30
20
10
0
-0.2
-0.1
0
0.1
0.2
0.3
0.4
0.5
NDIIb5
Canopy + Elevated Cover - Live (%)

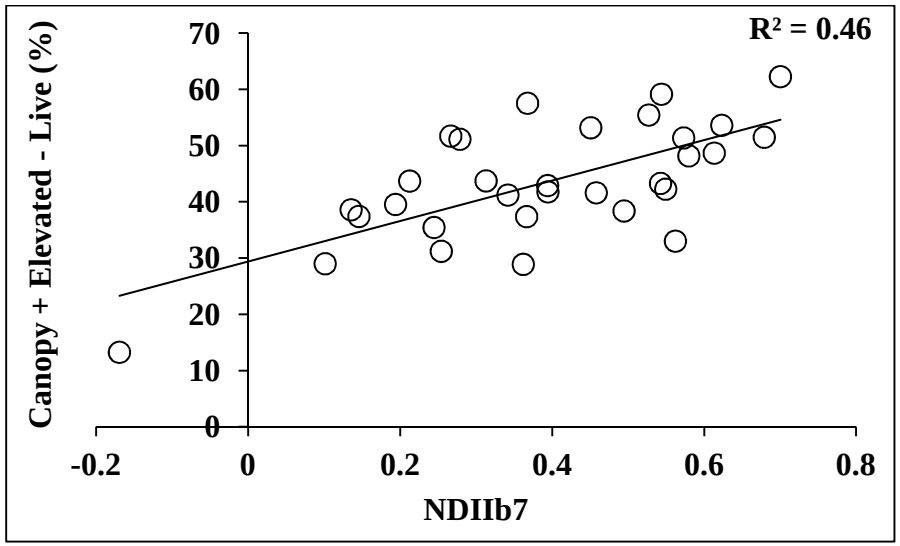
R² = 0.46
70
60
50
40
30
20
10
0
-0.2
0
0.2
0.4
0.6
0.8
NDIIb7
Canopy + Elevated - Live (%)

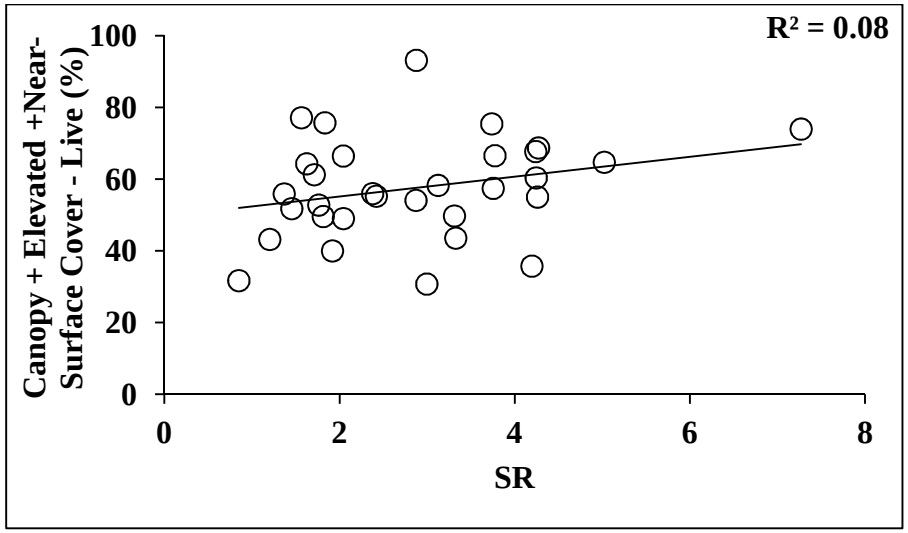
R² = 0.08
Canopy + Elevated +Near-Surface Cover - Live (%)
100
80
60
40
20
0
0
2
4
6
8
SR

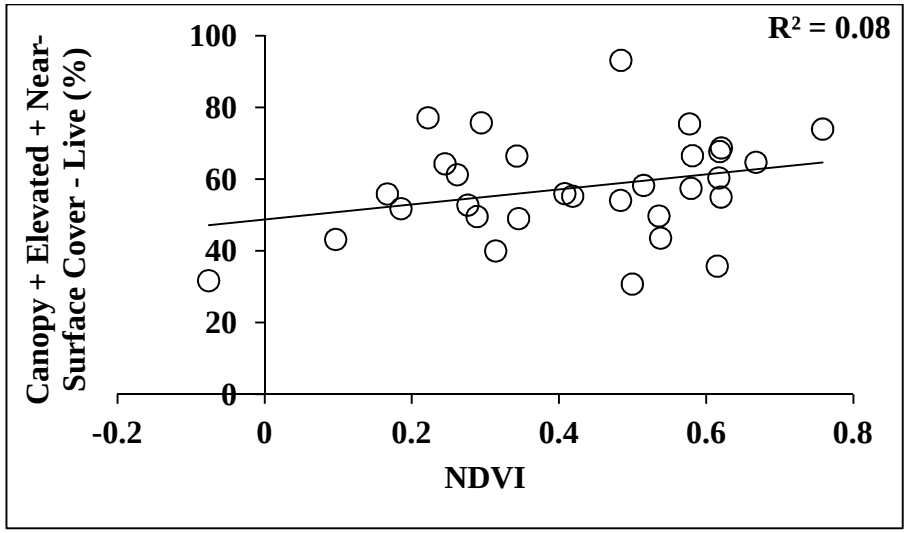
R² = 0.08
Canopy + Elevated + Near-Surface Cover - Live (%)
100
80
60
40
20
0
-0.2
0
0.2
0.4
0.6
0.8
NDVI

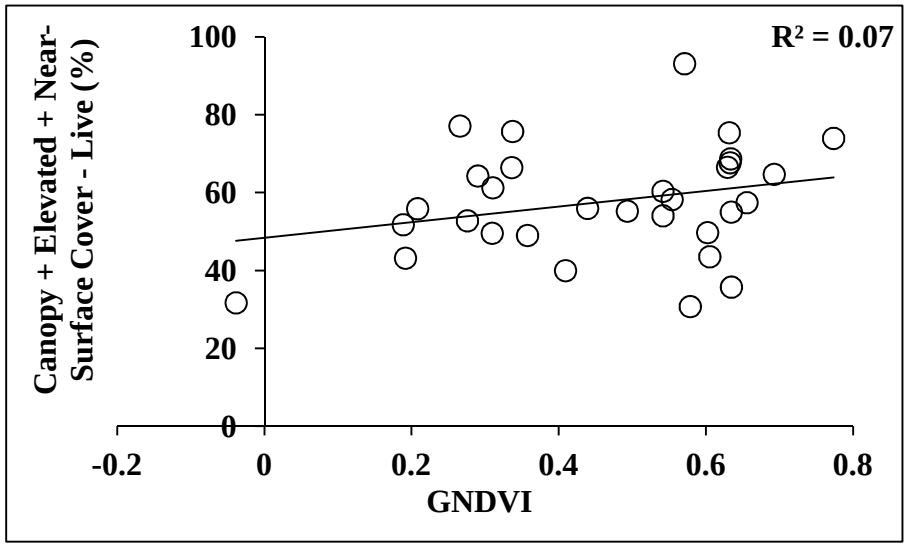
R² = 0.07
Canopy + Elevated + Near-Surface Cover - Live (%)
100
80
60
40
20
0
-0.2
0
0.2
0.4
0.6
0.8
GNDVI

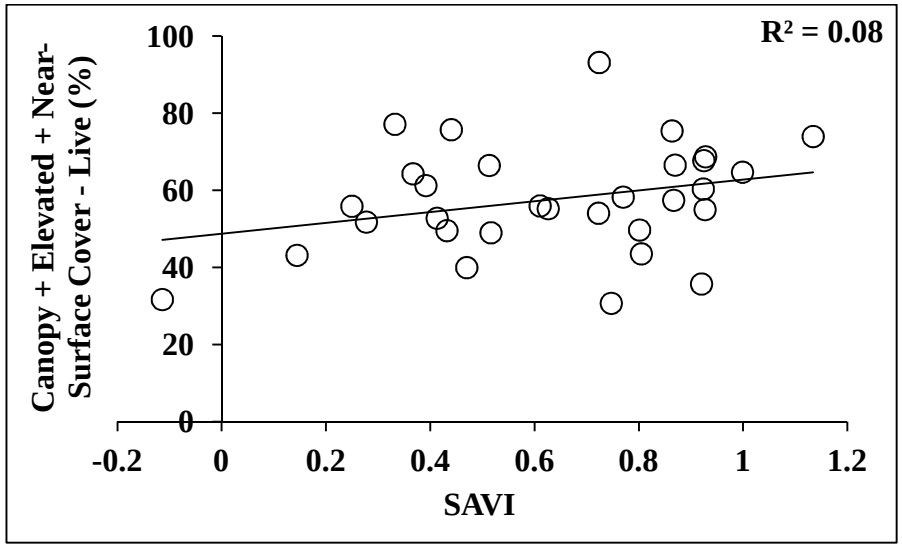
R² = 0.08
Canopy + Elevated + Near-Surface Cover - Live (%)
100
80
60
40
20
0
-0.2
0
0.2
0.4
0.6
0.8
1
1.2
SAVI

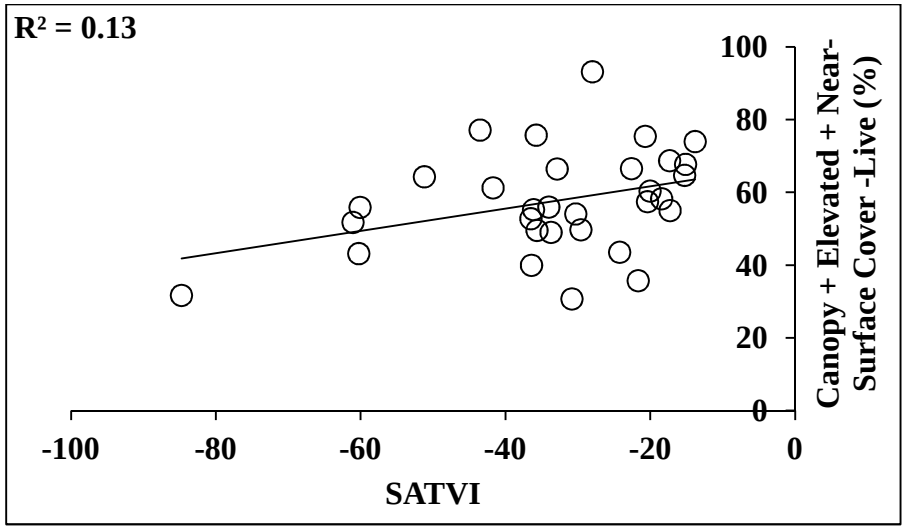
R² = 0.13
Canopy + Elevated + Near-Surface Cover -Live (%)
100
80
60
40
20
0
-100
-80
-60
-40
-20
0
SATVI

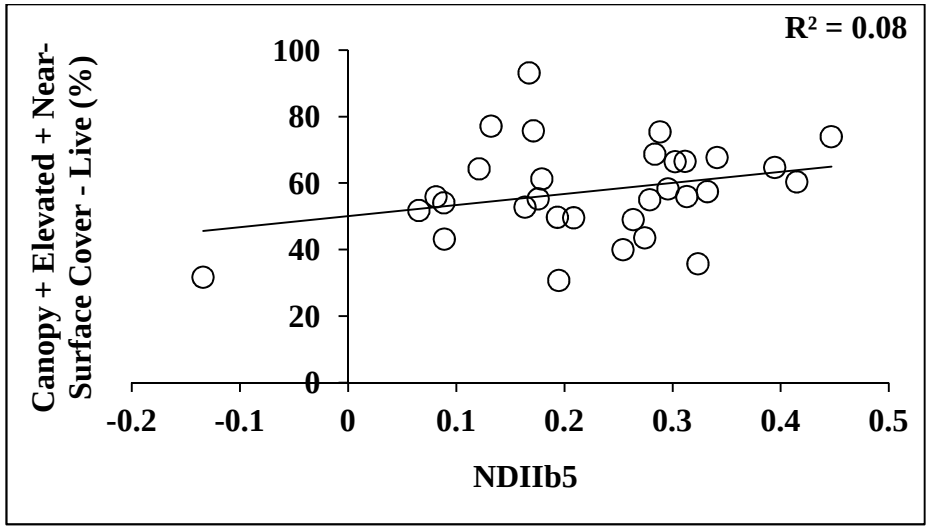
R² = 0.08
Canopy + Elevated + Near-Surface Cover - Live (%)
100
80
60
40
20
0
-0.2
-0.1
0
0.1
0.2
0.3
0.4
0.5
NDIIb5

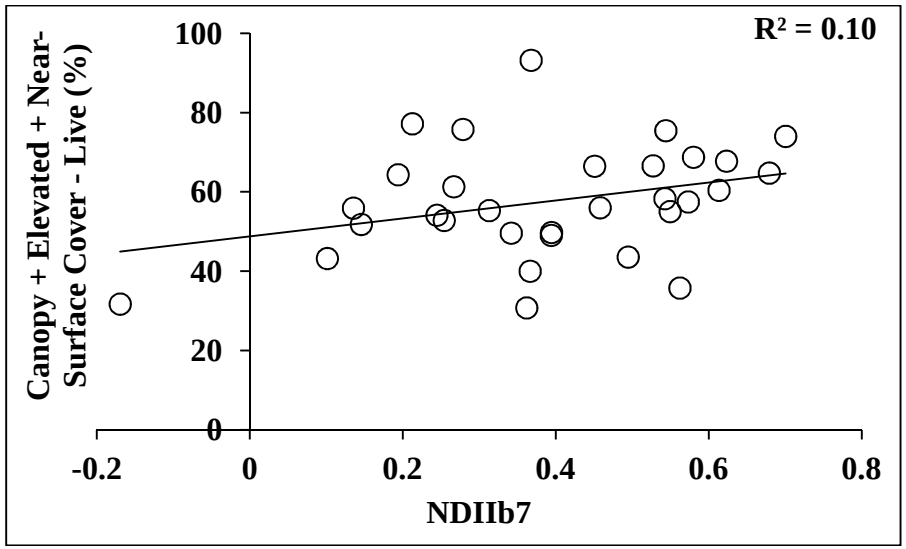
R² = 0.10
Canopy + Elevated + Near-Surface Cover - Live (%)
100
80
60
40
20
0
-0.2
0
0.2
0.4
0.6
0.8
NDIIb7